Deltares

Olivine weathering in field trials

Effect of natural environmental conditions on mineral dissolution and the potential toxicity of nickel

Olivine weathering in field trials

Effect of natural environmental conditions on mineral dissolution and the potential toxicity of nickel

Author(s)
Jos Vink
Daniel Giesen
Edvard Ahlrichs

Olivine weathering in field trials

Effect of natural environmental conditions on mineral dissolution and the potential toxicity of nickel

Client	TKI Nieuw Gas Topsector Energie
Contact	
Reference	
Keywords	Carbon Capture; Climate Change; CO2; Mineral Weathering; Nickel; Olivine; Risk Assessment;

Document control	
Version	1.0
Date	24-11-2022
Project nr.	11204378-000
Document ID	11204378-000-BGS-0002
Pages	62
Classification	
Status	final

Author(s)		
	Jos P.M. Vink Daniel Giesen Edvard Ahlrichs	

The allowed use of this table is limited to check the correct order-performance by Deltares. Any other client-internal-use and any external distribution is not allowed.

Doc. version	Author	Reviewer	Approver	Publish
1.0	Jos Vink	Hilde Passier	Rob Nieuwenhuis	
	Daniel Giesen			
	Edvard Ahlrichs			

Summary

One of the most common silicate minerals on earth is olivine, which has been a natural regulator for atmospheric carbon dioxide concentrations for millions of years. In the presence of water, CO_2 is chemically converted to calcareous products. In past years, the possibility of olivine applications to acquire negative emissions of CO_2 has received the attention of scientists and policy. The CO-Action project targeted the obstructions for the use of olivine to capture CO_2 such as scientific knowledge gaps that inhibited the estimation of mineral weathering rates, and addresses the bottlenecks for large scale applications in natural environments. Main obstructions are: 1) uncertainty of weathering rates of olivine under natural conditions; 2) toxicity risks of nickel that is incorporated in the mineral and is released upon weathering.

A two-year field experiment was conducted in the Netherlands to study mineral weathering rates under various conditions. Variables were: mineral source (Norwegian and Spanish olivine, Canadian wollastonite), type of application (on-top versus mixed-in), availability of moisture (rain-fed versus wet), and effect of vegetation (planted versus non-planted). All field plots contained mesocosms with similar treatments for mass-balancing. Pore water was sampled periodically over various depths, and different chemical extractions were applied to the soil. The numerical model OWCS, based on the shrinking core principle, was calibrated with data obtained from the field experiments. A separate risk assessment module for nickel was developed and incorporated in the model.

Results show that 6 to 8.5 percent of the initial mineral dose was dissolved after two years. Applying the Shrinking Core Model to each grain size, the dissolution over time could be calculated accurately. Of the smallest grain fraction (<2µm), 100 % of the mass is dissolved in two years. In the same period, 42.9 % of the fraction < 8 µm is dissolved. The larger fractions show decreasing dissolved portions respectively. Modelled and measured values show a good agreement.

Only marginal differences for extractable Mg and Ni were observed between dry and wet plots. Moisture content varied around 20 - 40 % in dry plots, indicating that the moisture content under natural precipitation conditions is not significantly limiting the chemical reaction compared to saturated conditions. The effect of vegetation (alternating winter barley and summer rye), and type of olivine application was of minor consequence, but the grain size distribution of the grounded minerals plays a decisive role in weathering rates. Due to weathering, and the release of alkaline products, the pH of the soil increased 0.2 to 0.5 unit over the course of the experiments.

Nickel concentrations in pore waters are elevated compared to the reference plot. However, 96 % of all Ni measurements are below the analytical upper reporting limit. Only two measurements (Norwegian olivine source) exceed the generic quality standards but only short after application. In the first period of weathering, most nickel is released from the ultrafine fraction. In all cases, the calculated No-effect concentration (PNEC) for nickel is larger than its measured value in pore water and are (far) below the risk characterization ratio (RCR < 1). This is a strong indication that no chronic toxic risks of nickel release are to be expected for the concentrations observed during the experiment.

Nederlandse samenvatting

Olivijn is één van de meest voorkomende silicaat mineralen op aarde en reguleert al miljoenen jaren de CO_2-concentratie in de atmosfeer. Bij aanwezigheid van water wordt CO_2 via natuurlijke chemische conversie omgezet in carbonaat (kalk). Het project CO-Action richt zich primair op het wegnemen van belemmeringen om olivijn te gebruiken om CO_2 te verwijderen, zoals wetenschappelijke hiaten en maatschappelijk-operationele knelpunten die grootschalige toepassingen van olivijn dreigen te hinderen. Deze knelpunten zijn: 1) de onzekerheid rond verweringssnelheden van het mineraal onder natuurlijke veldcondities; 2) de ecotoxicologische risico's van nikkel dat zit opgesloten in het mineraal. Een twee jaar durend veldexperiment is in Nederland uitgevoerd om de effecten van verschillende mineraalsoorten (Noors en Spaans olivijn, Canadese wollastoniet), de manier van toepassing, het vochtgehalte, en beplanting op de verweringssnelheid te kwantificeren. Hiervoor is periodiek het poriewater van de grond geanalyseerd op verweringsproducten, waarbij lysimeters werden gebruikt voor het bepalen van de massabalans van stoffen. Daarnaast zijn er verschillende soorten chemische extracties aan de bodem uitgevoerd. Het rekenmodel OWCS V6.3 is gekalibreerd met deze veldmetingen. Het model is uitgebreid met een risicomodule voor nikkel om de mogelijke effecten op grond- en oppervlaktewater te beoordelen. De resultaten laten zien dat de natuurlijke verwering van olivijn goed te voorspellen is met het rekenmodel. Na twee jaar is 6 tot 8,5 procent van de oorspronkelijke dosering verweerd, waarbij vooral de korrelgrootteverdeling bepalend is voor de verweringssnelheid. De gemiddelde neerslag lijkt weinig beperkend te zijn voor de snelheid van verwering vergeleken met vochtverzadigde condities. Door de vorming van alkalische verweringsproducten nam de pH in de bodem met 0,2 tot 0,5 eenheid toe. De hoeveelheid regenval (in Nederland) lijkt niet beperkend te zijn voor de verweringssnelheid, behalve voor oppervlaktedoseringen. Er zijn over de gehele testperiode geen chronische toxische effecten van nikkel aangetoond.

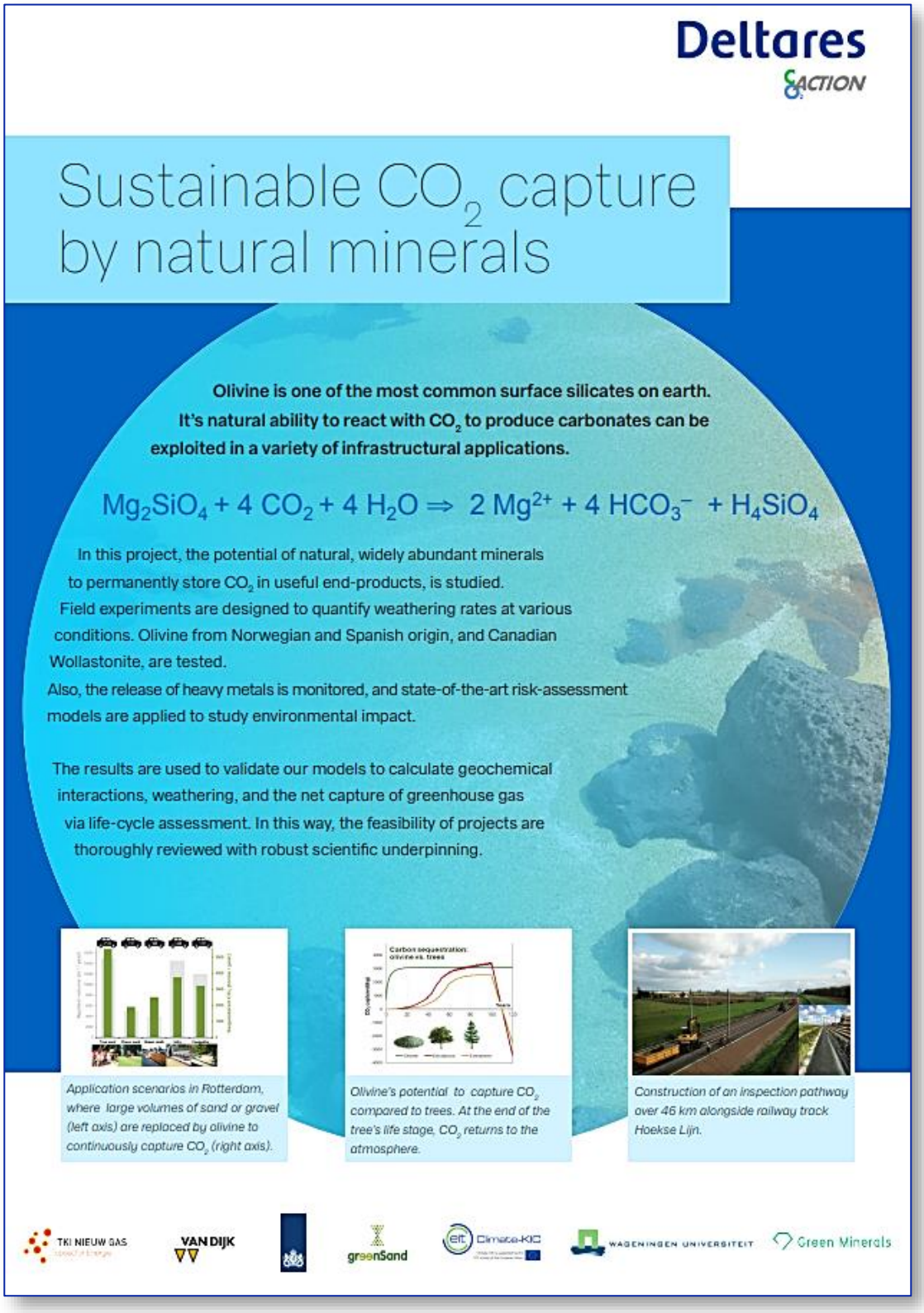

Information board at the field site.

Table of contents

1 Introduction

1.1 Rationale

Net negative CO_2 emissions are necessary to halt the effects of climate change. This requires drastic cuts in emissions but also the creation of permanent sinks, often referred as “negative emissions” (Dunsmore, 1992). Since awareness of climate change has drawn the interest of the both the scientific community and policy makers to produce (cost)effective mitigation measures, much attention is given to enhanced weathering of natural minerals such as the magnesium-silicate olivine (Bearat, H. et al., 2006; Schuiling & De Boer, 2010; Hartmann et al., 2013; Malik, 2017; Beerling et al., 2018; Lehmann & Possinger, 2020). Olivine is one of the most common silicate minerals on earth, and its natural ability to react with atmospheric CO_2 to produce insoluble carbonates and dissolved bicarbonates can be exploited in a variety of applications (Schuiling and Tickiell, 2010; Bakker et al., 2011; Vink and Den Hamer, 2012; Duerr, 2013; Kersbergen, 2020; Vink, 2021; 2022).

However, reliable predictions of weathering rates, and consequently the quantification of CO_2 sequestration, are lacking. Reliable scenario analyses for olivine applications in terrestrial or aquatic conditions are currently hampered. Also, the environmental impact of released nickel, which is incorporated in the mineral is hardly studied and, at best empirically determined in laboratory tests. For scenario analysis and modelling purposes there is a need for better-founded proxy for weathering under realistic field conditions. Also, the effect of environmental conditions on weathering rates requires scientific attention.

Field plots were realized on the Deltares campus in Delft. A 2-year monitoring campaign was started to investigate the behaviour of olivine in soil. The mineral wollastonite, a Ca-silicate, was also used for comparison with the olivine Mg-silicates. Field plots were designed to investigate the effect of mineral types and various environmental variables on weathering, including the behaviour of released nickel.

1.2 Project organization

The project **CO-Action** (Entitled “Sustainable CO2-capture in infrastructure projects by olivine”*)* was commissioned by *Topconsortia voor Kennis en Innovatie (TKI), Topsector Energie Nieuw gas.* Project set-up, organisation, time schedule and experimental design was discussed with project partners, who also contributed financially and/or in-kind. The project lead was with Deltares Foundation.

Partners in the project:

- Rijkswaterstaat
- Wageningen Universiteit
- Van Dijk Maasland
- GreenSand

Project contributors:

- Universiteit Antwerpen
- Green Minerals

1.3 Project goals

1. Quantification of weathering rates of olivine and wollastonite under realistic field conditions;
2. Quantification of the effect on weathering rates by the following environmental variables: mineral type; moisture availability; mode of application; presence of vegetation.
3. Assess the risk of nickel release to the environment during weathering of olivine and wollastonite, including ecotoxicity.

2 Materials and methods

2.1 Mineral characterization

In this field study, we used two types of olivine (magnesium silicates) to quantify weathering rates in soil under various environmental conditions. Next to this, we used Canadian wollastonite, a calcium silicate, in a limited set-up to compare geochemical behaviour with the magnesium silicates. Olivine (dunite rock) samples were obtained from two different geographic origins: from Spain (Pasek mine) and from Norway (Sibelco). Both batches were obtained in a grain size of 0-3 mm. Although many laboratory studies use very fine fractions (100-300 µm) for their experiments, because of its rapid weathering potential, we specifically used this grain size because this fraction is widely used in (infrastructural) projects. Main reasons for this are the practical (easy to apply and handle) as well as the commercial (relatively cheap) benefits of this grain size.

The elemental composition of the Spanish and Norwegian olivine prior to the experiments was analyzed by X-ray fluorescence (XRF, Thermo ARL 9400; pressed pellets). Grain size distributions of the mineral batches were analyzed by laser diffraction (Malvern particle sizer 2000s) after ultrasonic treatment.

2.2 Field trials

2.2.1 Experimental design

Field tests were designed to quantify weathering rates under realistic conditions. From earlier model calculations (Vink & Den Hamer, 2012; Vink & Knops, in prep.), some insights were gained as to which parameters were dominant in the theoretical calculation of olivine dissolution. The composition and the amount of the mineral potentially dictates the release of elements as a result of natural weathering. Also, the availability of water determines the continuity of the chemical reaction in soil. Nest to this, we wanted to test the release and possible emission of nickel, and link this to plant uptake.

In the field plots, the following environmental variables were tested:

1. Spanish versus Norwegian olivine;
2. Mg-silicate (olivine) versus Ca-silicate (wollastonite);
3. Doses applied on top or mixed into the soil;
4. Planted and non-planted soil;
5. Rainfed versus wet conditions.

Ad 1. Olivine (dunite rock) samples were obtained from two different geographic origins: from Spain (Pasek mine) and from Norway (Sibelco).

Ad 2. Wollastonite was kindly provided Bob Vasily (Canadian wollastonite).

Ad 3. In two plots, olivine was added onto the top of the soil. In the other plots, the same dose was mixed into the soil (section 2.2.3).

Ad 4. Two plots were planted throughout the year, alternating winter barley and summer rye.

Ad 5. Three plots with wet conditions were built in a lower region. Approximately 30 cm of topsoil, adjacent to a water body, was scraped of with a bulldozer to lower the plot. Groundwater level established at approximately 25 cm below ground level.

Plots had an open connection to the surrounding site, so rainwater could drain freely from the plot. To be able to mass-balance the fate of secondary weathering products, such as Mg, Si, Ca and Ni, **mesocosms** were installed in the plots. These mesocosms were constructed of polypropylene 35 L barrels, and contained the same soil, dose of mineral, and were subjected to the same environmental variables as the plot they were installed in. A non-dosed plot was used as a reference site. See Figure 1.

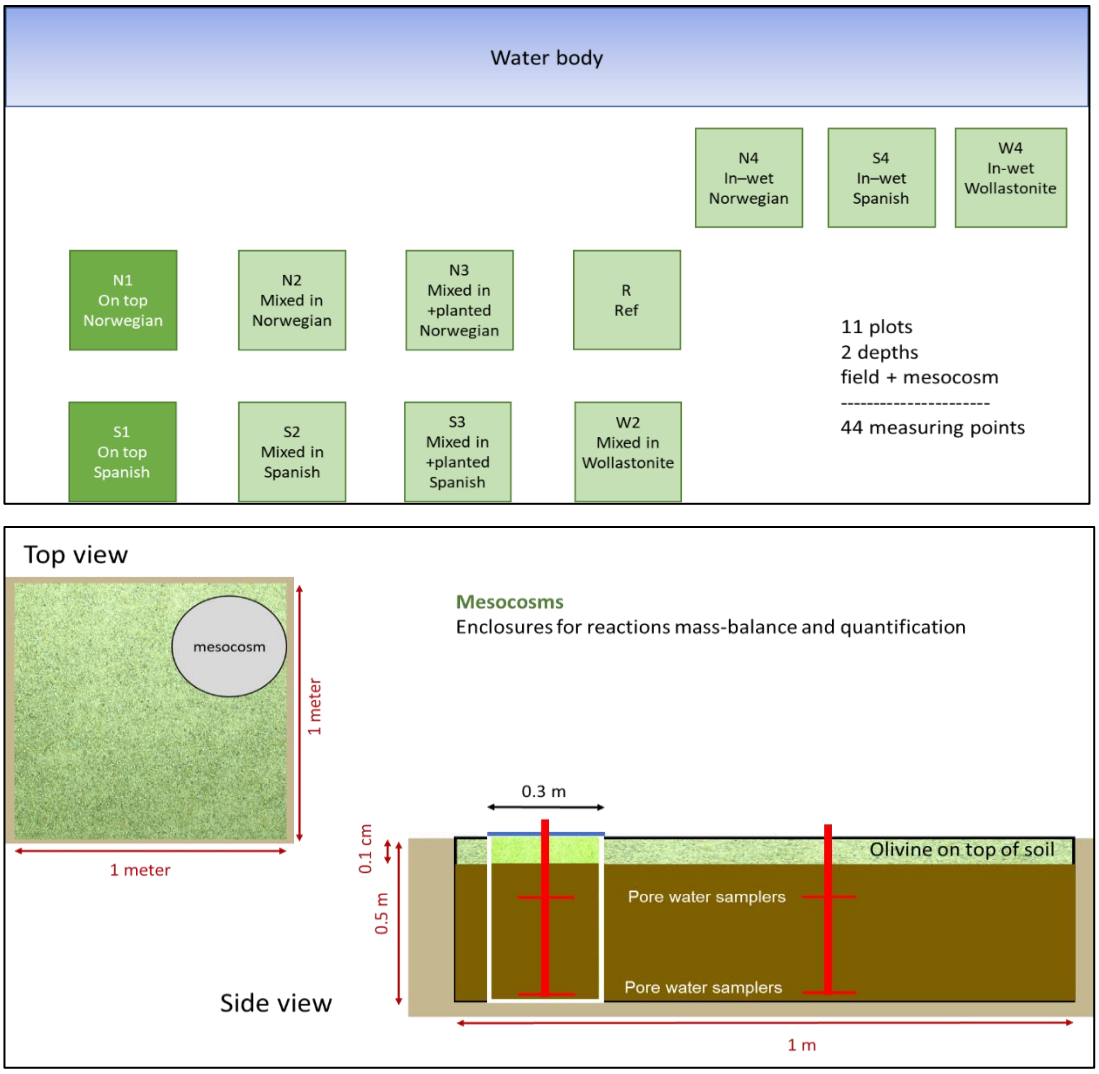

Fig. 1. Schematized experimental design of field plots. N= Norwegian olivine; S= Spanish olivine; W= wollastonite; R= Reference;

2.2.2 Soil composition

Main criteria for the design of the field plots was to use a homogeneous and representative soil composition, containing approximately 5% clay, 5% organic matter, and a slightly acidic pH. To achieve this, soil was composed and mixed by BVB Landscaping, De Lier, from the following components:

1. **Sand**. Sieved alluvial sand, grain size 150-250 µm.
2. **Compost**. “Green compost 0-15”, a mixture of leaf, wood, and grass.
3. **Garden peat**. “Tuinturf”, composed of >95% organic matter and a low pH.
4. **Clay**. Pristine river clay, sieved, quality certified.

The components were mixed in large tumblers, in ratios that would result in the required composition (see Appendix A for ratios, composition and quality). A total amount of 7 cubic metres (m^3) was composed and tested via analytical protocols. Five soil samples were mixed and analyzed in duplicate for composition.

On 22 April 2020, soil was mixed in mobile 150 L tumblers on site. Batches of 100 litres were mixed with olivine or wollastonite to acquire the desired dose (section 2.2.3; Appendix B). The excavated field plots were filled with the soil/mineral mixture, carefully burying the soil sensors for moisture and sampling in the field plots and mesocosms.

2.2.3 Dosage olivine

A literature survey was performed to get an indication of application dosages that were used in previous field or pot experiments. This yielded the following results:

Dietzen et al. (2018)	8 - 40 gr/kg soil = 6,4 – 32 kg /m^2 or 0.5 m^3
Taylor et al. (2015)	5 kg/m^2 in 10 cm = 31 gr/ kg soil = 25 kg/0.5 m^3
Amann et al. (2018)	22 kg/m^2
Renforth et al. (2015)	40 gr/kg mixed in = 32 kg/m^2
Ten Berge et al. (2012)	0.16, 0.82, 4, 20 kg/m^2

Main considerations in the establishment of a dose were grain size, environmental impact, and practicality/economics of potential large-scale applications. Ten Berge et al. (2012) showed that weathering rates decrease at higher doses, while increasing grain size decreases weathering potential dramatically (Renforth et al., 2015). Very fine grain sizes are unfavourable, both in terms of costs (grinding effort) and sustainability (CO_2-emission).

For the field plots, a dose of **4.04 kg ± 0.026** was used on a surface of 1 m^2, or mixed in 0.5 m^3 of soil (The variance is the measuring error of the weighing device). This dose is within the lower range of Dietzen et al. (2018) and Ten Berge et al. (2012). For a grain size, we selected a (cost-favourable) batch of **0 - 3 mm,** which is commonly used in large scale applications. See section 3.1.2 for size distribution analyses.

For Wollastonite, Haque et al. (2019; 2020a,b) used 3-20 $kg \cdot m^{-2}$ for soybean and 3-40 $kg \cdot m^{-2}$ for alfalfa in rooftop pot experiments. For comparison with the olivine plots, the same dose of 4.04 kg for wollastonite was used and mixed in 0.5 m^3 of soil.

From the composition of the various olivines (see section 3.1.3), a theoretical addition of the various elements to the soil (for example Mg, Ni) can be calculated via the olivine dose and stoichiometric dissolution of the minerals (see frame below). By definition, this theoretical addition assumes a homogeneous composition of the minerals and a homogeneous distribution in the soil. The calculated addition of these elements should coincide with measurements that were carried out via chemical destruction such as Aqua regia but not by a milder extraction such as Aqua nitrosa. See section 2.2.5.4 for further explanation.

Addition of dose per element

Dose of 4.04 kg/m^2 or kg/0.5m^3 or 417 kg dw soil = ***9.7 g olivine/kg dw soil.***
Added amount of magnesium (MgO via XRF) = 49% MgO (Norwegian) and 35% MgO (Spanish)
Corrected for Mg-MgO molar mass:
Norwegian: 0.6 x 49% x 9.7 g = ***2850 mg Mg/kg dw***
Spanish: 0.6 x 35% x 9.7 g = ***2040 mg Mg/kg dw***
Added amount of nickel to soil via olivine:
Ni content in mineral (via XRF) = 2110 mg/kg olivine (Norwegian), 1301 mg/kg (Spanish)
Added amount of Ni to soil:
(4.04 x 2110)/417 = ***20.4 mg Ni/kg dw soil*** *(Norwegian)*
(4.04 x 1301)/417 = ***12.6 mg Ni/kg dw soil*** *(Spanish)*

2.2.4 Plants

2.2.4.1 Field plots

Plant species were selected on the basis of two critera:

- Plants must develop extensive rooting in soil in a relatively short period;
- Plants are representative for agricultural crops.

Seeds of winter barley (winterrogge; *Secale cereale*) and summer rye (zomertarwe; *Triticum aestivum*) were acquired from the botanical garden in Utrecht. Seeds were sowed in two field plots (N3 and S3), including the mesocosm with the same dose, in the alternating seasonal periods (see Figure 2). Winter barley was sowed in the early autumns (August-September), summer rye was sowed in early spring (March-April) after harvesting the previous yield.

Fig. 2. Seedlings of winter barley (left) and full-grown summer rye on plots N3 and S3.

Plants were harvested, dried in a stove and stored. After ending of the field trials, whole plants including stem, leaf and seeds were grounded and analyzed according to the procedure of Temminghoff & Houba (2004).

2.2.4.2 Modelling nickel plant uptake

Next to the measurements described above, the uptake of Ni by plants was estimated via bioconcentration factors (BCF) acquired in scientific literature. A literature scan, specifically for nickel was performed to acquire uptake rates for BCF values, which were provided by

various review articles and field tests (Verkleij et al., 2000; Versluis & Otte, 2001; Schröder et al., 2006; Khan et al., 2015; Emurota & Onianwa, 2017; Eliku & Leta, 2017).
The equation from Schröder et al. (2005) was used to calculate the amount of Ni in the plant:

$$Ni_{Concentration\ in\ plant\ (mg/kg\ dw)} = Ni_{Concentration\ in\ soil\ (mg/kg)} \times BCF \qquad [1]$$

The BCF values for 41 different plant species were collected and used to calculate the Ni concentration in those plant species for various timesteps. Nickel concentrations in pore water were derived periodically from the various field plots.

2.2.5 Measurements

2.2.5.1 Continuous moisture content

Data on soil moisture content are crucial to interpret the measurements on the weathering of olivine: pore water concentrations depend on saturation status that varies with depth.To achieve this, sensors were installed at - 0.25 m below surface, both in the field plot and in the mesocosms. Sensors were installed horizontally and were inserted into the soil via the side of a 30 cm hole. In this way, air pockets around the sensors were avoided. A total of 22 sensors (2 per plot, 11 plots) were installed in this way, and monitored using a data logger.
Sensors were acquired from Meter (Decagon). Type ECH$_2$O EC5 sensors were used (see Table 1 and Figure 3). Soil moisture is detected by applying a current between the fork-shaped electrodes of the sensor. The electrical current is measured, including soil, air and water phase. Sensors use calibrating curves for soil types/components to calculate the in-situ moisture content. The EC-5 is less sensitive to variation in texture and electrical conductivity because it runs at a much higher measurement frequency. Therefore, its general calibration equation applies for all mineral soils up to 8 dS/m saturation extract. For the field plots, a mineral-soil-calibration curve was applied by the datalogger to convert the data to volumetric water content (m^3/m^3).

Table 1: Specifications of soil moisture sensor ECH$_2$O EC5.

Volumetric Water Content (VWC)	
Resolution	Range 0%–100%
Accuracy	0.001 m^3/m^3 VWC in mineral soils, 0.25% in growing media
Generic calibration	±0.03 m^3/m^3 typical in mineral soils that have solution EC < 8 dS/m
Medium-specific calibration	±0.02 m^3/m^3 in any porous medium (± 2%)

Fig. 3. Moisture sensors, installation and on-site monitoring via dataloggers.

2.2.5.2 Pore water collection

Pore water was collected periodically with 0.45 µm permeable macro-rhizon samplers (Eijkelkamp BV) of 20 cm length, with an effective sampling length 9 cm and a diameter of 4.5 mm. Rhizons were buried horizontally in two depths, at 10 cm and 30 cm below soil surface level, while filling the plots and mesocosms with the homogenized soil (see Figure 4). The rhizon samplers were connected with sampling tubes (1 m length) and were fixed in PVC tubes for long-term protection. Pore water was sampled periodically by using a LuerLock syringe of 50 ml, applying a vacuum to the sampler. Pore water was collected in boriumsilicate vials. Samples for metals plus macro-ions, DOC, and alkalinity were collected in separate sampling vials. The pH was measured on-site in the pore water vials directly after sampling using a calibrated electrode for pH 4-7-11.

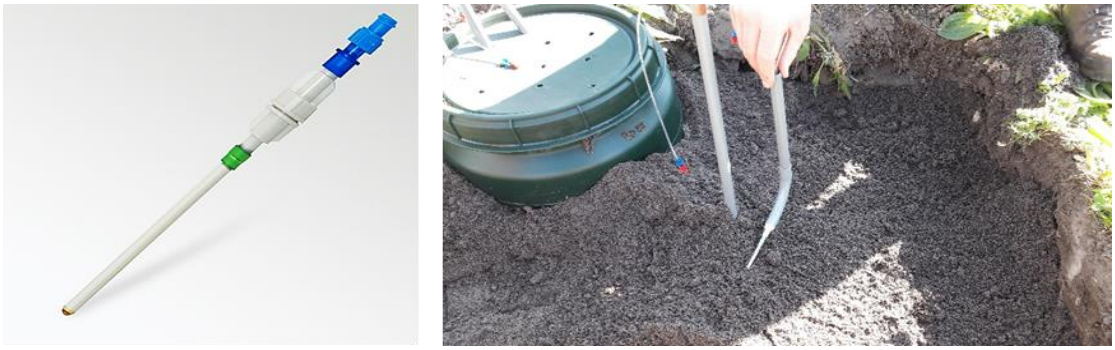

Fig. 4. Rhizon pore water sampler and installation in field plots.

The volume of pore water that could be extracted at the time of sampling depended on the moisture content at that time. Depending on the volume that could be extracted from the plots at the time of sampling, pore water samples were analysed in the following priority:
1) Secondary weathering products Mg, Ca, Fe, Ni, Si, P and S via ICP-MS (Perkin Elmer NexION 2000);
2) Total alkalinity (Metrohm - 665 Dosimat).
3) Total organic and inorganic carbon (via TC and acidification step; Shimadzu TOC-L).

2.2.5.3 Rainfall and temperature

Daily data on local precipitation and temperature were obtained from a 24-h atmospheric measuring station in Delft (www.hetweeractueel.nl/weer/delft/history) for the period of May 2020 till May 2022.

2.2.5.4 Soil chemical extractions

Soil samples were taken from the bulk batch in triplicate, homogenized, and subjected to various chemical extractions varying in ionic strength.
After two years, the plots were sampled individually. From each plot, including the mesocosms, 5 samples were taken, mixed, and subjected to chemical extractions.
The following extractions were applied:

1. Aqua Regia: Destruction of the soil matrix conform protocol NEN 6961:2014. A soil sample is extracted with a 3:1 HCl (35%) and HNO_3 (65%) acid mixture and heated for a minimum of 2 hours at 175 °C. This aggressive procedure dissolves all organic and inorganic components, including (part of the) silicate structures. The analysis is a measure of total content of elements in the sample.
2. Aqua Nitrosa: Extraction with a dilute (0.43M) HNO_3 nitric acid solution conform protocol ISO 17586:2016. This relatively mild extraction is a measure of the “chemical and biological reactive fraction” of elements (Groenenberg et al., 2017), also interpreted as “potentially bioavailable”.

2.3 Modelling set-up

2.3.1 Weathering reactions

The weathering reaction of olivine is thermodynamically irreversible, and is generally described by:

$$Mg_2SiO_4 + 4CO_2 + 4H_2O \rightarrow 2Mg^{2+} + 4HCO_3^- + H_4SiO_4 \qquad \Delta H = -84\ kJ/mol \qquad [2]$$

The reaction may be followed by the precipitation of Ca/Mg-carbonates. Molar conversion is dependent on environmental parameters such as pH and temperature. Mineral weathering may be described by the shrinking core model (SCM), which is widely used to describe situations in which solid particles are being consumed either by dissolution or chemical reaction and, as a result, the amount of the material being consumed is declining in size (Gbor & Jia, 2004). The SCM-model is used, for example, in pharmacokinetics and in dissolution-leaching studies. Assumptions of the SCM were described by e.g., Safari et al. (2009): particles are spherical, particle diameters shrink uniformly, and temperature remains constant.

Although the SCM model can in principle be applied for mineral weathering, there are practical limitations (Vink & Knops, in prep.). Weathering studies almost always assume particles to be monodisperse: i.e., all particles have a uniform (P50) size. Grinded batches of olivine have no uniform size, but show a large variety of particle sizes ranging from some micrometers to millimeters. Hangx & Spiers (2009) suggested that disregarding this particle size distribution may lead to large variations of calculated weathering rates.

To overcome the practical limitation of the SCM-model, we developed the model OWCS V6.3 (Olivine Weathering and CO_2 Sequestration) in order to quantify mineral weathering. The model calculates pH-dependent dissolution of olivine, its CO_2 sequestration capacity, and the release of magnesium and nickel. The model is coupled to a chronic toxicity model, based on Biotic Ligand Models, to allow for site-specific risk assessment of nickel (See section 2.3.2.2). This sequence of modelling (Figure 5) allows to interactively quantify:
i) size-specific weathering rates of olivine;
ii) the amount of carbon dioxide that is being consumed in the process;
iii) and the risk assessment of release of nickel (Ni) which is incorporated in the mineral.

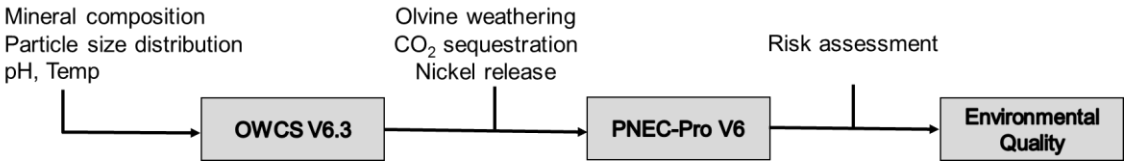

Fig. 5. Procedure of coupling of weathering model, CO2 calculation and nickel risk assessment.

Many studies have reported on the relationship between mineral dissolution rate (r) of olivine and pH (Pokrovsky and Schott, 2000a,b; Wogelius & Walther, 1991), temperature (White et al., 1999), mineral saturation (Nagy et al., 1991; Wogelius & Walther, 1992), and surface area (Holdren and Speyer, 1985; Palandri and Kharaka, 2004). Olsen (2007) found a strong pH relationship and clear break near pH=6:

$$Log\ r_{pH<6} = -0.48\ pH - 6.9 \qquad [3]$$
$$Log\ r_{pH>6} = -0.18\ pH - 8.8 \qquad [4]$$

The reaction rate (r) and rate constant (k) are described using the generic Arrhenius function:

$$ln\ k_T = ln\ k_{T.R} - E_a / R\ (1/T-1/T_r) \quad [5]$$

in which T is temperature, R is the gas constant, and E_a is the activation energy. We adopted this principle to each single size fraction of the mineral batch. Using the analyzed grain size distribution, dissolution rates were calculated for each given time step. The amount of olivine added (to soil) is coupled to the surface area of the plots on which the application was done in order to calculate dissolved concentrations in pore water. The total volume of pore water is derived from the moisture content from which concentrations in soil is calculated.

Dissolution was calculated for each time step over 40 years. In each following time step, the remaining mass from the previous time step is subjected to weathering until a fraction is depleted. The following model conditions were applied: Rainfall and temperature was used from measurements (section 2.2.5.3). The pCO_2 was initialized at 410 ppm (coinciding with atmospheric concentration), although soil-CO_2 may be higher. Both the particle size distribution and the applied dose of olivine are used to calculate the mass of each fraction, resulting in the reduction in diameter of particles and, consequently, mass loss in each sequential time step. The mineral composition (XRF) of the applied olivine is used for input to calculate released mass of elements per volume unit. Using molar conversion from the weathering equation [2] presented above, the sequestered CO_2 is calculated. Released Mg and Ni is calculated and converted from solid to dissolved phase using the Biochem-Orchestra database for chemical partitioning (Vink and Meeussen, 2007).

Statistical comparison between plots for elements Mg, Ca, Cr and Ni was carried out in Excel statistical data analysis, using paired T-test ($p<0.05$ two tailed). The term Δ (delta) is used for the difference between a (mean) value minus the reference value from plot R (= reference).

2.3.2 Nickel risk assessment

2.3.2.1 Environmental Quality Standards

Generic chemical quality standards exist for various environmental compartments, like soil, aquatic sediment, and groundwater. These standards are valid for all conditions, regardless of pH, composition, etc. Table 2 summarizes the EQS for nickel in The Netherlands.

Table 2. Environmental quality standards for nickel for various environmental compartments.

Compartment	Value	EQS
Soil	35 mg/kg	Background value (Achtergrondwaarde)
	39 mg/kg	Maximum value Urban (Max waarde functieklasse Wonen)
	100 mg/kg	Maximum value Industry (Max waarde functieklasse Industrie)
Sediment	44 mg/kg	Maximum Tolerable Risk (MTR)
Surface water	4 µg/L	Year average (JG-MKN)
	34 µg/L	Maximum permissible value (MAC-MKN)
Ground water	15 µg/L	Target value undeep (Streefwaarde ondiep)
	20 µg/L	Threshold value (Drempelwaarde)
	75 µg/L	Intervention value (Interventiewaarde)
Drinking water	20 µg/L	Drinking water (Drinkwater norm)

Generic quality standards are also known as a “first-tier assessment”. Although EQS have their protective purpose, they are, however, not good indicators for actual risks at various environmental conditions. Environmental risks are addressed with “higher-tiered” methods, that take the chemical and bioavailability of a compound into account.

2.3.2.2 Biotic Ligand Models

Ecotoxicological consequences of nickel release due to olivine weathering was addressed with higher-tiered risk assessment using Biotic Ligand Models, BLM (EC, 2011; Verschoor et al., 2011; Rüdel et al., 2015; EC, 2016). BLMs are sophisticated risk assessment tools that compute toxicological “no-effect” concentrations for metals, accounting for chemical speciation and toxicity based on semi-mechanistic processes and toxic endpoints for biota (e.g., Rüdel et al., 2015). Competitive interactions between metals and macro-ions (Ca, Na, Mg) for biotic ligand-binding and complexation directly relate water composition to metal toxicity. BLMs for Ni are well studied and were published in scientific literature since over two decades. Their value for regulatory frameworks is recognized (SCHER, 2010; EC, 2011) and laid down in European Technical Guidance (EU, 2019) for water quality assessment of metals.

The nickel-BLMs account for chemical speciation (the distribution of a metal over adsorbing and complexing phases; Vink, 2002; 2009) and water composition (e.g., dissolved organic matter, pH, macro-ions). Based on these environmental variables, free metal activities (FIA) are calculated and No-Effect concentrations (PNEC) are derived using the concept of Species Sensitivity Distribution (EU, 2008) for biota of various trophic levels. For nickel, the toxicity database consists of 233 chronic toxicity data of 28 aquatic species. Simplified routines of the BLM models (Verschoor et al., 2017) were used in the software tool PNEC-pro (Vink et al., 2016) and coupled to the OWCS weathering model. In this way, release and ecotoxicological risk assessment of nickel was directly coupled to time-dependent weathering of olivine.

3 Results and discussion

3.1 Soil and mineral characterization

3.1.1 Soil characterization

Composition of the initial homogeneous field soil is shown in Table 3. The soil is characterized as a loamy sand, and is slightly acidic.

Table 3. Initial composition of homogeneous field soil (section 2.2.2).

Parameter	Value
Silt (<16um)	6.1 ± 0.3
C elemental (g/kg)	46.3 ± 0.4
N elemental (g/kg)	1.47 ± 0.8
pH	6.0
Dry weight (kg/m^3)	629
Dump weight (kg/m^3)	835

3.1.2 Soil particle size distribution

Particle size distribution of the initial homogeneous field soil is shown in Table 4.

Table 4. Particle size distribution of initial homogeneous field soil (Section 2.1).

Particle Diameter µm	Mean Volume % <	St. dev. Volume % <
2	1.88	± 0.16
16	6.10	± 0.37
50	9.82	± 0.82
63	10.85	± 0.92
125	16.3	± 0.71
250	55.85	± 0.07
500	90.4	± 0.85
1000	97.75	± 0.78
2000	100	± 0

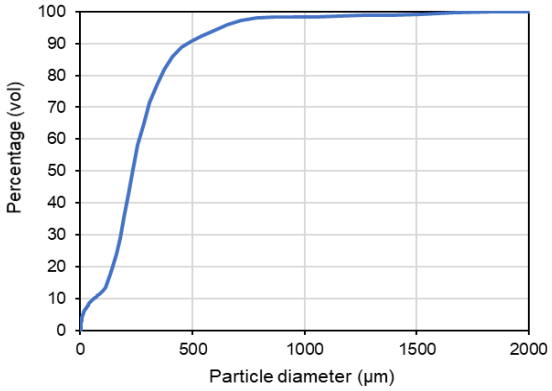

3.1.3 Mineral characterization of olivine and wollastonite via XRF

Table 5 shows the results of elemental X-ray fluorescence of the two types of olivine and wollastonite. The values are averaged duplicates which showed little variations in all cases.

The composition of the olivine types is slightly different. The olivine from Norway contains more Mg and Ni compared to the Spanish olivine. The Spanish olivine has a slightly higher Fe content and contains more Al, Ca, V, Sr and S compared to the olivine from Norway. Total mass recovery of the Spanish olivine is slightly lower than the Norwegian, possibly due to a higher weathering state and/or amorphous $MgCO_3$ precipitation which is not detected by XRF.

Table 5 . Geochemical composition of Norwegian and Spanish olivine and wollastonite, derived from XRF.

	Mass %					
	Norwegian olivine		Spanish olivine		Wollastonite	
SiO2	41.08	± 0.02	40.86	±0.01	56.22	±0.17
MgO	49.00	± 0.05	35.11	±0.04	3.70	±0.24
Fe2O3	7.20	± 0.03	7.89	±0.01	1.91	±0.06
Al2O3	0.35	± 0.00	2.82	±0.01	5.86	±0.03
MnO	0.10	± 0.00	0.13	±0.00	0.04	±0.00
Na2O	0.00	± 0.00	0.06	±0.01	2.08	±0.01
TiO2	0.00	± 0.00	0.05	±0.00	0.21	±0.00
CaO	0.08	± 0.01	2.15	±0.05	23.93	±0.20
K2O	0.01	± 0.00	0.08	±0.01	2.27	±0.03
P2O5	0.00	± 0.00	0.01	±0.00	0.08	±0.00
Total	97.8	± 0.11	89.16	±0.01	96.29	±0.09
	Elements (mg/kg)					
Cr	2201	± 99.8	2281	±62.4	24.1	±3.5
Ni	2110	± 105.5	1301	±0.6	20.6	±2.8
Sr	9.97	± 0.00	32.2	±0.64	1591	±14.7
Zr	126.2	± 7.8	158.8	±1.3	180.7	±34.7
Ba	0.00	± 0.00	35.8	±13.5	321.1	±2.8

3.1.4 Mineral particle size distribution

Figure 6 shows the distribution of particle sizes of the minerals that were used in the field experiments. Although the commercially acquired fractions are marketed as “0 - 3 mm”, both batches do have particles that are larger than 3 mm, with a maximum of approximately 10 mm.

The Spanish olivine has a slightly higher mass fraction in the ultrafine fraction (< 250 µm) and in the coarse fraction (> 2 mm), but the overall median value of the grain size of the Norwegian olivine is slightly lower than for the Spanish olivine. Wollastonite has a large fraction of ultrafine grains (65% is < 250 µm).

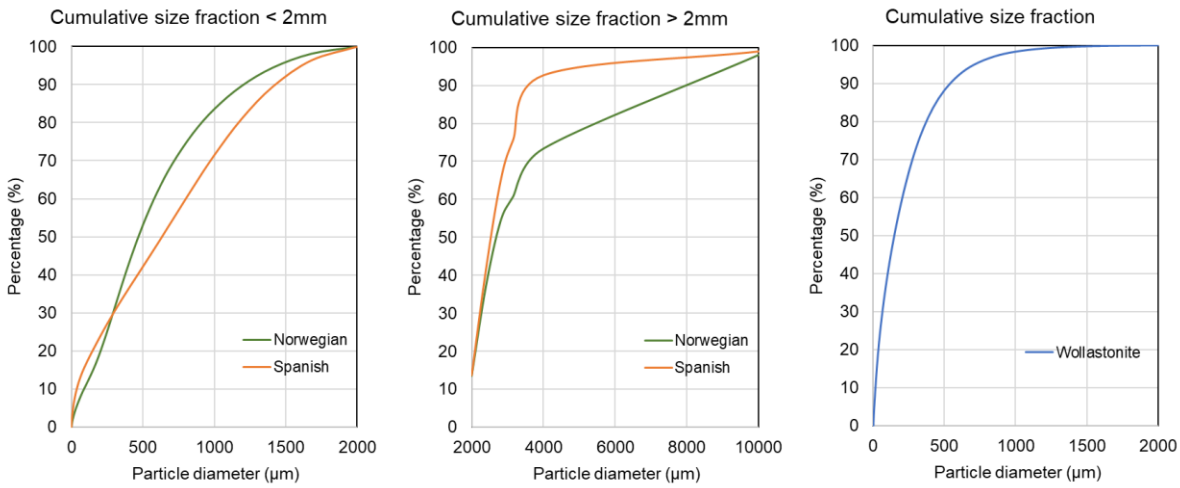

Fig. 6. Particle size distribution of Norwegian and Spanish olivine, and wollastonite.

3.2 Rainfall and temperature

Figure 7 shows the data of daily precipitation and temperature over the monitoring period of two years. Spring 2020 started very dry, with almost no moisture in May, but precipitation started to pick up in June. Table 6 shows the cumulative precipitation over various periods during the two-year experiment. Average values during the experiments did not deviate from average annual data.

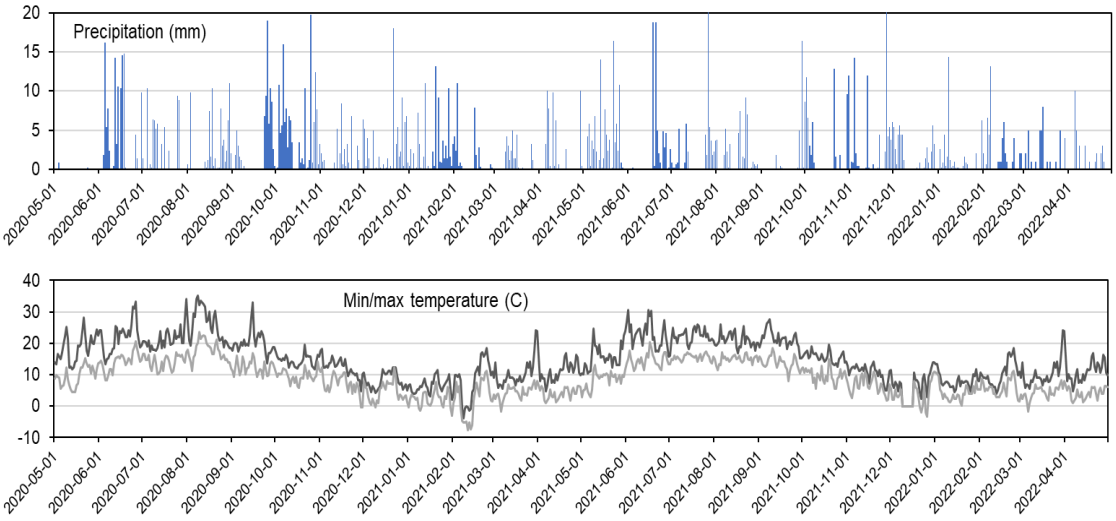

Fig. 7. Precipitation (top) and min/max temperatures over the 2-year period.

Table 6. Cumulative precipitation over experiment periods.

Period	Precipitation (mm)
May – Dec 2020	599
Jan – Dec 2021	697
Jan – May 2022	164

3.3 Moisture content

Figure 8 and Appendix C shows the moisture content, measured continuously with buried sensors in field plots and mesocosms.

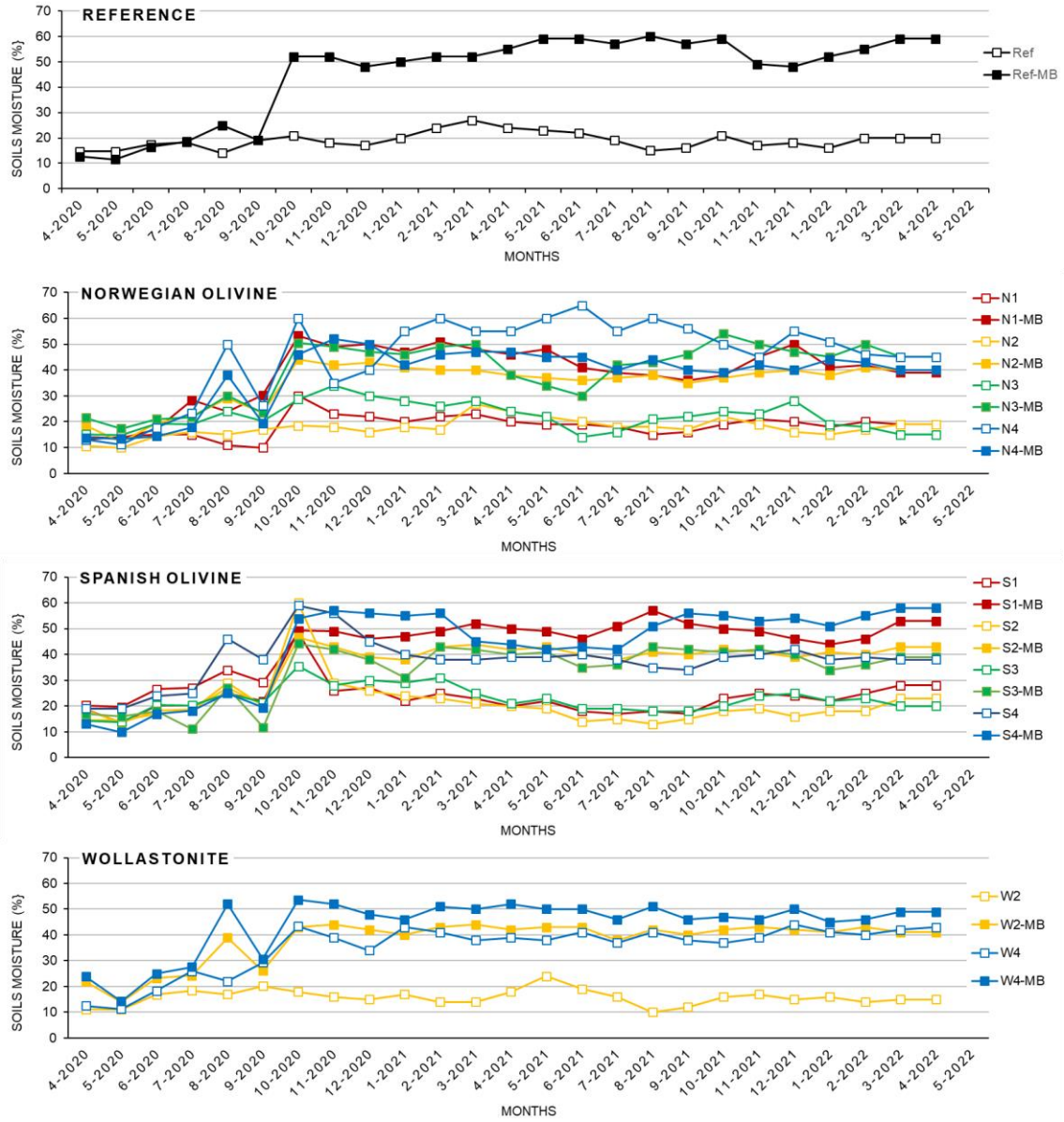

Fig. 8. Moisture content in field plots (open markers) and mesocosms (closed markers). Ref = Reference plot; S = Spanish olivine; N = Norwegian olivine; W = Wollastonite; MB = mesocosm.

After a relatively dry start in spring, moisture content normalized from June 2020 and onwards. As intended, the wet plots S4, N4, and W4, have an almost systematic higher moisture content than plots 1-3 and have 50 to 100% higher moisture contents. The rather high values of wet plot N4 is yet unexplained.

The same applies to the mesocosms: moisture content in mesocosms is approximately 50-100% higher than in open field plots, caused by the lack of natural drainage. As a consequence, the higher moisture content in mesocosms may affect the mineral weathering rate compared to the open plots. This can be verified by normalizing the pore water concentrations of elements by a “uniform” moisture content.

3.4 Pore water concentrations over time

Pore water collection was performed periodically as explained in section 2.2.5.2. Analysis of elements was prioritized depending of the amount of collected volume. In most cases, pore water volumes were sufficient to analyze the elements released from mineral weathering (Mg, Si, Ca, Ni and other elements), but not always for alkalinity and dissolved (in)organic carbon. The analysis of these components requires additional and separate volumes (5-20 ml), which are not always available from soil pore water extractions via Rhizon samplers.

Next to this, alkalinity measurements in open field systems are extremely challenging. The equilibrium between dissolved and atmospheric CO_2, the amount of rainfall, the water saturation of soil, and the (daily, temperature-dependent) dissolution and sorption of alkaline species, result in highly fluctuating concentrations of HCO_3^- and CO_3^{2-} in pore water. These temporal fluctuations, which obviously occur under field conditions, makes the quantification of dissolved inorganic carbon and the direct link to mineral sources, very difficult. For this reason, the alkalinity and inorganic-C measurements were not used for the interpretation of weathering rates.

All pore water measurements from field plots, mesocosms and adjacent surface water are collected in Appendix D.

3.4.1 pH

During pore water collection, pH was measured on-site immediately after collection to avoid alterations during collection or storage. Figure 9 shows a summary of all plots, and the adjacent surface water of the wet plots (all data in Appendix D). The values represent average values of pore waters collected from a specific plot, including the mesocosms.

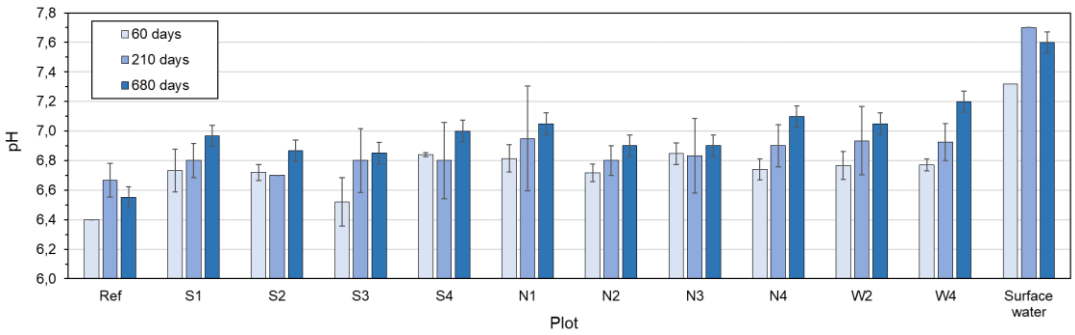

Fig. 9. Averaged pH in field plots and mesocosms at 60, 210 and 680 days. Vertical bars are standard deviations (n=4) of averaged measurements.

Figure 9 shows that all plots have a slight increase in pore water pH compared to the reference plot. Differences between olivine source (Norwegian or Spanish) are statistically not significant ($p<0.05$). The wet plots (N4, S4, and W4) show slightly higher and increasing pH-values compared to the dry plots. This may be explained by three reasons: 1) Mineral weathering in wet plots is higher than in dry plots; 2) The influence of adjacent surface water with a relatively high pH; 3) Differences in organic matter decomposition rates and pathways, i.e. anaerobic production of alkalinity.

In general, the applied mineral dose of 4 kg/m^2 results in a pH-increase in the pore water of approximately 0,2 to 0,5 pH-unit over the measured period.

Alkalinity measurements in open field systems are extremely challenging. The equilibrium between dissolved and atmospheric CO_2, the amount of rainfall, the water saturation of soil, and the (daily, temperature-dependent) dissolution and sorption of alkaline solid phases,

result in highly fluctuating concentrations of HCO_3^- and CO_3^{2-} in pore water. These temporal fluctuations, which obviously occur under field conditions, makes the quantification of dissolved inorganic carbon and the direct link to mineral sources, very difficult. For this reason, the alkalinity and inorganic-C measurements were not used for the interpretation of weathering rates

3.4.2 Weathering products Mg, Si, Ca

All measurements in time, depth, in individual plots and mesocosms are presented in Appendix D. To visualize differences between the studied minerals and applied treatments, some representative results are shown below. The shown trendlines between data points are interpolated weighed averages, accounting for the different time periods between measurements.

3.4.2.1 Open field plot versus mesocosm

Figure 10 shows some examples of the time-dependent concentrations of magnesium, silica and calcium for the selected experiments. For representative examples we selected the dry, unplanted, mixed-in field plots for this figure in order to discard masking effects of treatments.

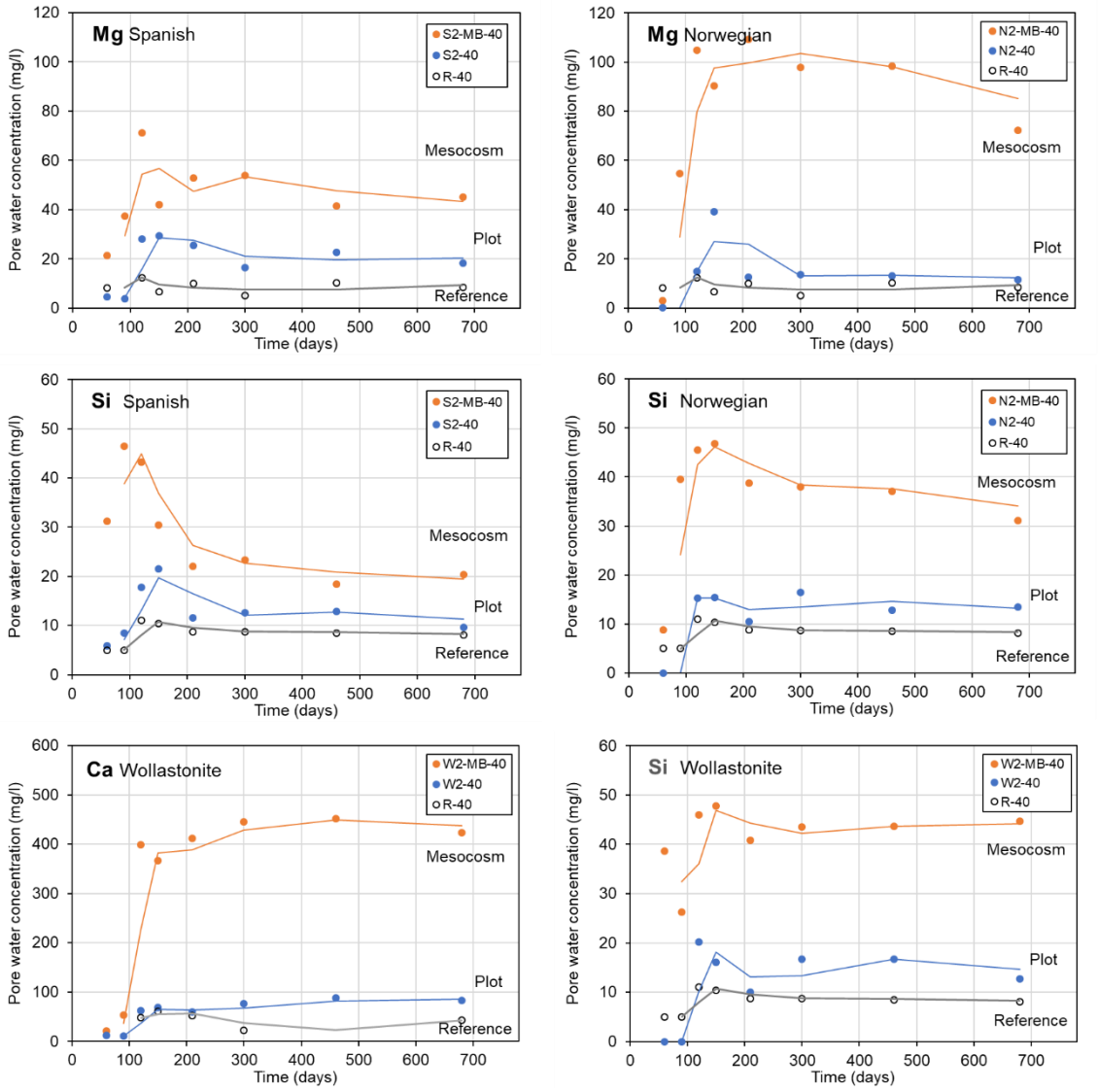

Fig. 10. Pore water concentrations of Mg, Si and Ca over time in open field plots and mesocosms (MB).

Results clearly show that Mg and Si (and Ca for wollastonite) are elevated compared to the concentrations measured in the reference. Concentration ratios of Mg and Si coincide with the molar ratio (Mg_2SiO_4) of the mineral's composition. This is strong evidence that the elevated Mg and Si concentrations are the result of weathering, and release of these elements from the mineral to pore water.

Without exception, concentrations in mesocosms are higher than in open field plots, possibly for two reasons:

1. No natural drainage occurs from mesocosms, as opposed to the open plots where compounds may migrate to subsoil with drainage water;
2. Moisture content in mesocosms is generally higher than in open plots, therefore possibly promoting chemical reaction.

Mesocosm concentrations of Mg appear to be significantly higher for the Norwegian olivine than for the Spanish olivine. This may possibly be attributed to the chemical composition of the two minerals. Norwegian olivine has a MgO content of 49.0 %, while Spanish olivine has a MgO content of 35.1 % MgO. Also, Norwegian olivine has a finer grain size distribution, which may promote faster weathering. The fact that Si-concentrations are also higher (with comparable SiO composition of the two minerals) also strongly points into the direction of faster weathering.

Wollastonite shows a significant Ca- and Si-release, particularly in the mesocosms and in the wet plot (see following sections). Dissolution of particulate carbonates (e.g., $CaCO_3$) may be largely excluded for this slightly acidic soil, although some minor sources may be present in the clay fraction.

3.4.2.2 Olivine applied on top versus mixed in

Figure 11 shows some examples of the time-dependent concentrations of dissolved magnesium and silica for the two olivines. Plots 1 and 2 were used for a direct comparison of concentrations with depth, at -10 cm and -40 cm below the surface. Since no significant differences were observed for the Norwegian plots, only examples are shown only for Spanish olivine.

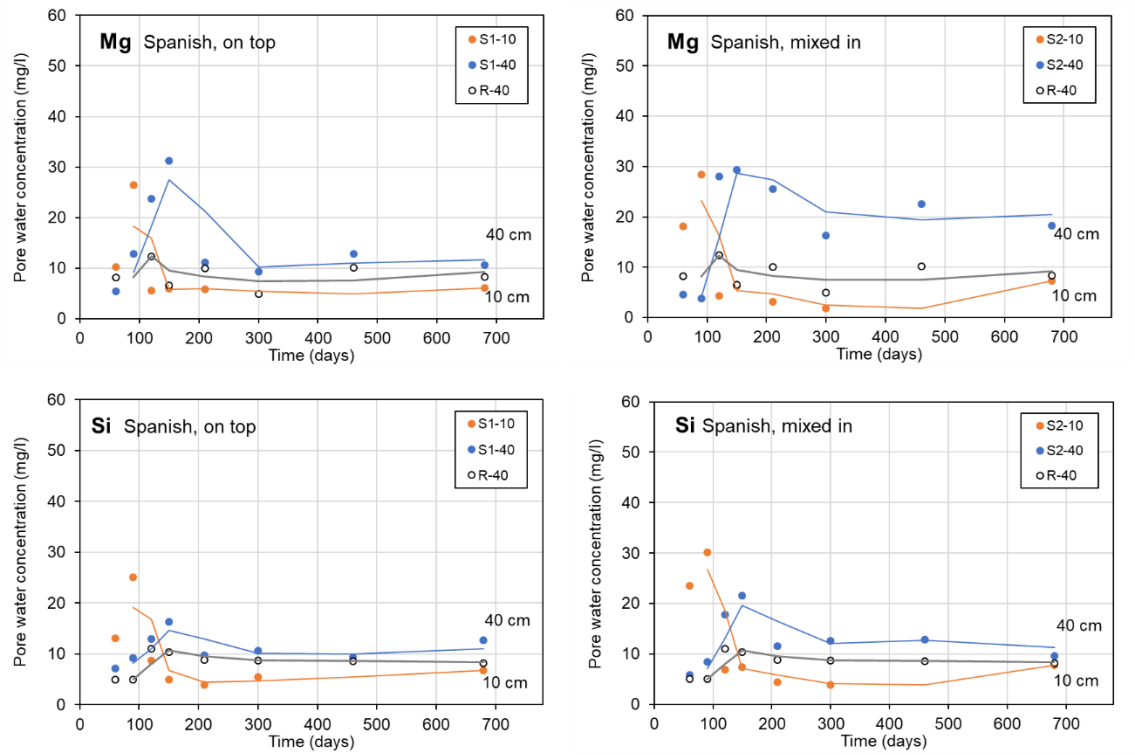

Fig. 11. Pore water concentrations of Mg and Si over time in open field plots, with a surface-application (plots 1) and a mixed-in treatment (plots 2), for two depths.

Concentrations of Mg and Si are in all cases higher in the deeper (-40 cm deep) zone than in the shallow (-10 cm deep) zone, even in the plots where olivine is applied on top. Possible reasons of this are:

1. The top layer of the soil dries out faster in natural conditions than the deeper layer, so chemical reactions are periodically limited;
2. Leaching of Mg and Si occurs from topsoil to subsoil.

3.4.2.3 Dry versus wet conditions

Figure 12 shows some examples of the time-dependent concentrations of Mg, Si and Ca for the various treatments. Plots 2 and 4 were used for direct comparison, since both plots have a mixed-in application.

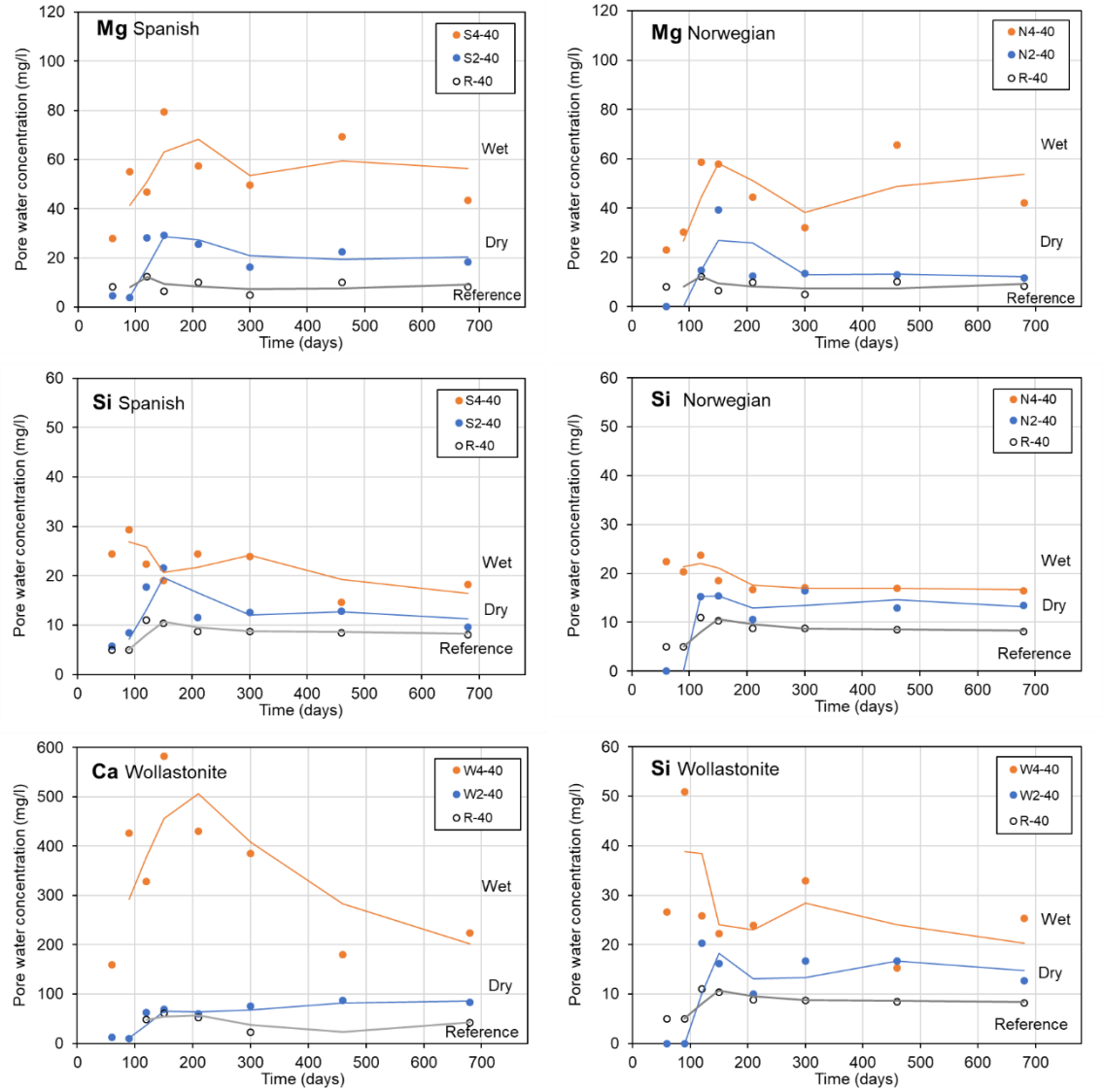

Fig. 12. Pore water concentrations of Mg, Si and Ca over time in open field plots, dry (plots 2) and wet (plots 4) conditions.

In all cases, concentrations in the wet plots of Mg, Si and Ca are elevated compared to the dry plots (factor 2 to 3). The effect is most pronounced for wollastonite, where the Ca concentration is elevated up to a factor of 4 to 5 in the first year.

These elevated concentrations do not necessarily indicate that weathering rates in wet conditions are also a factor of 2 to 3 higher than in dry conditions. Wet plots typically have a hydrological regime that may not allow leaching to occur in the same manner as in the dry plots. The saturated zone in the wet plots regulated by the canal is fairly stable at -35 cm. This may inhibit the transport of dissolved elements to the surrounding environment. Also, it may reduce weathering rates if concentrations become oversaturated and secondary mineral precipitation starts to take place.

3.4.2.4 Planted versus non-planted

In plots 3, alternating summer rye and winter barley was grown throughout the years. Plots 2 were kept clean and any infestations of vegetation was removed periodically by hand. Figure 13 shows examples at 40 cm depth in both plots for both olivine minerals.

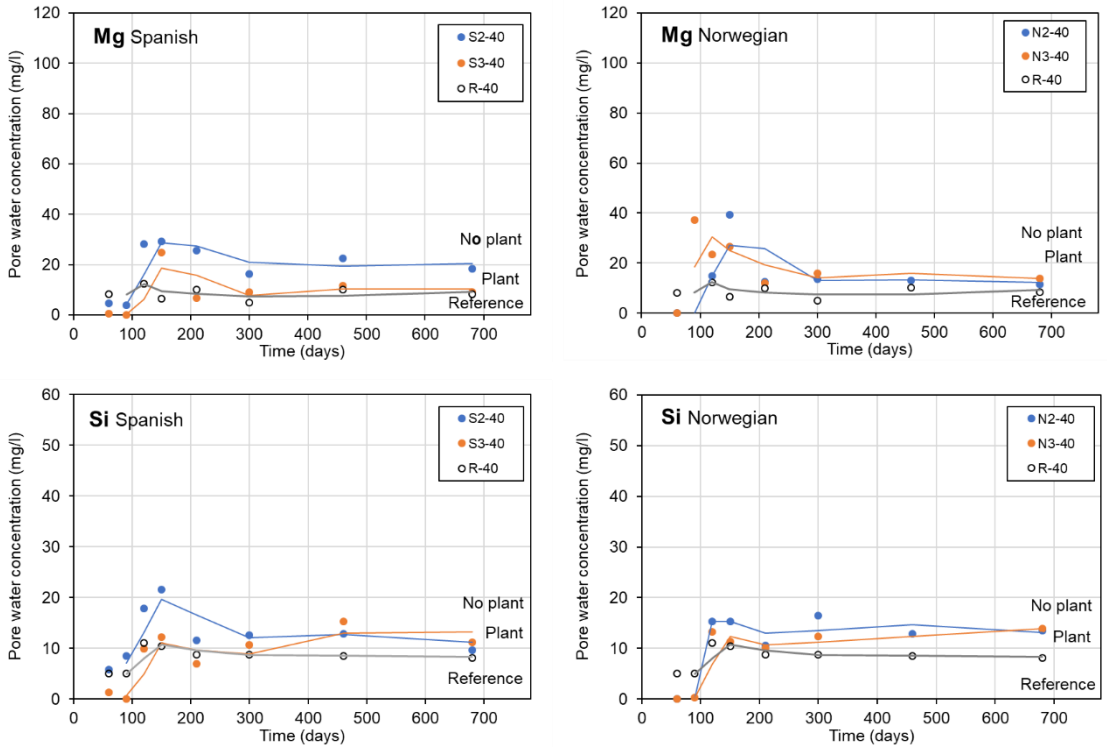

Fig. 13. Pore water concentrations of Mg and Si over time in open field plots, non-planted (plots 2) and planted (plots 3).

It was expected that the presence of plants may affect the soil characteristics of the field plots in various ways that may potentially affect mineral weathering:

- Intensive rooting may increase the soil permeability and drainage;
- Intensive rooting may increase the soil pCO_2;
- Intensive rooting may decrease pH;
- Plants will take up Mg as a nutrient;

Differences in pore water concentrations between planted and non-planted treatments appear to be small, although the concentrations of Mg in the Spanish plots (S2 and S3) are statistically different ($p < 0.05$). This could be an indication that plants have extracted a portion of the (available) Mg from soil. However, this is not in line with the results of the chemical extractions of the soil (see section 3.6).

3.4.3 Nickel

Nickel concentrations in pore water received much attention in this study, since it is considered a priority pollutant according to the Water Framework Directive (WFD). Main priority in this study was to investigate whether nickel would exceed environmental quality standards after the application of olivine. This is the first check, also indicated as “compliance”. Consequently, risk assessments are discussed (“second-tier”) to evaluate possible toxicity of nickel to biota. Figure 14 summarizes all measurements of nickel in pore waters of all plots.

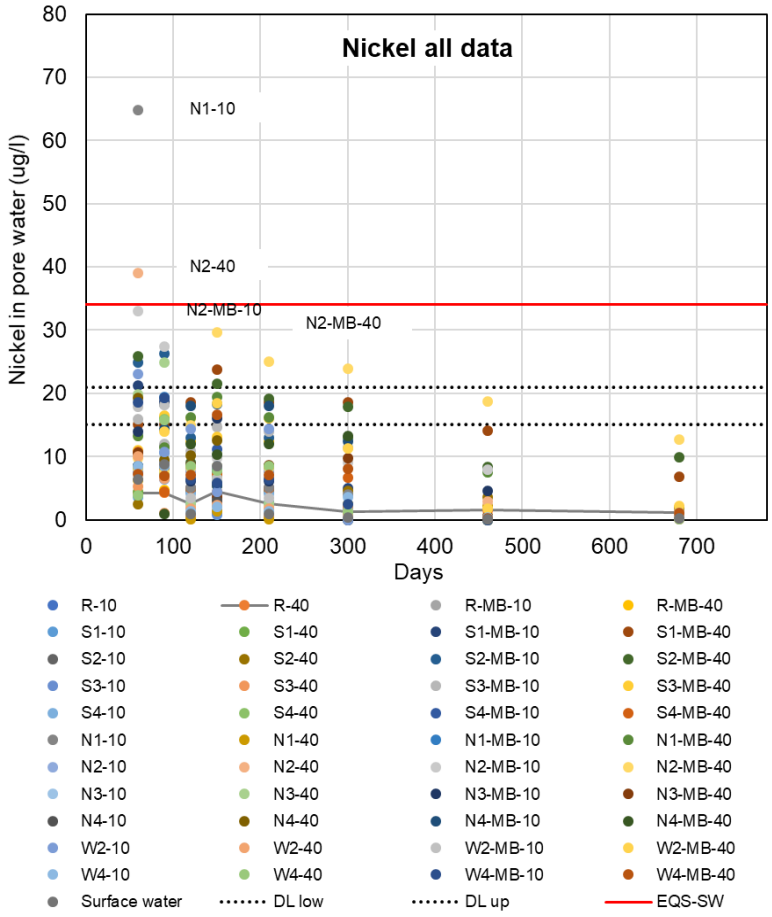

Fig. 14. Nickel concentrations over time in pore water of field plots and mesocosms. Dotted lines are upper and lower analytical reporting limits. The Red line is the WFD-environmental quality standard of nickel in surface water.

Results show that, compared to the reference plot, nickel concentrations in pore waters are elevated. Also, 96 % of all Ni measurements are below the analytical upper reporting limit (100 % of all wollastonite). Only 2 measurements exceed the environmental quality standard (EQS) of surface water, and only after the first 60 days after application. These are N1-10 (Norwegian olivine, top application) and N2-40 (Norwegian, mixed-in). After this period, no exceedance of the EQS was observed.

The 5 highest Ni-concentrations recorded are all from plots with Norwegian olivine. Norwegian olivine has a higher nickel content than the Spanish olivine (2110 versus 1301 mg/kg), which becomes available upon weathering. The decrease of nickel concentrations over time is a result of sorption to soil matrix, hence extracting nickel from pore water and binding is to soil constituents as organic matter, clay, or inorganic complexes. Vink & Knops (2022, in prep.) showed that in the first period of weathering, most nickel is released from the ultrafine fraction (< 250 µm) which is dissolved after some time. Release from the larger fractions is slower and possibly coincides with the rate of sorption to soil constituents.

3.5 Plants

From plots N3 and S3, winter barley and summer rye were harvested twice over the two-year period of the experiment. Whole plants including stem, leaf and grain, but not roots, were mixed and analyzed. Results of plant analyses are shown in Table 7.

Table 7. Nickel concentrations in two plant species over two years (mg/kg dw).

	Norwegian olivine (N3)		Spanish olivine (S3)	
Year	Summer rye	Winter barley	Summer rye	Winter barley
2020/2021	0.213	0.197	<0.05	0.118
2021/2022	<0.05	0.082	<0.05	<0.05

Results show that summer rye and winter barley from the Norwegian olivine plot have accumulated some nickel in the first year. In the second year, concentrations were below analytical reporting limit. In the Spanish olivine plot, only Winter barley accumulated some nickel in the first year.

To compare the measurements with the plant-uptake model, bioconcentration factors (BCF) for nickel were collected from scientific literature for a variety of plant species (Lenferink, 2019. See also section 2.2.4.2). Here, we use the BCF values for plant species that agree with or resemble the species used in the field experiment. This yielded:
$BCF_{Summer\ rye} = 1.72.10^{-2}\ kg_{soil} / kg_{plant\ dw}$
$BCF_{Winter\ barley} = 2.06.10^{-2}\ kg_{soil} / kg_{plant\ dw}$

Using the nickel content in soil from section 2.2.3:
20.4 mg Ni/kg dw soil (Norwegian olivine plots)
12.6 mg Ni/kg dw soil (Spanish olivine plots)

And the equation [1]:
$Ni_{Concentration\ in\ plant\ (mg/kg\ dw)} = Ni_{Concentration\ in\ soil\ (mg/kg)}\ x\ BCF$

Table 8 shows the results of calculated nickel in summer rye and winter barley for the two olivine treatments. In order of magnitude, there is a good agreement between the measured and calculated values.

Table 8. Calculated Ni in plants via BCF.

	Norwegian olivine (N3)		Spanish olivine (S3)	
	Summer rye	Winter barley	Summer rye	Winter barley
Calculated	0.351	0.420	0.217	0.260

Figure 15 shows the nickel concentration in pore water of the planted and non-planted plots. Nickel concentrations are elevated specifically in plot with Norwegian olivine, specifically in the first 3 - 4 months. After 6 months, Ni-concentrations in these plots are not statistically different from the reference.

The decline in concentrations after the first period was discussed earlier (section 3.4.2). Firstly, the ultrafine fraction of the olivine is weathered more rapidly than the coarser fractions, yielding a relatively fast release of weathering products among which nickel. Secondly, adsorption to soil matrix occurs, extracting elements from solution into the solid (less available) phase. Pore water is the most bioavailable source of elements. Dissolved elements are most likely to be taken up by plants, since no de-sorption or dissolution from solid phases has to occur before uptake. Antonkiewicz et al. (2016) reported on bioaccumulation factors based on dissolved nickel, rather than total nickel in soil. BAF values tended to decrease when nickel concentrations increased. They found that nickel accumulated mainly in roots of the test plants (maize, bean).

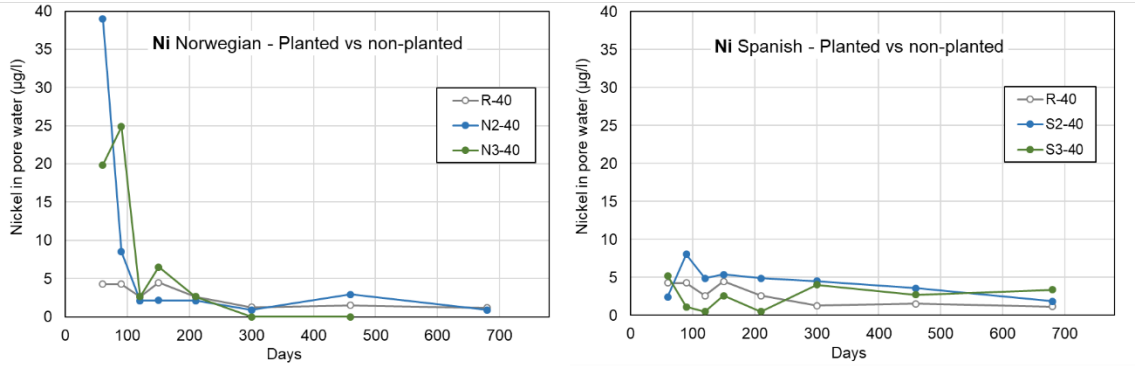

Fig. 15. Nickel pore water concentrations in the two olivine treatments in time (plots 3 = planted; plots 2 = non-planted; R = reference).

For plants, nickel is considered as an essential element, although the need for Ni is generally very low: approximately 0.1 mg/kg dw (Labrecque et al., 1995; Rozema & Verhoef, 2003). In seeds of cereals (*Dactylis glomerate* and *Avena barbata*), typical concentrations of 0 – 4.7 mg Ni /kg dw were found in Norwegian soils (Sunderman, 1991). Beet contained 0.5 – 95.6 mg Ni /kg dw when grown on sewage sludge (Sanders et al., 1987). Willow trees (*Salix)* contained up till 20 mg Ni /kg dw in the leaves in soil containing 45 mg/kg nickel (Labrecque et al., 1995). Phytotoxicity may occur at high nickel concentrations, resulting in necrosis of the leaf, using nutrient solutions of 0.6 – 6 mg Ni/L (Das et al., 1978). Wang (1986) tested *Lemna minor* and reported an EC50 of 470 µg Ni/L in surface water. Ni concentrations in surface water of 1000 µg Ni /L caused growth inhibition of 30 to 70%, the latter in water with low alkalinity (Wang, 1987).

The Panel on Contaminants in the Food Chain recently updated the nickel risk assessment in food. The tolerable daily intake (TDI) of nickel was established at 13 µg/kg body weight (Schrenk et al., 2020). This means for an average person of 70 kg an average daily intake of 0.91 mg. With the measured concentrations in the plants of the field plots (Table 7), this means that the limits for food are not exceeded by a factor of at least 4.

3.6 Chemical soil extractions

Soil samples were taken from the bulk soil batch in triplicate, homogenized, and subjected to various chemical extractions varying in ionic strength (see section 2.2.5.4 for further explanation). The following extractions were carried out in triplicate of samples from the soil batch:

1. Aqua Regia: This aggressive destruction is a measure of total content of an element in the sample, including the incorporated elements in solid (olivine, wollastonite) minerals and adsorbed and absorbed by soil constituents.
2. Aqua Nitrosa: This relatively mild extraction is a measure of the “chemical and biological reactive fraction” of elements, including adsorbed and dissolved fractions.

At the end of the field experiment, soil samples were taken from all individual plots and subjected to the same chemical extractions as the initial soil. With a dose of 4.04 kg olivine per plot (see section 2.2.3), the theoretical enrichment of Mg and Ni to the soil was calculated. The enrichment is compared to the initial soil composition to calculate loss of elements due to leaching and plant uptake.

Results of the extractions for Mg, Ca and Ni are presented in Table 9 for the initial soil that was used to construct the field plots. All data are presented in Appendix E.

Table 9. Elemental composition of the initial soil determined via chemical extractions.

	Destruction Aqua regia mg/kg		Extraction Aqua nitrosa mg/kg	
Al	5244	± 757	385.6	± 47.3
Ca	3181	± 338	3017	± 914
Fe	6731	± 1121	1115	± 92
Mg	1168	± 214	338	± 129
K	1220	± 216	194	± 81
Cr	10.5	± 1.0	0.50	± 0.04
Ni	9.7	± 0.8	1.50	± 0.15

The Aqua regia (AR) destruction obviously yields higher values than the Aqua nitrosa (AN) extraction (Vink & Osté, 2021). An exception is calcium (Ca), which is mostly present as calcite (lime) which can fairly easily be dissolved by a mild acid. AN extractions of elements Cr and Ni are factors lower (20 and 10, respectively) than the AR extractions, indicating that the major part is (strongly) bound to the soil components such as clay, iron(hydr)oxides and organic matter.

Figure 16 gives a visualization of the chemical fractions that are extracted by Aqua regia and Aqua nitrosa respectively. The dissolved phase is the pore water, including salts and adsorbed amounts to dissolved organic matter (DOC).

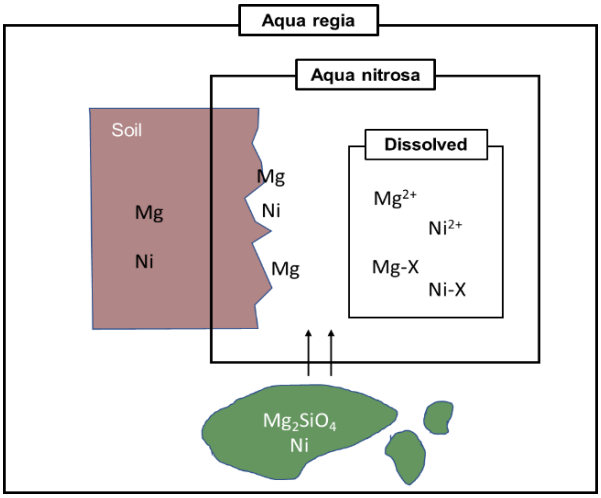

Fig. 16. Extraction methods indicative of chemical phases.

The following sections will discuss the extraction results related to experimental variables in the plots (and mesocosms). We exclude cross-relations with multiple treatments, since these cannot be linked to a single treatment. The following treatments are discussed:

1. Open field plot versus mesocosm
2. Spanish versus Norwegian olivine
3. Olivine applied on top versus mixed in
4. Dry versus wet conditions
5. Planted versus non-planted

3.6.1 Open field plot versus mesocosm

The open field plots allow for free drainage to subsoil < 0.5 m. The mesocosms, indicated by MB (= Mass Balance), are closed systems without drainage.

Figure 17 shows the results of chemical destructions (AR; left columns) and extractions (AN; right colums) of the open field plots and the accompanying mesocosms in that plot.
As discussed before, Mg is used as a proxy for mineral weathering, supported by Ni.
In section 2.2.3, the calculated addition of magnesium via the olivine applications was 2850 mg/kg dw in the Norwegian plots, and 2040 mg/kg dw in the Spanish plots. Since AR represents chemical destruction, the total amount of Mg should therefore also include Mg present in the original soil. Hence:

$$Mg_{Soil} = Mg_{Olivine\ addition\ AR} + Mg_{Soil\ (reference)\ AR} \quad [6]$$

This yields for the Norwegian plots: 2850 + 1018 = 3868 mg/kg dw, and 2040 + 1018 =3058 mg/kg dw for Spanish plots.
Figure 17 shows that measured values (AR) are in most cases somewhat lower than the calculated value, which may be attributed to loss of mass via leaching through weathering, and/or to incomplete dissolution of the mineral phase. For wollastonite, which has very little Mg incorporated in the mineral, the values coincide with the ones from the reference plots. The same observation applies to nickel.

Differences between AR-destructions from open plots and mesocosms can be explained by:

- Mass loss through leaching ($AR_{open\ plot} < AR_{mesocosm}$);
- Plant uptake;
- Sample heterogeneity and analytical error.

In almost all plots, including the reference, $AR_{open\ plot} < AR_{mesocosm}$. This is however not the case for for the two planted plots (N3 + S3), where Mg content in open plots is higher than in the mesocosm. The only plausible explanation may be that plant uptake of Mg in mesocosms is larger than in open plots, possibly via moisture availability and/or a more intensive root system in mesocosm. This was not further investigated. We excluded N3 and S3 from the forthcoming calculations.

Mass loss of magnesium via leaching is approximated by:

$$Mass\ loss\ Mg = (Mg_{mesocosm} - Mg_{open\ plot}) / Mg_{mesocosm} \times 100\% \quad [7]$$

The calculated average loss-of-mass for all plots is 14.1% ± 13.6. The lowest mass loss occurred in the wet plots N4 and S4 (1.0 – 1.3% respectively) where leaching is most probably inhibited by the hydraulic condition i.e., the presence of a shallow water table.

Differences between Aqua nitrosa (AN) extraction from open plots and mesocosms are generally small and may be explained by differences in moisture content (see section 3.3) and/or chemical precipitation and complexation. For more accurate interpretation, dissolved concentrations should be considered. Here, we assume that the net increase of element concentrations - compared to the reference - are the result of mineral weathering of olivine and wollastonite. In contrast to chemical destruction, the mild extraction distinguishes between solid phases and (potentially) available phases. Release of Mg and Ni through weathering will be available in the adsorbed and dissolved phase, not in insoluble solid or absorbed phases. Here we hypothesize that the Δ AN-fraction (AN minus Ref) may be considered as a quantitative measure for mineral weathering, and can be described by:

$$\Delta Mg_{AN} = Mg_{AN} - Mg_{AN\ Soil\ (reference)} \quad [8]$$

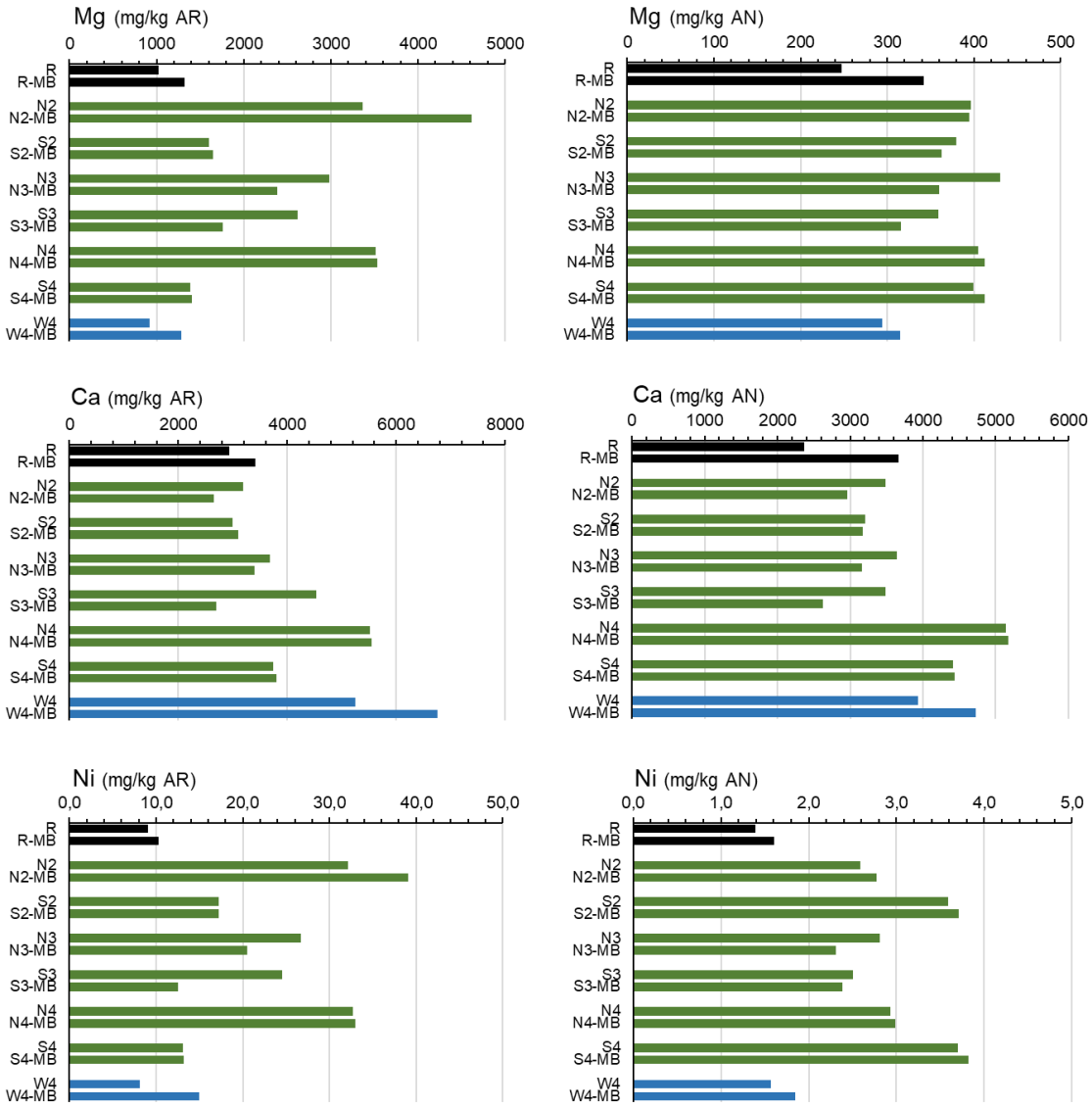

Fig. 17. Extractions from open plots and accompanying mesocosms.
AR=Aqua regia (left columns); AN=Aqua nitrosa (right columns); R=Reference; N=Norwegian olivine; S=Spanish olivine; W=wollastonite; MB=Mass balance (mesocosm). Plot numbers and treatments: see section 2.2.1.

3.6.2 Spanish versus Norwegian olivine

Figure 18 shows the results of chemical destructions and extractions of the open field plots for Norwegian and Spanish olivine. The wollastonite plots are included for comparison.

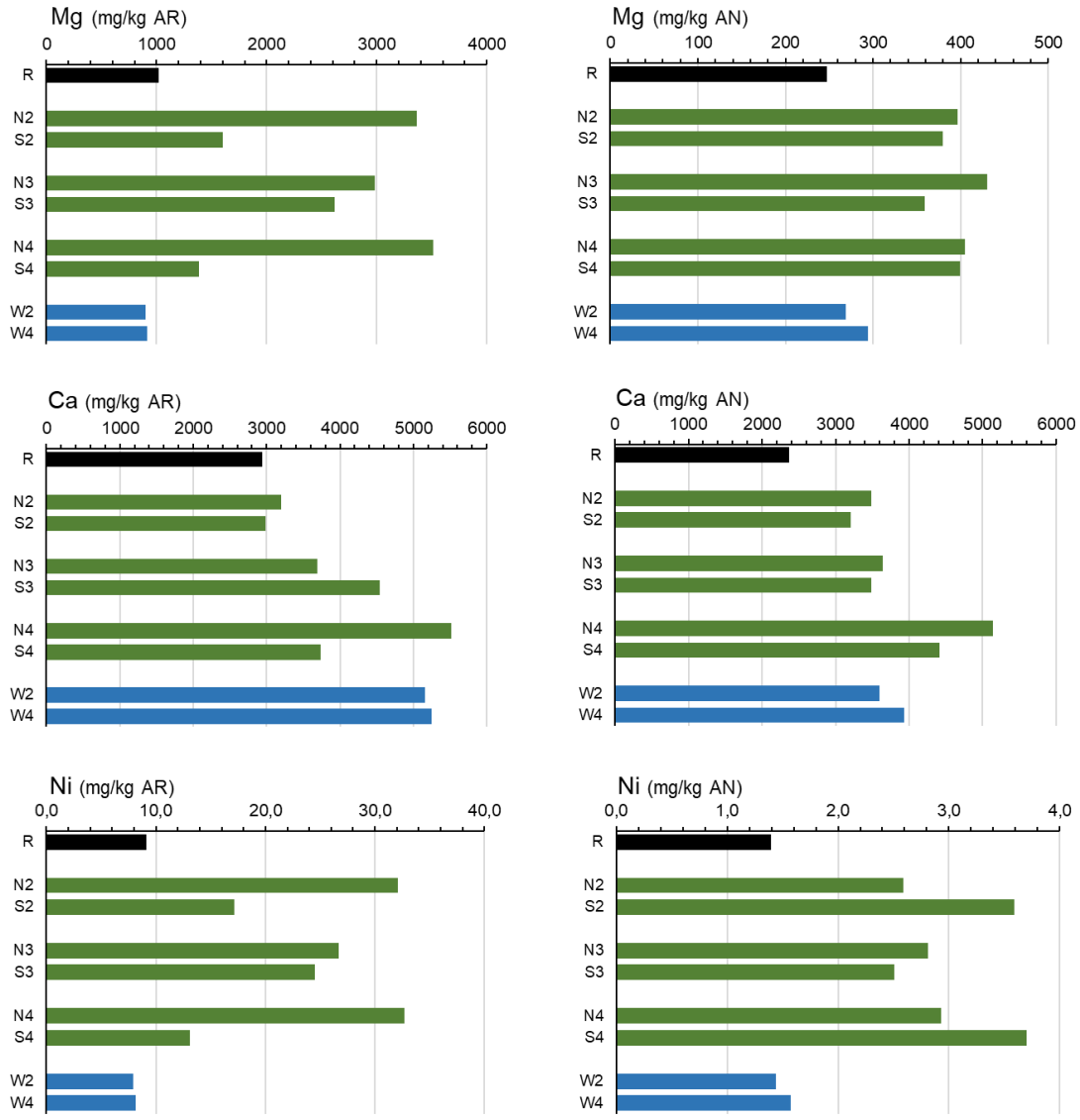

Fig. 18. Extractions from open plots of Norwegian and Spanish olivine, and wollastonite. AR=Aqua regia (left columns); AN=Aqua nitrosa (right columns); R=Reference; N=Norwegian olivine; S=Spanish olivine; W=wollastonite; Plot numbers and treatments: see section 2.2.1.

In all olivine plots, Mg and Ni are elevated compared to the reference. For all treatments, the Norwegian olivine plots have higher AR-extractable amounts of Mg and Ni than Spanish olivine plots. This is explained by the 40 % higher amount of added Mg through the dosage (2850 vs 2040 mg/kg dw soil, respectively) and the 62 % higher nickel amount (20.4 vs 12.6 mg/kg dw soil; see section 2.2.3).

Differences in AN fractions are smaller than observed for the AR fractions. Potential available concentrations of Mg in the Spanish plots are only slightly lower than in the Norwegian plots. The planted plot N3 has slightly higher extractable Mg than the non-planted plot, which may indicate enhanced weathering. This is not observed in the Spanish equivalent plots.
For nickel, the AN fractions in Spanish plots S2 and S4 are significantly higher. This is in contrast with the pore water measurements, which showed higher concentrations of nickel in the Norwegian plots (see section 3.4.3 and 3.5).

For wollastonite, the calculated added amount of Ca to the soil 1646 mg/kg dw soil. This is in agreement with AR-extracted amounts (Added + Ref). Extracted amounts of Mg and Ni are in the same order as the reference, both for AR and AN.

3.6.3 Olivine applied on top versus mixed in

In plots number 1 olivine was applied on top of the soil surface, in plots number 2 the dose was mixed in. Layers of -10 cm depth and -40 cm depts in plots number 1 were sampled individually.

As expected, Mg and Ni content in the top layer of plots 1 yielded the highest AR-extractable content (Fig. 19). This is in agreement with pore water concentrations, that were highest for nickel in Norwegian plot N1-10. However, the deeper layer in the Norwegian plot (N1-40) had elevated Mg content, both compared to the reference and the Spanish plot. This can only be explained by translocation and/or leaching of mass from the surface into deeper layers. This is also the case for nickel in the Norwegian plot.

Notable is the little difference of AN-extractable amounts between the deeper layers of the “on-top” plots and the “mixed-in” plots. This is observed for both olivine types. This suggests that the type of application (on-top or mixed in) has marginal effect on the potential available fraction of both Mg and Ni after a period of two years.

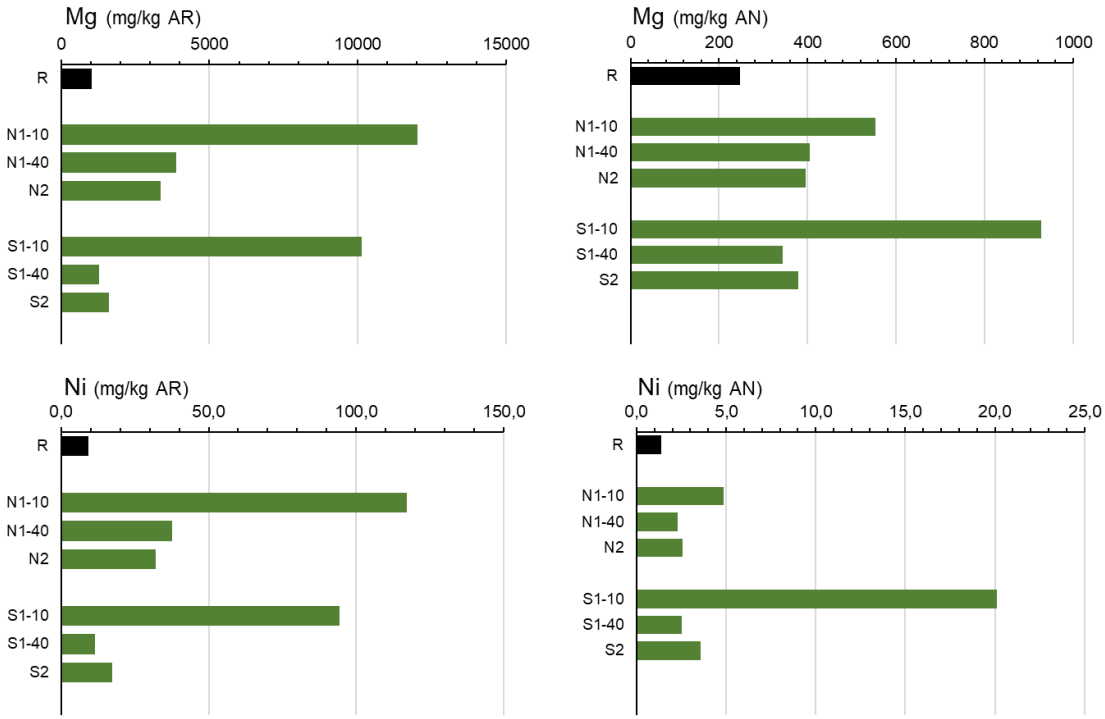

Fig. 19. Extractions of soil layers from plots with on-top and mixed-in application.
AR=Aqua regia (left columns); AN=Aqua nitrosa (right columns); R=Reference; N=Norwegian olivine; S=Spanish olivine; W=wollastonite; Plot numbers and treatments: see section 2.2.1.

3.6.4 Dry versus wet conditions

Dry, mixed-in plots (number 2) are compared to wet mixed-in plots (number 4).

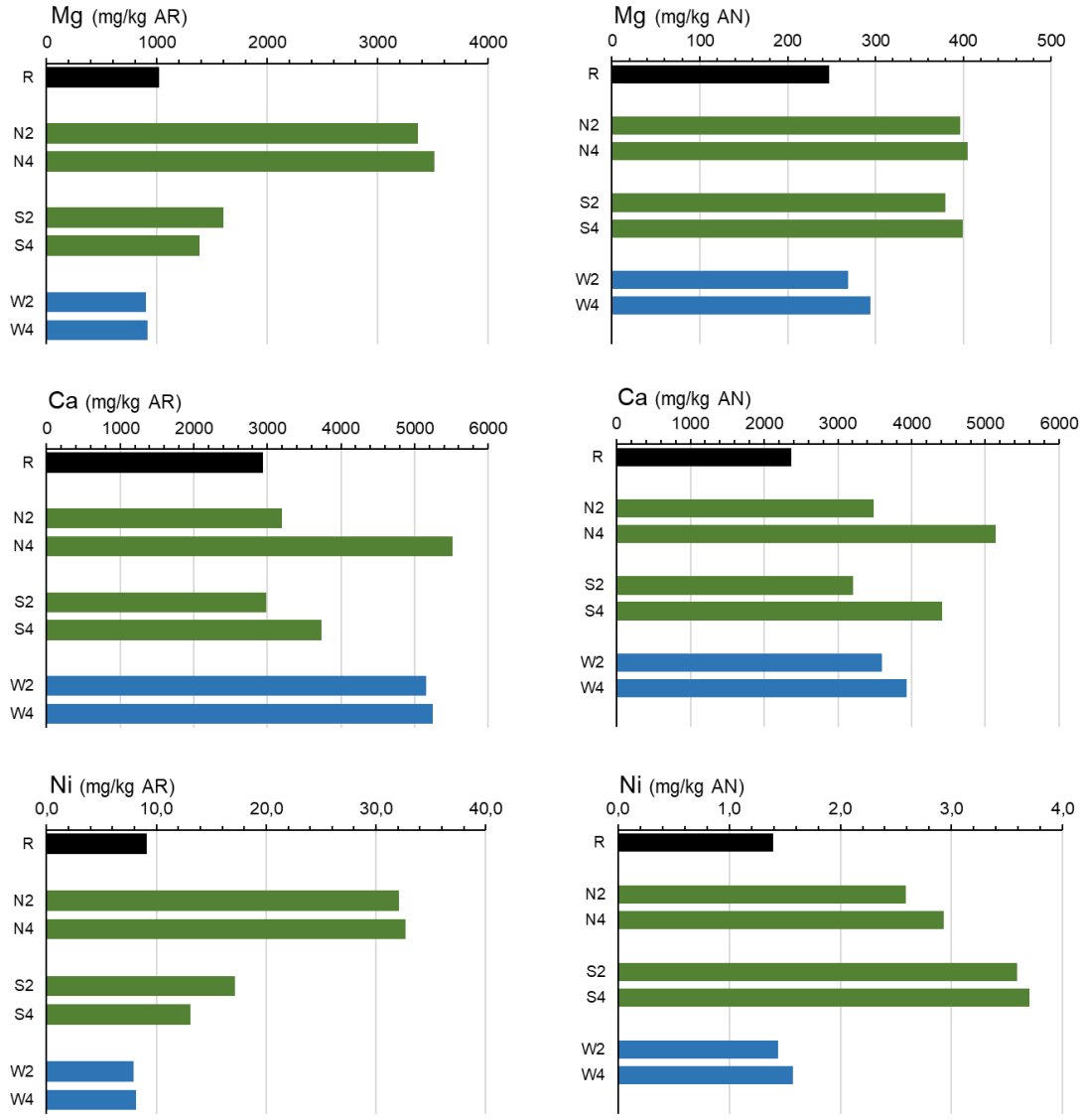

Fig. 20. Extractions of soils from dry (#2) and wet (#4) plots.
AR=Aqua regia (left columns); AN=Aqua nitrosa (right columns);
R=Reference; N=Norwegian olivine; S=Spanish olivine; W=wollastonite; Plot numbers and treatments: see section 2.2.1.

The chemical reaction of mineral weathering requires the presence of water (see section 2.3.1). Wet plots were introduced in the experimental design to test whether saturated conditions would facilitate (or increase) the weathering rate of the used minerals. However, only marginal differences for Mg and Ni were observed between dry and wet plots (Fig. 20). Moisture content varied around 20-40 % in dry plots and was never below 15 %. This strongly suggests that the moisture content of “dry” plots, i.e., under natural precipitation conditions, is not significantly limiting the chemical reaction compared to saturated conditions. Additionally, it is possible that water saturated conditions may lower the pCO_2 in the soil, which may in turn inhibit the chemical reaction rate. Also, the lack of transport of reaction products could have played a role via possible secondary mineral formation and/or supersaturation.

3.6.5 Planted versus non-planted

Planted plots (number 3) are compared to non-planted plots (number 2).

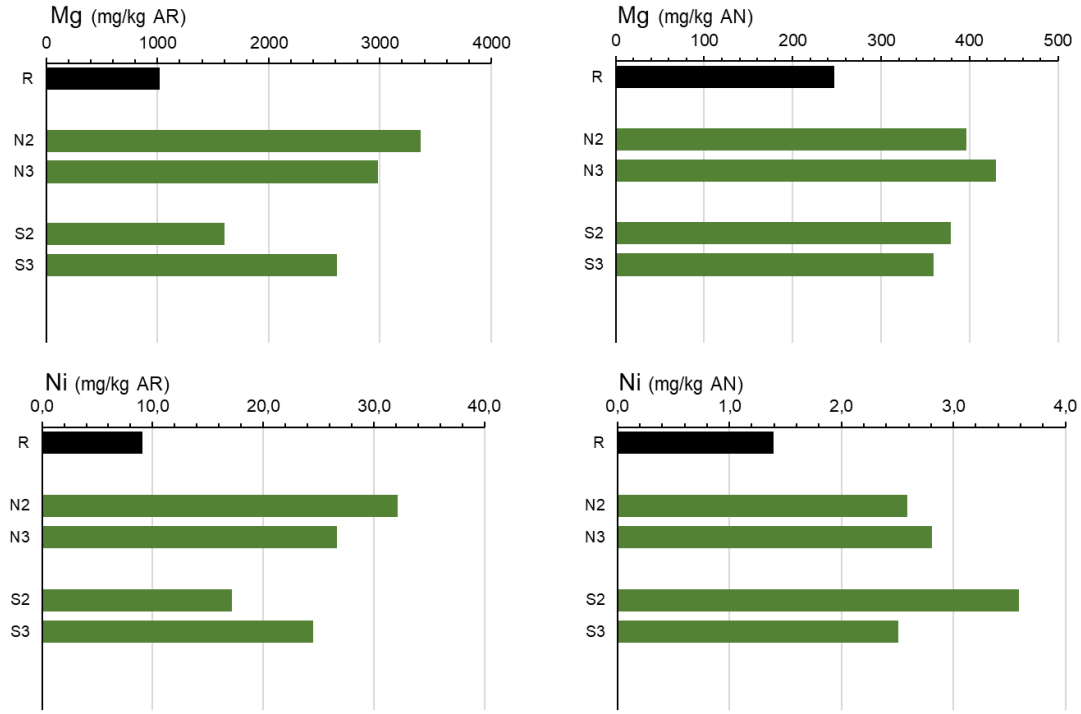

Fig. 21. Extractions of soils from planted (#3) and non-planted (#2) plots.
AR=Aqua regia (left columns); AN=Aqua nitrosa (right columns); R=Reference; N=Norwegian olivine; S=Spanish olivine; Plot numbers and treatments: see section 2.2.1.

Total Mg (via AR extraction) in Norwegian plots is higher than in Spanish plots, as was discussed earlier. The planted Norwegian plot shows slightly lower total-Mg than the non-planted plot (Fig. 21), which could be explained by plant uptake. However, the Spanish plots show the opposite trend: more total-Mg in the planted plot than in the non-planted. The same is observed for nickel. In all cases, the potential available fractions (via AN extraction) show opposite trends compared to total fractions, both for Mg and Ni. Since we found no significant differences in pore water pH in the planted and non-planted plots, these observations remain yet unexplained. When compared to the effect of olivine source (Norwegian or Spanish), the effect of deeply rooted plants on olivine weathering does not seem a dominant variable, as was confirmed by pore water analysis.

3.7 Empirically derived weathered fraction of olivine

Previous sections discussed the pore water concentrations and extractable amounts of various chemical fractions in mineral-added plots and mesocosms under various treatments. This allows for an approximation of mass-loss as a result of weathering.

Empirical weathering rates are derived separately for Norwegian and Spanish olivine. For this, the plots with on-top application were excluded from the analyses, because of the dose differences between soil layers. All other plots with mixed-in application (numbers 2, 3, 4) are used for analyses.

It was assumed that the potential extractable Mg-fraction serves as a proxy for weathering of olivines (section 3.6.1). Hence, the addition of Mg to soil via mineral weathering is then approximated by:

$$\Delta Mg = AN_{Field\ plot} - AN_{Reference} \quad [9]$$

Using the data obtained from mesocosms, the amount of mass loss as a result of leaching was estimated (section 3.6.1) via:

$$Mass\ loss\ Mg = (Mg_{mesocosm} - Mg_{open\ plot}) / Mg_{mesocosm} \times 100\% \quad [10]$$

We use a generic value of 14 % (section 3.6.1) for normalization of Mg mass loss. Hence, measured values are normalized to compensate for the lost fraction due to leaching:

$$\Delta Mg = (AN_{Field\ plot} - AN_{Reference}) \times (1 + 0.141) \quad [11]$$

Table 10 shows the calculation steps to derive mass loss and amount of olivine weathered for the various experimental plots in detail.

Table 10. Empirically derived mass loss through weathering of olivine. For plot numbers and treatments see section 2.2.1.

Plot	Δ Mg (MB – Ref)	Δ Mg normalized	Δ Mg dissolved olivine (mg/kg)	Initial dose (mg/kg)	Fraction mass loss of initial dose	% mass olivine weathered
N2	396.4-246.9	(396.4-246.9)*1.141	170.6	2850	170.6/2850	6.0 %
N3	430.2-246.9	(430.2-246.9)*1.141	209.1	2850	209.1/2850	7.3 %
N4	405.2-246.9	(405.2-246.9)*1.141	180.6	2850	180.6/2850	6.3 %
S2	397.2-246.9	(397.2-246.9)*1.141	171.5	2040	171.5/2040	8.4 %
S3	359.4-246.9	(359.4-246.9)*1.141	128.4	2040	128.4/2040	6.3 %
S4	399.5-246.9	(399.5-246.9)*1.141	174.1	2040	174.1/2040	8.5 %

Results show that the olivine weathering over the 2-year period is between 6.0 – 8.5 % of the mass of the total applied dose. The weathering rate of the Spanish olivine is slightly higher than the Norwegian source. The differences between rainfed- and saturated conditions are small. Effect of planting is not conclusive: plant-stimulated weathering is observed in the Norwegian plots, but not in the Spanish plots.

For wollastonite, the extractable Mg could not be used as a proxy, since wollastonite is a Ca-silicate. Wollastonite follows a different weathering reaction than olivine (see section 2.3.1), described by, o.a., Te Pas (2020):

$$CaSiO_3 + 2CO_2 + 3H_2O \rightarrow Ca^{2+} + 2HCO_3^- + H_4SIO_4 \leftrightarrow CaCO_3 + CO_2 + H_2O + H_4SiO_4 \quad [12]$$

Applying the same methodology for Ca (the CaO content in wollastonite is 23.9 %; section 3.1.3), this would yield weathering percentages of 84 % and 102 % for plots W2 and W4, respectively. Although the weathering rate of wollastonite might be higher than the olivines

based on the grain-size distribution (fine fraction is larger), these values seem unrealistic. We conclude that the presented methodology is not applicable for wollastonite using Ca as a proxy. The reactions of wollastonite compared to olivine, and the CO_2 sequestration potential compared to olivine is discussed in detail by Te Pas (2020).

3.8 Model results, calibration, and prognosis

3.8.1 Dissolution of olivine

Applying the Shrinking Core Model (SCM) to each grain size class (see section 2.3.1), the dissolution of each grain size class over time was calculated. The smallest size fraction rapidly decreases in diameter because of its relatively large surface area compared to mass. This is followed by the second-smallest size fractions in progressing time intervals. Although all grains start weathering from t = 0, regardless of size, the larger particle size fractions exert a relatively small contribution to the overall weathering, since small grains have a progressive larger surface-to-volume ratio than large grains.

The results of this size-specific approach on the dissolution of olivine is shown in Table 11 (Norwegian olivine as an example). After two years, 100 % of the mass of grain size fraction < 2 µm is dissolved. In the same period, 42.9 % of the fraction < 8 µm is dissolved, leaving a residual particle diameter of 4 µm, etcetera. The larger fractions show decreasing dissolved portions respectively.

Table 11. Changes in particle sizes after two years, and calculated fraction dissolved (% mass) per grain size fraction (SCM model).

Initial particle diameter (µm)	Particle diameter after 2 years (µm)	Dissolved per fraction (%)
2000	1996	0,14 %
1141	1137	0,24 %
1000	996	0,27 %
707	703	0,38 %
420	416	0,65%
250	246	1,1 %
150	146	1,8 %
88	84	3,1 %
50	46	5,6 %
16	12	19,0 %
8	4	42,9 %
2	0	100 %

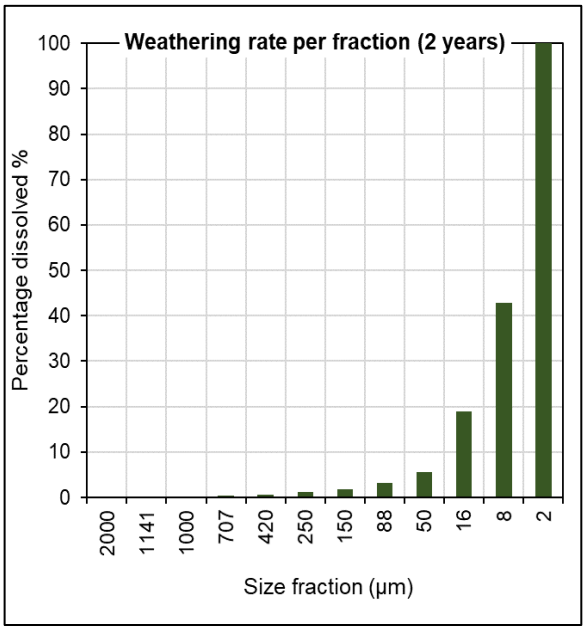

Using the SCM principle in the weathering model OWCS, and the measured data for calibration, a dissolution rate k of 7.43E-11 mol/m^2/s was derived for both olivine types. Figure 22 shows the result of the model exercises, along with the measured weathering rates derived from the various experimental plots. Results show a good agreement between the modelled and the measured values from Table 11.

The difference in Figure 22 between the Norwegian and the Spanish olivine is directly related to the grain size distribution (see section 3.1.4). The Spanish olivine has a larger ultrafine

grain fraction (< 250 µm) compared to the Norwegian. After this point, the Norwegian olivine has a finer grain size distribution.

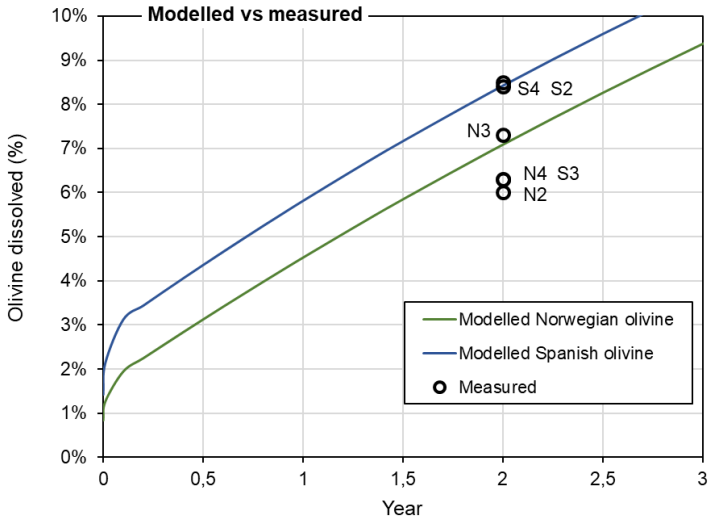

Fig. 22. Modelled and measured dissolution of olivine over time. Labels denote the field plots. Model results derived with OWCS V6.3.

With the settings of the calibrated OWCS model for two years, a prognosis was done for a period of 100 years. This is presented in Figure 23. In the first decennium, the dissolution rate of the Spanish olivine exceeds that of the Norwegian, but after some time a turning point is reached after which the Norwegian olivine is dissolved more rapidly. Half of the Norwegian olivine is dissolved after 42 years, which is 50 years for the Spanish olivine. After 100 years, approximately 75 % of the olivine is dissolved, versus 68 % for the Spanish olivine.

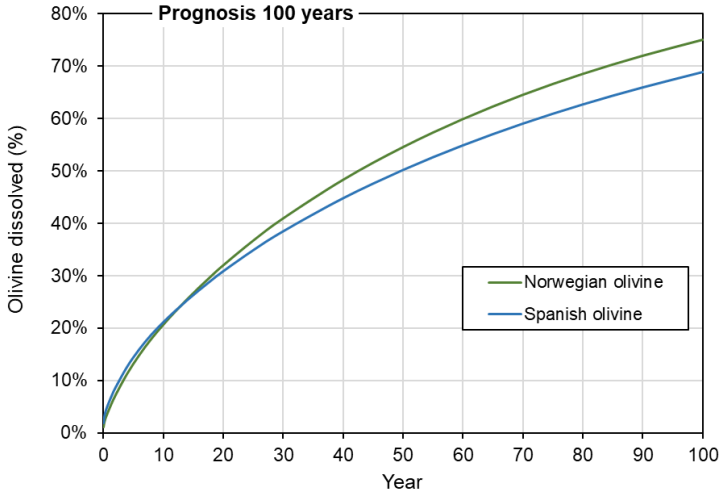

Fig. 23. Prognosis of dissolution of two olivine types over a period of 100 years.

It should be noted that the prognosis for 100 years should be interpreted with certain care. Obviously, calibration of the model was performed for the first 2 years of weathering, which was the duration of the experiments. Extrapolation to future time steps may, a-priori, introduce uncertainty. Nevertheless, the good agreement between modelled and measured results, and the logical shapes of the curves which have a direct relation with the olivine-source specific size distribution, provides confidence in the calculation methodology.

3.8.2 Nickel toxicity assessment

To assess the actual risks of nickel, Biotic Ligand Models for nickel were applied using the nickel concentrations that were measured over two years in pore water in the experimental plots (section 2.3.2.2). BLMs take environmental parameters such as pH, and concentrations of DOC, Mg, and Ca into account to calculate concentrations for which no toxic effects are expected (PNEC). This is done for a large variety of biota using the software PNEC-pro V6. Toxicity is based on chronic nickel exposure. Measured nickel concentrations are compared to the accompanying calculated PNEC as a risk indicator. The Risk Characterization Ratio (RCR) is defined as:

$$RCR = [C_{Ni}] / PNEC \qquad [13]$$

If RCR > 1, a toxicity risk is expected, since the calculated no-effect concentration is lower than the measured value;
If RCR <1, no toxicity risk is expected.

Environmental input parameters and calculated values of PNEC are shown in Appendix F. Figure 24A shows the relation between measured Ni concentration and accompanying PNEC. In all cases, the calculated No-effect concentration is larger than its measured value in pore water. This indicates that the concentration level for which toxic effects may start to manifest are not reached.

Figure 24B shows the calculated RCR for all measured data points. All values are (far) below the RCR = 1 ratio, indicating that no chronic toxic risks are expected. Only for one data point (N1-10; C = 64.8 µg/L, PNEC = 64.4 µg/L), there is a probability of 54 % that toxicity may occur in that point of time.

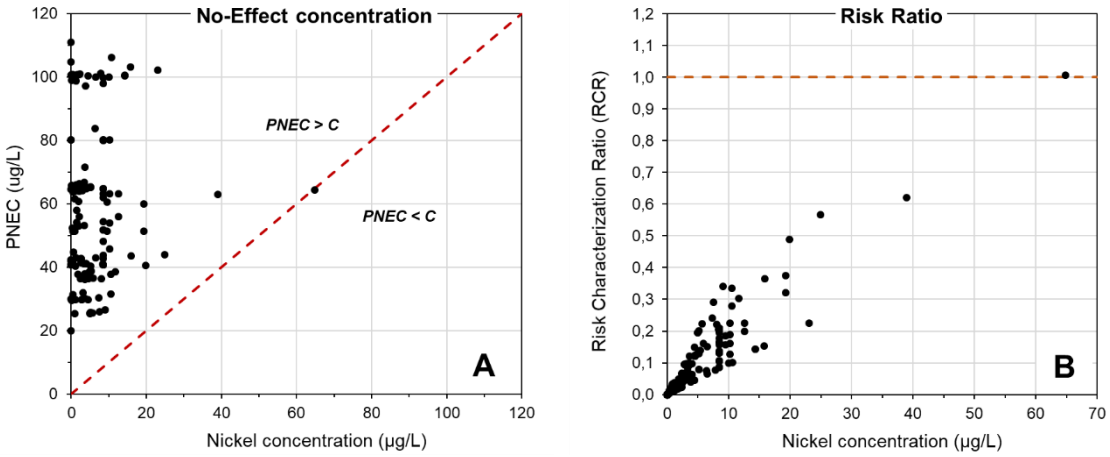

Fig. 24A. Measured nickel concentrations in all plots versus the calculated no-effect concentrations. In all cases, the PNEC is larger than the measured concentration, indicating less toxicity than suggested by the generic environmental quality standard.
Fig. 24B. Measured nickel concentrations and the accompanying Calculated Risk Characterization Ratio (RCR). All measurements except one are well below the safe toxicity risk boundary of 1.

4 Synthesis

4.1 Conclusions

Experimental

1. A two-year field experiment was performed with olivine of Norwegian and Spanish origin, and Canadian wollastonite for comparison. Open field plots contained mesocosms for mass-balancing measured concentrations and to quantify the amount of leaching. Plots and mesocosms had various treatments (Norwegian vs Spanish olivine, rainfed vs. wet conditions, on-top vs mixed-in application, planted vs non-planted). Summer rye and winter barley was sown in alternate seasons in the planted plots. Weathering products were measured in pore water periodically at two depths. Various chemical soil extractions yielded information on total and available fractions of elements *(Section 2.2.1)*.

2. The composition of the olivine types is different. The olivine from Norway contains more Mg and Ni compared to the Spanish olivine, which has slightly higher Fe content. The Spanish olivine has a slightly higher part in the ultrafine fraction (< 250 µm) and in the coarse fraction (> 2 mm), but the overall grain median value of the Norwegian olivine is slightly lower than the Spanish olivine. Wollastonite has a large fraction of ultrafine grains (65% < 250 µm) *(Section 3.1.2, 3.1.3)*.

3. The cumulative precipitation over the course of the two-year experiment did not deviate from average annual rainfall of previous years *(Section 3.2)*.

Olivine weathering

4. Pore water concentration ratios of Mg and Si are comparable to the molar ratio of the mineral's composition. This is strong evidence that the elevated Mg and Si concentrations are the result of mineral weathering, and release of these elements from the mineral to pore water *(Section 3.4)*.

5. The applied mineral dose of 4 kg/m^2 results in a pH-increase in the pore water of approximately 0.2 to 0.5 pH-unit over the course of two years *(Section 3.4.1)*.

6. The average loss-of-mass for all plots is approximately 14 % which is attributed to leaching. The lowest mass loss occurred in the wet plots where leaching is most probably inhibited by the presence of a shallow water table *(Section 3.6.1)*.

7. Concentrations of Mg and Si are in all cases higher in the deeper (-40 cm) zone than in the shallow (-10 cm) zone, even in the plots where olivine is applied on top. This is attributed to two reasons: a) In natural conditions, the top layer of the soil dries out faster than the deeper layer, so chemical reactions are periodically inhibited; b) Leaching of Mg and Si occurs from topsoil to subsoil *(Section 3.6.3)*.

8. For all treatments, the Norwegian olivine plots have higher AR-extractable amounts of both Mg and Ni than Spanish olivine plots. This is explained by the 40 % higher amount of added Mg through the dosage and the 62 % higher nickel content *(Section 3.6.2)*.

9. Olivine weathering over the 2-year period is between 6.0 – 8.5 % of the total applied dose. The weathering rate of the Spanish olivine is slightly higher than the Norwegian olivine *(Section 3.7)*.

10. Applying the Shrinking Core Model to each grain size, the dissolution over time could be calculated accurately. Of the smallest grain fraction (2µm), 100 % of the mass is dissolved in two years. In the same period, 42.9 % of the fraction < 8 µm is dissolved. The larger fractions show decreasing dissolved portions respectively *(Section 3.8.1).*

11. A dissolution rate k of 7.43E-11 mol/m^2/s was derived for both olivine types *(Section 3.8.1)*.

12. Results of dissolution over time show a good agreement between the modelled and the measured values *(Section 3.8.1)*.

13. With the settings of the calibrated OWCS model, a prognosis was done for a period of 100 years. Half of the Norwegian olivine is dissolved after 42 years, and 50 years for the Spanish olivine. Although these prognoses should be interpreted with care, the good agreement between modelled and measured results, and the logical shapes of the curves that have a direct relation with the olivine-source specific size distribution, provides confidence in the calculation methodology *(Section 3.8.1)*.

14. Compared to other treatments, grain size distribution is the dominant factor affecting weathering rates *(Section 3.8)*.

Plot treatment effects

15. As intended, the wet plots with shallow groundwater table have a systematic higher moisture content of 50 to 100 % compared to plots with free drainage *(Section 3.3)*.

16. Only marginal differences for extractable Mg and Ni were observed between dry and wet plots. Moisture content varied around 20-40 % in dry plots and was never below 15 %. This strongly suggests that the moisture content of “dry” plots, i.e., under natural precipitation conditions, is not significantly limiting the chemical reaction compared to saturated conditions. Additionally, water saturated conditions may lower the pCO_2 in soil, which may in turn inhibit the chemical reaction rate *(Section 3.3, 3.6.4)*.

17. Wet sites typically have a hydrological regime that may not allow leaching to occur in the same manner as in the free-drainage sites. This may inhibit the translocation of dissolved elements to the surrounding environment *(Section 3.4.2).*

18. The hypothesis that plants (alternating barley and rye) stimulate olivine weathering could not be confirmed. Differences in pore water concentrations between planted and non-planted treatments are small, although possible enhanced weathering is observed in the Norwegian plots but not in the Spanish plots. Plant species were selected for their intensive rooting ability, but it cannot be excluded that other plant species may show different effects *(Section 3.4.2, 3.5, 3.6.5)*.

19. There are strong indications that the type of application (on-top versus mixed in) has marginal effect on the potential available fraction of both Mg and Ni after a period of two years. Notable is the little difference of AN-extractable amounts between the deeper layers of the “on-top” plots and the “mixed-in” plots. This is observed for both olivine types *(Section 3.6.3)*.

Risk assessment of nickel release

20. Nickel concentrations in pore waters are elevated compared to those in the reference plot. However, 96 % of all Ni measurements are below the analytical upper reporting limit. Only two measurements exceed the environmental quality standard (EQS) of surface water, and only after the first 60 days after application. After this period, no exceedance of the EQS was observed *(Section 3.4.3)*.

21. The five highest Ni-concentrations recorded are from plots with Norwegian olivine. Nickel concentrations are elevated specifically in the first 3 to 4 months. After 6 months, Ni-concentrations in these plots do not statistically differ from the reference. Norwegian olivine has a higher nickel content than the Spanish olivine which becomes available upon weathering. The decrease of nickel concentrations over time is a result of sorption to soil matrix which extracts nickel from pore water and binding it to soil constituents *(Section 3.4.3)*.

22. In the first period of the weathering experiment, most nickel is released from the ultrafine fraction (< 250 µm). Release from the larger fractions is slower and possibly occurs at the same rate as sorption to soil constituents *(Section 3.4.3, 3.8).*

23. Nickel content in plants could well be approximated by a bioconcentration factor for summer rye and winter barley *(Section 3.5)*.

24. Nickel content in plants show that the quality standards for food are not exceeded by a factor of at least 4 *(Section 3.5)*.

25. In all cases, the calculated No-effect concentration (PNEC) for nickel is larger than its measured value in pore water. The concentration for which toxic effects may start to manifest are not reached. All values are (far) below the risk characterization ratio (RCR < 1), indicating that no chronic toxic risks of nickel release are expected *(Section 3.8.2)*.

Visual main results

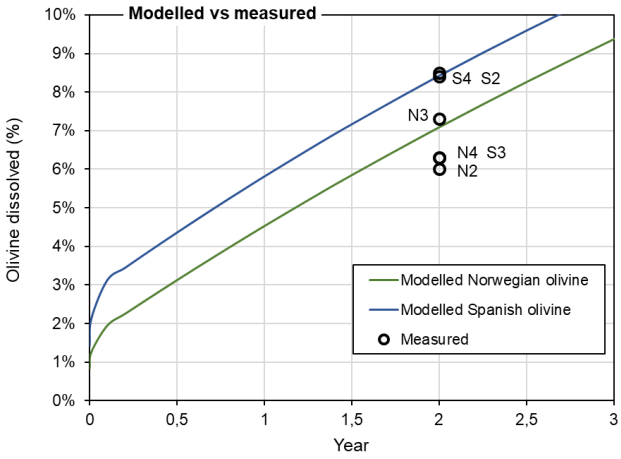

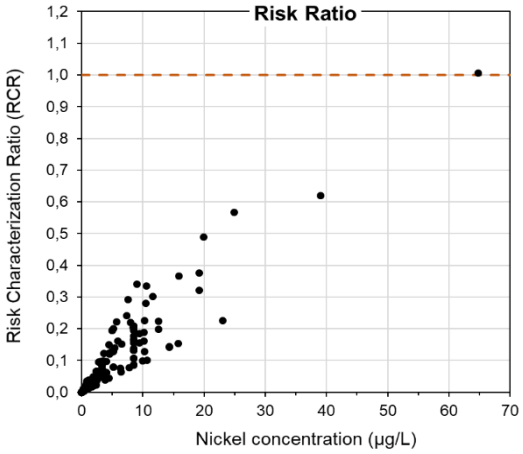

Left: Modelled and measured weathering rate for two olivine sources are in agreement (section 3.8.1). Right: Chronic toxicity of nickel upon weathering is not expected (section 3.8.2).

4.2 Recommendations

1. Prior to (large-scale) application of olivines or comparable minerals in the environment, modeling exercises should be performed to estimate weathering efficiency and perform environmental risk assessment via legal accepted methods. This may underpin claims on carbon capture and/or environmental benefits.

2. Monitoring pore water alkalinity in field plots proves to be very challenging as a result of many interfering reactions. To estimate olivine weathering rates, it is recommended to monitor robust weathering products such as Mg, Si and Ni as a proxy for weathering, accompanied by accurate mass-balancing.

3. As a consequence of variability in dissolved inorganic carbon species, especially after extraction of pore water and exposure to ambient atmosphere, pH measurements must be performed on-site.

4. Weathering of olivine releases Mg in the bioavailable (easily extractable and pore water) fractions in soil. Being a macro-nutrient for plants, the potential beneficial effect on production and growth should be further evaluated.

5. It was demonstrated that the modelling exercises, applying the shrinking core model (SCM) to individual grain size distributions, provide useful insight in weathering pathways. The dissolution rate of a mineral is directly derived from this. However, it is yet unclear to what extent this may be influenced by the precipitation of calcareous products around the grain. The formation of a “weathering shield” may overestimate the derived dissolution rate. It is recommended to address quantitatively the occurrence of precipitates in the estimation of weathering rates. A first step would be a laboratory experiment using electron microscopy and X-ray techniques to quantify the formation of such shields.

6. This study addresses the dissolution of olivine in a terrestrial environment. However, recent initiatives for large scale application of olivine are specifically targeted at the marine environment. In order to facilitate this, we refer to the recommendations done by Vink & Hoving (2022) where current scientific gaps are addressed.

References

Amann, T., J. Hartmann, E. Struyf, W. de Oliveira Garcia, E.K. Fisher, I. Janssens, P. Meire, J. Schoelynck (2018). Constraints on enhanced weathering and related carbon sequestration: a cropland mesocosm approach. *Biogeosciences Discussions*, https://doi.org/10.5194/bg-2018-398.

Antonkiewicz, J., Jasiewicz, C., Koncewicz-Baran, M., Sendor, R. (2016). Nickel bioaccumulation by the chosen plant species. Acta Physiologiae Plantarum 38/40.

Bakker, D.J., V. Beumer, N. Hartog, W. Snijders, M. Sule, J.P.M. Vink (2011). Toepassing van olivijn in RWS werken; Inventarisatie van mogelijkheden voor pilots (*Applications of olivine in RWS constructions; Inventory of possibilities for pilots*). Deltares rapport 1203661, Utrecht.

Bearat, H., M.J. McKelvy, A.V.G. Chizmeshya, D. Gormley, R.Nunez, R.W. Carpenter, L. Squires, G.H. Wolf (2006). Carbon sequestration via aqueous olivine mineral carbonation: Role of passivating layer formation. *Environ. Sci. Technol.* 40(15): 4802-4808.

Beerling, D.J., J.R. Leake, S.P. Long, J.D. Scholes, J. Ton, P.N. Nelson, M. Bird, E. Kantzas, L.L. Taylor, B. Sarkar, M. Kelland, E. DeLucia, I. Kantola, C. Müller, G.H. Rau, J. Hansen (2018). Farming with crops and rocks to address global climate, food and soil security. Nature Plants 4:138-147

Das, P.K., Kas, & Mishra, M. (1978). Ni nutrition in Plants: I. Effect of nickel on some oxidase activities during rice (Oryza sativa L.) seed germination. Z. Pflanzenphysiol. 90:225-233.

Dietzen, C., R. Harrisona, S. Michelsen-Correac (2018). Effectiveness of enhanced mineral weathering as a carbon sequestration tool and alternative to agricultural lime: An incubation experiment. *Int. J. Greenhouse Gas Control* 74:251-258

Duerr, J.S. (2013). Enhanced chemical weathering as a geoengineering strategy to reduce atmospheric carbon dioxide, supply nutrients, and mitigate ocean acidification. *Reviews of Geophysics* 51:113-149.

Dunsmore, H.E. (1992). A geological perspective on global warming and the possibility of carbon dioxide removal as calcium carbonate mineral. *Energy Convers. Mgmt.* 33/5-8:565-572.

Eliku, T., Leta, S. (2017). Heavy metals bioconcentration from soil to vegetables and appraisal of health risk in Koka and Wonji farms, Ethiopia. Environ. Sci. Pollut. Res. 24(12):11807-11815.
Emurotu, J., Onianwa, P. (2017). *Bioaccumulation of heavy metals in soil and selected food crops cultivated in Kogi State, north central Nigeria.* Environmental Systems Research. DOI 10.1186/s40068-017-0098-1.

European Commission (2011). Common Implementation Strategy for the Water Framework Directive (2000/60/EC) Guidance Document No. 27 Technical Guidance For Deriving Environmental Quality Standards. European Communities.

European Commission (2016). Science for Environment Policy. Advances in fresh water risk assessment: experiences with biotic ligand models. Issue 441, January 2016.

European Union (2008). European Union risk assessment report. Nickel and nickel compounds. Prepared by The Danish Environmental Protection Agency, on behalf of the European Union.

European Union (2019). Guidance Document No. 38 Technical Guidance for implementing Environmental Quality Standards (EQS) for metals; Consideration of metal bioavailability and natural background concentrations in assessing compliance. 2000/60/EC

Gbor, P.K., C.Q. Jia (2004). Critical evaluation of coupling particle size distribution with the shrinking core model. *Chem. Engineering Sci.* 59/10:1979-1987.

Groenenberg, J.E., Romkens, F.A.M., Van Zomeren, A., Rodrigues, S.M., Comans, R.N.J. (2017). Evaluation of the single dilute (0.43 M) Nitric acid extraction to determine geochemically reactive elements in soil. Environ. Sci. Technol. 51: 2246-2253.

Hangx, S.J.T. and Spiers, C.J. (2009). Coastal spreading of olivine to control atmospheric CO_2 concentrations: A critical analysis of viability. International Journal of Greenhouse Gas Control, 3(6): 757-767.

Haque F, Y.W. Chiang, R.M. Santos (2020a). Risk assessment of Ni, Cr, and Si release from alkaline minerals during enhanced weathering. *Open Agriculture* 5:166-175.

Haque, F., R.M. Santos, Y.W. Chiang (2020b). Optimizing inorganic carbon sequestration and crop yield with wollastonite soil amendment in a microplot study. Front. Plant Sci. DOI 10.3389/fpls.2020.01012.

Haque, F., R.M. Santos, A. Dutta, M. Thimmanagari, Y.W. Chiang (2019). Co-benefits of wollastonite weathering in agriculture: CO2-sequestration and promoted plant growth. ACS Omega 4(1): 1425-1433.

Hartmann, J., A.J. West, P. Renforth, P. Koehler, C.L. De La Rocha, D.A. Wolf-Gladrow, H.H. Duerr, J. Scheffran (2013). Enhanced chemical weathering as a geoengineering strategy to reduce atmospheric carbon dioxide, supply nutrients, and mitigate ocean acidification. Reviews of Geophysics 51:113-149.

Holdren G.R., P.M. Speyer (1985). Reaction rate-surface area relationships during the early stages of weathering 1. *Geochim. Cosmochim. Acta* 49:675-681.

Kersbergen, G. (2020). The possibilities of olivine enhanced weathering in paved road construction. Rep. 4233670, Utrecht university.

Khan, A., Khan, S., Khan, M.A., Quamar, Z., Waqas (2015). The uptake and bioaccumulation of heavy metals by food plants, their effects on plant nutrients, and associated health risk: a review. Environ. Sci. Pollut. Res. 22(18):13772-13799.

Kleint, C., Pichler, T., & Koschinsky, A. (2017). Geochemical characteristics, speciation and size-fractionation of iron (Fe) in two marine shallow-water hydrothermal systems, Dominica, Lesser Antilles. Chemical Geology, 454, 44-53.

Köhler, P., J.F. Abrams, C. Völker, J. Hauck, D.A. Wolf-Gladrow (2013). Geoengineering impact of open ocean dissolution of olivine on atmospheric CO2 surface ocean pH and marine biology. Environ. Res. Lett. 8:014009 (9pp).

Labrecque M et al. (1995). Effects of wastewater sludge on growth and heavy metal bioaccumulation of two Salix species. Plant & Soil, 171,303-316.

Lehmann, J., A. Possinger (2020). Atmospheric CO2 removed by rock weathering. Nature 583:204-205.

Lenferink, J. (2019). Does olivine weathering result in nickel toxicity? Combining terrestrial and aquatic risk modules to the weathering of olivine and subsequent release of nickel. Deltares Intern report, Utrecht.

Malik, A. (2017). Kinetics of olivine dissolution in column experiments. Thesis 1234567, University Hamburg.

Nagy K.L. A.E. Blum, A.C. Lasaga (1991). Dissolution and precipitation kinetics of kaolinite at 80 degrees C and pH 3; the dependence on solution saturation state. *Am. J. Sci.* 291:649-686.

Olsen, A.A. (2007). Forsterite dissolution kinetics: applications and implications for chemical weathering. Thesis Fac. Virginia Polytechnic Institute State University, Blacksburg, Virginia.

Palandri, J.L., Y.K. Kharaka (2004). A compilation of rate parameters of water-mineral interaction kinetics for application to geochemical modelling. US Geological Survey.

Pokrovsky, O. S., & Schott, J. (2000a). Forsterite surface composition in aqueous solutions: a combined potentiometric, electrokinetic, and spectroscopic approach. Geochimica et Cosmochimica Acta, 64(19), 3299-3312.

Pokrovsky O.S., J. Schott (2000b). Kinetics and mechanism of forsterite dissolution at 25C and pH from 1 to 12. *Geochim. Cosmochim. Acta* 64:3313-3325.

Renforth, P., P.A.E. von Strandmann, G.M. Henderson, 2015. The dissolution of olivine added to soil: Implications for enhanced weathering. Appl. Geochem. 61:109-118

Rozema J, Verhoef H.A. (2003). Leerboek Toegepaste Oecologie.VU, ISBN 9789053832882, Amsterdam.

Rüdel, H., C. Díaz Muñiz, H. Garelick, N. Kandile, B. Miller, L. Pantoja Munoz, W.G.M. Peijnenburg, D. Purchase, Y. Shevah, P. van Sprang, M.G. Vijver, J.P.M. Vink (2015). Consideration of the bioavailability of metal/metalloid species in freshwaters: experiences regarding the implementation of biotic ligand model-based approaches in risk assessment frameworks. *Environ. Sci. Poll. Res.* 22/10:7405-7421.

Safari, V., G. Arzpeyma, F. Rashchi, N. Mostoufi, N. (2009). A shrinking particle – shrinking core model for leaching of a zinc ore containing silica. *Intl. J. Mineral Processing* 93/1:79-83.

Sanders, J.R, S.P. McGrath, T.M. Adams (1987). Zinc, copper and nickel concentrations in soil extracts and crops grown on four soils treated with metal-loaded sewage sludge; Environmental pollution 44:193-210.

SCHER (2010). Opinion on the Chemicals and the Water Framework Directive: Technical Guidance for Deriving Environmental Quality Standards. Scientific Committee on Health and Environmental Risks, European Union, Brussels.

Schrenk, D., Bignami, M., Bodin, L., Chipman, J.K., Del Mazo, Grasl-Kraupp, B. et al. (2020). Udate of the risk assessment of nickel in food and drinking water. EFSA Journal 18(11). DOI.org/10.2903/j.efsa.2020.6268.

Schröder, T., Cornelisen, P., Vink, J., & Zee, S. v. (2006). *Uptake of Cd, Cu, Ni, Pb and Zn by a plant vegetation in embanked floodplains of the rivers Rhine and Meuse.* Deltares.

Schuiling, R.D., De Boer, P.L. (2010). Coastal spreading of olivine to control atmospheric CO2 concentrations; A critical analysis of viability. Comment: Nature and laboratory experiments are different. Short Comm. Int. J. Greenhouse Gas Control 4:855-856.

Schuiling, R.D., O. Tickiell (2010). Enhanced weathering of olivine to capture CO2. *J. Appl. Geochem.* 4:510-519.

Sunderman W.F. (1991). Nickel. In: Merian, E. (Ed.) "Metals and their compounds in the environment", p.1101-1126.

Taylor, L.L., J. Quirk, R.M.S. Thorley, P.A. Kharecha, J. Hansen, A. Ridgwell, M.R. Lomas, S.A. Banwart, D.J. Beerling (2015). Enhanced weathering strategies for stabilizing climate and averting ocean acidification. Nature Climate Change, DOI 10.1038/NCLIMATE2882.

Temminghoff, E.J.M., V.J.G. Houba (2004). Plant analysis procedures. ISBN: 978-1-4020-2976-9, Springer.

Te Pas, E. (2020). Is the CO2 hyunter a green, black or white mineral? Exploring the enhanced weathering potential of olivine, basalt, wollastonite, anorthite, and albite to improve agricultural production and mitigate climate change. PhD thesis, Wageningen University.

Ten Berge, H.F.M, H.G. van der Meer, J.W. Steenhuizen, P.W. Goedhart, P. Knops, J. Verhagen (2012). Olivine Weathering in Soil, and Its Effects on Growth and Nutrient Uptake in Ryegrass (Lolium perenne L.): A Pot Experiment. Plos One 7(8): e42098.

Verkleij, J., Ten Bookum, W., Sneller, E. en Bernhard, R. (Red. J.P.M. Vink) (2000). Mechanismen van opname, accumulatie en toxiciteit van zware metalen in uiterwaardenvegetatie. RIZA rapport 2000.016, ISBN 90-369-5310-3, Lelystad.

Verschoor, A., J.P.M. Vink, M.G. Vijver, G. De Snoo (2011). Geographical and temporal variation in Cu, Zn, Ni bioavailability and species sensitivity. *Environ. Sci. Technol.* 45:6049-6056.

Verschoor, A., M.G. Vijver, J.P.M. Vink (2017). Refinement and cross-validation of nickel bioavailability in PNEC-pro, a regulatory tool for site-specific risk assessment of metals in surface waters. *Environ. Toxicol. Chem.* 36(9):2367-2376.

Versluijs, C., Otte, P. (2001). *Accumulatie van metalen in planten.* Bilthoven: RIVM rapport 711701 024.

Vink, J.P.M. (2022). Olivine weathering efficiency in marine environments Physical & chemical transformations and CO2 capture in batch experiments and model scenarios. Deltares report 11206646, Utrecht.

Vink, J.P.M. (2021). Geschiktheid van olivijn als ballastmateriaal; haalbaarheidsstudie voor spoorwegtoepassing. Deltares report 11207232, Utrecht.

Vink, J.P.M. (2009). The origin of speciation: trace metal kinetics and bioaccumulation by Oligochaetes and Chironomids in undisturbed water-sediment interfaces. *Environ. Pollut.* 157:519-527.

Vink, J.P.M. (2002): Measurement of heavy metal speciation over redox gradients in natural water-sediment interfaces and implications for uptake by benthic organisms. *Environ. Sci. Technol.* 36/23:5130-5138.

Vink, J.P.M., D. den Hamer (2012). Olivijn legt CO2 vast in de gemeente Rotterdam. Mogelijkheden voor praktijktoepassingen en klimaatdoelen *(Olivine captures CO2 in the city of Rotterdam; possibilities for practical applications and climate targets*). Deltares report 1206650, Utrecht.

Vink, J.P.M., A. Hoving (2022). Olivine weathering efficiency in marine environments; Physical and chemical transformations and CO2 capture in batch experiments and model scenarios. Deltares technical report 11206646-000-BGS-0004, Utrecht.

Vink, J.P.M, P. Knops (in prep). Size-fractionated Weathering of Olivine, its CO_2-Sequestration Rate, and Ecotoxicological Risk assessment of Nickel Release.

Vink, J.P.M., J.C.L. Meeussen (2007). BIOCHEM-ORCHESTRA: a scenario-DSS for heavy metal speciation and ecotoxicological impacts in river systems. *Environ. Poll.* 148:833-841.

Vink, J.P.M., L. Osté (2022). Afleiding kwaliteitsnormen voor metalen en fosfaat in grond en bagger. Achtergronden en overwegingen bij het Milieuhygiënisch Toetsingskader en de inbedding in de Regeling Bodemkwaliteit. Deltares report 11208090, Utrecht.

Vink, J.P.M., A. Verschoor, M.G. Vijver (2016). PNEC-pro. Software release version 6. http://www.pnec-pro.com. Deltares, Utrecht.

Wang, W. (1986). Toxicity tests of aquatic pollutants by using common duckweed. Environ. Poll. 11:1-14. 221.

Wang, W. (1987). Toxicity of nickel to common duckweed (*Lemna minor*). Environ. Tox. Chem. 6:961-967.

White A.F., A.E. Blum, T.D. Bullen, D.V. Vivit, M. Schulz, J. Fitzpatrick (1999). The effect of temperature on experimental and natural chemical weathering rates of granitoid rocks. *Geochim. Cosmochim. Acta* 63:3277-3291.

Wogelius, R. A., & Walther, J. V. (1991). Olivine dissolution at 25 C: Effects of pH, CO2, and organic acids. Geochimica et Cosmochimica Acta, *55*(4), 943-954.

Wogelius, R. A., & Walther, J. V. (1992). Olivine dissolution kinetics at near-surface conditions. Chemical Geology, 97(1-2), 101-112.

A Composition of soil mixture

Object	Basismengsel proef Olivijn Deltares - van Dijk Maasland																								
grondstof	mengver-houding	los lever	droog	verzadigd	lutum		organische stof		stikstof		fosfaat		kali		magnesium		respiratie mmol O2 / kg OS / uur		Chloride		CaCO3		pH H2O		EC
		kg/m3	kg/m3	kg/m3	% ds		% ds		mg/100 gr		mg/100 gr		mg/100 gr		mg/kg				mg/l		%-DS				mS/cm
cocopeat	0	300	75	871	0	0	90	90	0	0	0	0	0	0	0	0	2	2	0	0	0	0	5,5	6	0,3	1
Cocofibre	0	29	100	0	0	0	95	95	0	0	0	0	0	0	0	0	2	2	0	0	0	0	6,4	6,4	0,09	0,09
bark 10-15	0	265	175	0	0	0	95	95	0	0	0	0	0	0	0	0	8	8	0	0	0	0	4,3	5,2	0,06	0,16
zand 0-250	30	1300	1200	0	0	2	0	0,3	4	20	3	9	4	9	14	15	0	0	18	18	1,8	2,9	8,1	8,1	0,14	0,14
zand 300	0	1225	1175	0	0	1,3	0,32	0,37	4	20	3	9	4	8	14	15	0	0	18	18	1,8	2,9	6,7	8,8	0,05	0,18
steenslag 2-6	0	1300	1275	0	1,3	2,7	0,4	0,46	4	10	3	4	3	5	13	19	0	0	18	18	0,1	0,1	6,6	9,3	0,03	0,11
SD-Compost	0	0	400	0	7,4	8,7	19,1	30	413	621	135	151	179	399	460	834	4,5	5,88	36	391	0,1	0,6	6,4	7,3	0,85	3,09
groenompost 0-15	22	650	420	950	3,3	7,4	24,5	28,3	639	811	188	292	384	576	463	658	5,35	9,1	426	657	0,1	0,8	7,4	8,5	1,81	3
tuinturf A4 MG	33	425	125	0	3,4	5,4	91	93,6	1092	1187	5	8	17	18	884	931	1,28	1,4	18	18	0,1	0,1	4	4,8	0,09	0,52
klei florisol 0-3	0	1175	1100	0	21,9	21,9	3,6	3,6	92	92	32,7	32,7	6	6	192	192	0	0	18	18	0,1	0,1	7,2	8,3	0,09	0,55
lava 3-8	0	1150	960	1240	2,7	3,4	1,3	2	4	23	22	35	1653	1715	153	249	0	0	18	36	0,1	0,76	8,2	9,2	0,09	0,18
zand S 0-1	0	1250	1200	0	1,3	1,3	0,13	0,13	1	1	2	2	1	1	5	5	0	0	18	18	0,1	0,1	6,3	8	0,02	0,07
klei florisol 0-3	0	1175	1100	0	21,9	21,9	3,6	3,6	92	92	32,7	32,7	6	6	192	192	0	0	18	18	0,1	0,1	7,2	8,3	0,09	0,55
Klei Den Boer	15	1075	900	0	37,5	39,5	8	8,1	286	322	30	35	16	17	440	450	1,2	1,2	36	36	0,1	0,5	7,2	8	0,25	0,65
kleikorrels 4-8 G	0	400	400	530	2,2	4,7	0,1	1,6	4	10	3	22	82	1505	1	166	0	0	18	36	0,1	0,29	4,5	7,4	0,18	0,59
zand 0-250	0	1300	1200	0	0	2	0	0,3	4	20	3	9	4	9	14	15	0	0	18	18	1,8	2,9	8,1	8,1	0,14	0,14
Triplesuperfosfaat	0		100	0	0	0	0	0	0	0	45000	45000	0	0	0	0	0	0	0	0	0	0	0	0	0,58	0,58
Kieseriet	0		100	0	0	0	0	0	0	0	0	0	0	0	27000	27000	0	0	0	0	0	0	0	0	0,84	0,84
DCM mix 2	0		100	0	0	0	0	0	7000	7000	6000	6000	12000	12000	4000	4000	0	0	0	0	0	0	0	0	0,78	0,78
	100	zv	zv	zv																						
Totaal	100	835	629	209	8,76	11,07	11,3	12,2	229,3	277,7	36,1	56,1	63,3	94,6	228,6	263,0	2,57	3,83	110,5	161,3	1,1	1,9	4,9	5,6	0,51	0,97
					3,00	8,00	5	10	80	240	50	200	30	120	100	300	0	5	0	200			6	7		

los gewicht	835	kg/m3	stikstof	253,5	mg/100 gram	2534,87	mg/kg	NO3	0,86	Ca	0,60	HCO3	1,56	mmol/l	Fe	29,9	µmol/l	M50	284,6	µm
droog gewicht	629	kg/m3	fosfaat	46,1	mg/100 gram	461,17	mg/kg	NH4	0,79	Mg	0,23	Na	0,96	mmol/l	Mn	1,58	µmol/l	D60	345,4	µm
verzadigd gewicht		kg/m3	kali	79,0	mg/100 gram	496,41	mg/ltr	H2PO4	0,15	SO4	0,42	Cl	2,79	mmol/l	Zn	0,35	µmol/l	D10	133,1	µm
			magnesium	245,8	mg/kg	154,52	mg/ltr	K	3,18	Sl	0,30			mmol/l	B	12,43	µmol/l	D60/D10	2,59	
Lutum	9,9	%													Cu	0,39	µmol/l	MKI	€ 3,73970	per m3
OS	11,8	%	respiratie	3,20	mmol O2 / kg OS / uur			EC	0,74	Chloride	135,9	mg/l	pH	5,3	Mo	0,37	µmol/l	MKI	€ 4,48136	per ton

Base composition. Mengverhouding = Mixing ratio.

Organische stof = organic matter; Zand = sand; Groencompost = bioorganic compost; Tuinturf = Garden peat; Kalk = lime; Klei = Clay

B Field plot realization

Excavation of field plots; mixing composite soil with olivine and wollastonite; inclusion of mesocosms and probes for sampling and continuous moisture detection. Two plots were planted with winter barley and summer rye, seasonally alternated.

C Moisture content over time

Moisture content over time (%) in field plots via installed electronic sensors.

		Time period		Moisture content (%)																				
	Plot	4-2020	5-2020	6-2020	7-2020	8-2020	9-2020	10-2020	11-2020	12-2020	1-2021	2-2021	3-2021	4-2021	5-2021	6-2021	7-2021	8-2021	9-2021	10-2021	11-2021	12-2021	1-2022	2-2022	3-2022	4-2022
Top	N1	13	14	15	15	11	10	30	23	22	20	22	23	20	19	19	18	15	16	19	21	20	18	20	19	19
	N1-MB	14	14	17	28	24	30	53	49	50	47	51	48	46	48	41	39	38	36	38	45	50	41	42	39	39
Mixed	N2	11	10	14	16	15	17	19	18	16	18	17	27	24	22	20	18	18	17	22	19	16	15	17	19	19
	N2-MB	19	12	20	22	29	23	44	42	43	41	40	40	38	37	36	37	38	35	37	39	40	38	41	40	40
Plants	N3	15	15	19	19	24	20	29	34	30	28	26	28	24	22	14	16	21	22	24	23	28	19	18	15	15
	N3-MB	22	17	21	22	30	24	50	49	47	46	49	50	38	34	30	42	43	46	54	50	47	45	50	45	45
Wet	N4	13	11	18	23	50	26	60	35	40	55	60	55	55	60	65	55	60	56	50	45	55	51	46	45	45
	N4-MB	14	13	14	18	38	19	46	52	50	42	46	47	47	45	45	40	44	40	39	42	40	44	43	40	40
Top	S1	20	20	27	27	34	29	48	26	27	22	25	23	20	22	18	17	18	17	23	25	24	22	25	28	28
	S1-MB	19	14	20	20	25	22	49	49	46	47	49	52	50	49	46	51	57	52	50	49	46	44	46	53	53
Mixed	S2	15	15	17	18	29	20	60	29	26	24	23	21	20	19	14	15	13	15	18	19	16	18	18	23	23
	S2-MB	19	14	18	19	27	20	47	43	39	38	43	44	42	43	40	38	41	40	42	41	39	41	40	43	43
Plants	S3	14	14	20	20	25	21	36	28	30	29	31	25	21	23	19	19	18	18	20	24	25	22	23	20	20
	S3-MB	17	16	18	11	27	12	44	42	38	31	43	42	40	41	35	36	43	42	41	42	40	34	36	39	39
Wet	S4	19	19	24	25	46	38	59	56	45	40	38	38	39	39	40	38	35	34	39	40	42	38	39	38	38
	S4-MB	13	10	17	18	25	19	54	57	56	55	56	45	44	42	43	42	51	56	55	53	54	51	55	58	58
	W2	11	11	17	18	17	20	18	16	15	17	14	14	18	24	19	16	10	12	16	17	15	16	14	15	15
	W2-MB	22	14	23	24	39	26	43	44	42	40	43	44	42	43	43	38	42	40	42	43	42	41	43	41	41
	W4	13	11	18	26	22	29	43	39	34	43	41	38	39	38	41	37	41	38	37	39	44	41	40	42	43
	W4-MB	24	14	25	28	52	31	54	52	48	46	51	50	52	50	50	46	51	46	47	46	50	45	46	49	49
	Ref	15	15	17	18	14	19	21	18	17	20	24	27	24	23	22	19	15	16	21	17	18	16	20	20	20
	Ref-MB	13	12	16	19	25	19	52	52	48	50	52	52	55	59	59	57	60	57	59	49	48	52	55	59	59

D Pore water measurements over time

JULY 2020	Ca	Fe	Mg	Ni	Si	P	S	pH
60	mg/l	mg/l	mg/l	mg/l	mg/l	mg/l	mg/l	
R-10-072020	nd	nd	nd	nd	nd	nd	nd	6,4
R-40-072020	nd	nd	8,2	nd	nd	nd	nd	6,4
R-MB-10-072020	nd	nd	nd	nd	nd	nd	nd	6,4
R-MB-40-072020	12,66	0,13	2,90	0,01	7,37	2,70	1,37	6,4
S1-10-072020	46,74	0,01	10,18	0,00	13,14	1,48	15,99	6,86
S1-40-072020	28,25	0,04	5,49	0,00	7,21	1,38	1,32	6,54
S1-MB-10-072020	228,64	0,78	55,68	0,02	47,20	6,68	2,07	6,82
S1-MB-40-072020	49,58	0,48	10,44	0,02	19,34	5,18	19,19	6,71
S2-10-072020	70,01	0,06	18,15	0,01	23,48	2,07	24,68	6,76
S2-40-072020	17,55	0,01	4,54	0,00	5,83	0,51	6,16	6,77
S2-MB-10-072020	118,83	3,31	34,38	0,02	36,62	11,83	2,03	6,69
S2-MB-40-072020	86,53	0,19	21,39	0,03	31,25	6,68	44,97	6,66
S3-10-072020	33,68	0,01	9,40	0,01	14,07	1,93	6,80	6,31
S3-40-072020	1,98	0,06	0,47	0,01	1,34	0,56	0,42	6,65
S3-MB-10-072020	133,80	1,52	33,66	0,02	30,04	9,53	2,17	6,65
S3-MB-40-072020	13,72	0,18	3,26	0,01	9,76	4,43	2,13	6,47
S4-10-072020	nd	nd	nd	nd	nd	nd	nd	
S4-40-072020	98,71	0,06	27,82	0,01	24,45	0,61	5,14	6,83
S4-MB-10-072020	nd	nd	nd	nd	nd	nd	nd	
S4-MB-40-072020	74,27	1,54	15,54	0,01	14,12	3,97	0,76	6,85
N1-10-072020	50,11	0,38	0,08	0,06	0,08	13,18	25,89	6,75
N1-40-072020	nd	nd	nd	nd	nd	nd	nd	
N1-MB-10-072020	nd	nd	nd	nd	nd	nd	nd	
N1-MB-40-072020	153,72	0,72	37,00	0,01	31,03	6,65	4,75	6,88
N2-10-072020	nd	nd	nd	nd	nd	nd	nd	
N2-40-072020	18,22	0,13	0,04	0,04	0,02	2,89	10,30	6,77
N2-MB-10-072020	252,53	0,46	72,76	0,03	53,64	10,49	3,70	6,65
N2-MB-40-072020	11,64	0,16	3,10	0,01	8,81	3,34	1,71	6,73
N3-10-072020	nd	nd	nd	nd	nd	nd	nd	
N3-40-072020	10,65	0,12	0,04	0,02	0,02	2,21	5,36	6,93
N3-MB-10-072020	97,85	3,37	26,91	0,01	24,37	8,72	1,60	6,82
N3-MB-40-072020	20,45	0,13	4,87	0,01	12,92	5,03	5,51	6,79
N4-10-072020	nd	nd	nd	nd	nd	nd	nd	
N4-40-072020	85,63	0,02	23,19	0,02	22,44	2,09	36,84	6,69
N4-MB-072020	nd	nd	nd	nd	nd	nd	nd	
N4-MB-40-072020	92,28	1,08	23,44	0,01	19,98	4,65	0,60	6,79
W2-10-072020	132,15	0,02	24,71	0,02	46,38	4,94	71,20	6,83
W2-40-072020	11,94	0,09	0,02	0,01	0,01	2,04	3,59	6,63
W2-MB-10-072020	260,14	0,50	58,56	0,02	53,34	7,77	2,63	6,83
W2-MB-40-072020	20,66	0,13	3,99	0,01	38,59	7,08	2,11	6,78
W4-10-072020	nd	nd	nd	nd	nd	nd	nd	
W4-40-072020	159,19	0,03	24,60	0,00	26,63	0,32	54,88	6,73
W4-MB-10-072020	332,11	0,90	64,91	0,02	53,61	3,10	2,80	6,81
W4-MB-40-072020	39,56	0,32	7,00	0,01	39,93	4,85	5,73	6,77
Surface water	76,19	0,31	11,91	0,01	9,46	0,16	9,42	7,32

AUG 2020	Ca	Fe	Mg	Ni	Si	P	S	pH
90	mg/l	mg/l	mg/l	mg/l	mg/l	mg/l	mg/l	
R-10-082020	nd	nd	nd	nd	nd	nd	nd	
R-40-082020	nd	nd	nd	nd	nd	nd	nd	
R-MB10-082020	nd	nd	nd	nd	nd	nd	nd	
R-MB-40-082020	19,35	0,02	3,48	0,00	4,59	0,47	1,84	6,7
S1-10-082020	119,84	0,19	26,38	0,01	25,11	1,86	81,85	7,18
S1-40-082020	72,08	53,77	12,80	0,01	9,22	56,28	15,25	6,86
S1-MB-10-082020	312,11	25,20	73,33	0,02	45,48	15,92	2,89	6,51
S1-MB-40-082020	131,63	4,78	31,11	0,01	32,60	7,77	0,98	6,6
S2-10-082020	109,64	2,42	28,39	0,01	30,12	5,08	1,12	7,17
S2-40-082020	16,85	0,08	3,82	0,01	8,47	2,38	3,68	6,76
S2-MB-10-082020	196,85	13,72	55,49	0,03	40,28	17,05	2,69	6,73
S2-MB-40-082020	139,36	3,31	37,41	0,02	46,52	12,01	1,81	6,6
S3-10-082020	54,31	0,01	16,13	0,01	18,75	2,34	9,42	7,15
S3-40-082020	1,44	0,07	0,02	0,00	0,00	0,96	0,12	6,92
S3-MB-10-082020	159,01	9,20	40,32	0,01	29,76	10,76	2,17	6,75
S3-MB-40-082020	239,22	13,62	61,83	0,02	41,57	14,96	0,93	6,73
S4-10-082020	nd	nd	nd	nd	nd	nd	nd	
S4-40-082020	193,00	3,77	55,18	0,02	29,32	2,51	28,46	6,73
S4-MB-10-082020	nd	nd	nd	nd	nd	nd	nd	
S4-MB-40-082020	188,54	1,22	35,32	0,00	53,04	5,59	3,58	6,81
N1-10-082020	nd	nd	nd	nd	nd	nd	nd	
N1-40-082020	nd	nd	nd	nd	nd	nd	nd	
N1-MB-10-082020	334,01	11,79	77,86	0,02	44,14	8,58	3,59	7,15
N1-MB-40-082020	120,35	6,09	27,08	0,01	20,17	6,16	1,26	7,3
N2-10-082020	92,35	185,75	44,60	0,01	0,07	53,03	1,59	7,12
N2-40-082020	nd	nd	nd	nd	nd	nd	nd	
N2-MB-10-082020	169,66	0,05	46,74	0,03	34,20	4,29	94,51	6,9
N2-MB-40-082020	195,96	7,27	54,61	0,01	39,50	10,54	0,97	6,87
N3-10-082020	nd	nd	nd	nd	nd	nd	nd	
N3-40-082020	160,91	1576,46	37,19	0,02	0,32	210,98	15,60	6,99
N3-MB-10-082020	200,13	9,98	53,35	0,02	36,92	12,11	3,66	6,88
N3-MB-40-082020	65,04	0,40	19,75	0,02	16,85	2,47	39,66	6,98
N4-10-082020	nd	nd	nd	nd	nd	nd	nd	
N4-40-082020	106,46	3,46	30,27	0,01	20,31	7,15	1,48	7,34
N4-MB-10-082020	140,93	0,51	39,16	0,01	30,97	2,55	7,10	7,17
N4-MB-40-082020	36,17	0,97	6,45	0,00	7,63	2,10	0,38	6,94
W2-10-082020	30,64	248,70	67,61	0,01	0,07	42,91	2,55	6,8
W2-40-082020	10,13	0,44	0,09	0,01	0,01	1,14	1,65	6,81
W2-MB-10-082020	336,99	13,05	72,57	0,02	51,14	11,85	3,21	6,94
W2-MB-40-082020	52,63	0,01	12,03	0,01	26,25	1,28	27,23	6,62
W4-10-083020	nd	nd	nd	nd	nd	nd	nd	
W4-40-083020	425,64	11,77	90,53	0,02	50,95	4,11	192,43	6,76
W4-MB-10-0820	429,05	6,62	79,54	0,02	53,93	5,24	3,35	7,14
W4-MB-40-0820	271,07	5,35	51,04	0,01	53,25	10,05	1,90	6,9
Surface water	75,42	0,50	11,80	0,01	9,43	0,19	9,30	7,47

Deltares

NOV 2020	Ca	Fe	Mg	Ni	Si	P	S	pH
120	mg/l	mg/l	mg/l	mg/l	mg/l	mg/l	mg/l	On-site
R 10 112020	nd	nd	nd	nd	nd	nd	nd	
R 40 112020	47,74	0,04	12,35	<dl	11,02	1,6	5,75	6,5
R MB10 112020	219,55	24,34	54,15	<dl	39,28	20,52	1,17	
R MB40 112020	214,86	20,36	53,28	<dl	39,17	18,24	1,11	6,8
S1 10 112020	29,76	0,02	5,59	<dl	8,64	0,48	3,66	6,5
S1 40 112020	120,11	0,08	23,75	<dl	12,94	0,85	23,74	6,5
S1 MB10 112020	275,61	24,68	67,22	<dl	34,03	13,46	0,7	6,5
S1 MB40 112020	339,43	41,81	85,08	<dl	39,08	19,37	2,54	6,5
S2 10 112020	17,23	0,06	4,26	<dl	6,93	1,53	1,67	7,3
S2 40 112020	98,7	2,5	28,07	0,02	17,8	1,47	2,99	6,7
S2 MB10 112020	169,83	18,93	48,75	<dl	25,47	13,54	1,47	6,5
S2 MB40 112020	247,36	26,33	71,15	<dl	43,21	22,76	1,31	6,6
S3 10 112020	18,5	0,04	5,23	<dl	6,36	1,23	1,01	7
S3 40 112020	78,46	0,01	12,49	<dl	9,87	0,87	9,87	7
S3 MB10 112020	123,39	15,39	30,3	<dl	15,92	10,12	1,1	6,5
S3 MB40 112020	nd	22,91	64,55	<dl	33,99	19,46	0,82	6,5
S4 10 112020	149,26	0,09	17,49	<dl	13,11	1,2	42,64	7,2
S4 40 112020	327,09	10,5	46,73	<dl	22,34	11,31	2,99	7
S4 MB10 112020		25,83	76,64	<dl	39,2	18,71	0,74	6,9
S4 MB40 112020	nd	15,29	29,01	<dl	14,25	7,83	0,81	6,8
N1 10 112020	27,69	0,13	5,55	<dl	10,14	1,83	< MDL	7,7
N1 40 112020	59,96	0,01	13,81	<dl	10,79	1,48	36,79	7,1
N1 MB10 112020	283,42	30,01	71,58	<dl	35,29	15,86	0,91	7
N1 MB40 112020	386,54	44,81	92,35	<dl	38,7	17,42	2,78	6,6
N2 10 112020	20,63	0,26	6,04	<dl	15,58	4,04	< MDL	7,3
N2 40 112020	72,12	< MDL	14,8	<dl	15,31	1,46	32,63	7,1
N2 MB10 112020	284,71	24,8	82,01	<dl	37,25	17,89	0,66	6,6
N2 MB40 112020	355,74	41,25	104,7	<dl	45,54	23,33	3,16	6,5
N3 10 112020	302,68	28,3	84,38	<dl	37,04	17,36	1,55	6,5
N3 40 112020	113,64	0,01	23,59	<dl	13,32	1,3	61,15	7,1
N3 MB10 112020	95,5	4,8	25,74	<dl	17,52	3,76	< MDL	8
N3 MB40 112020	109,41	11,24	30,99	<dl	14,32	6,3	0,97	6,7
N4 10 112020	276,88	0,09	33,49	<dl	13,08	0,59	86,82	6,9
N4 40 112020	376,91	7,17	58,69	<dl	23,78	9,11	7,22	6,9
N4 MB10 112020	303,52	37,78	96,79	<dl	45,09	24,05	2,73	6,9
N4 MB40 112020	96,18	11,26	23,37	<dl	10,62	6,43	0,67	6,9
W2 10 112020	31,24	< MDL	5,76	<dl	25,01	1,94	< MDL	7,3
W2 40 112020	62,29	0,02	8,61	<dl	20,26	0,85	8,28	7,3
W2 MB10 112020	303,25	13,49	58,44	<dl	46,19	15,56	0,9	6,6
W2 MB40 112020	399,17	33,17	88,04	<dl	45,94	18,78	2,65	6,6
W4 10 112020	597,34	14,29	72,9	<dl	31,77	7,45	78,42	6,9
W4 40 112020	327,61	0,43	33,01	<dl	25,79	1,35	76,01	7,3
W4 MB10 112020	373,62	18,02	71,86	<dl	47,42	16,66	1,14	6,9
W4 MB40 112020	508,52	34,44	95,35	<dl	48,89	16,17	2,61	6,7
Surface water	121,46	0,28	16,06	<dl	8,67	<dl	35,34	7,4

DEC 2020	Ca	Fe	Mg	Ni	Si	P	S	pH
150	mg/l	mg/l	mg/l	mg/l	mg/l	mg/l	mg/l	
R-10-122020	2,31	0,08	0,56	0,00	1,03	0,21	0,39	6,6
R-40-122020	61,35	0,02	6,59	0,00	10,37	37,23	1,67	6,6
R-MB-10-122020	188,08	14,71	45,64	0,01	42,63	1,96	17,03	6,7
R-MB-40-122020	nd	nd	nd	nd	nd	nd	nd	nd
S1-10-122020	30,23	0,02	5,97	0,00	4,97	2,75	0,51	7,56
S1-40-122020	142,60	1,22	31,27	0,00	16,29	44,45	2,08	7,43
S1-MB-10-122020	226,78	17,34	53,45	0,01	35,01	1,11	11,34	6,91
S1-MB-40-122020	327,17	35,73	76,81	0,02	42,23	2,99	18,22	7,51
S2-10-122020	26,41	0,08	6,33	0,01	7,37	5,40	1,92	7,33
S2-40-122020	110,74	2,22	29,32	0,01	21,54	11,80	3,47	6,63
S2-MB-10-122020	224,88	19,37	62,02	0,02	47,72	1,68	19,04	6,41
S2-MB-40-122020	146,35	5,15	42,07	0,02	30,47	2,07	8,45	7,45
S3-10-122020	13,16	0,03	3,74	0,00	3,63	0,76	1,03	8,1
S3-40-122020	85,86	0,07	24,92	0,00	12,22	10,10	1,35	7,62
S3-MB-10-122020	270,55	22,85	69,84	0,01	40,62	1,31	18,54	6,93
S3-MB-40-122020	118,73	12,24	29,37	0,01	20,40	1,45	10,50	6,85
S4-10-122020	322,18	1,30	36,84	0,00	15,44	117,09	2,14	nd
S4-40-122020	326,44	3,55	79,28	0,01	19,04	135,69	2,17	7,22
S4-MB-10-122020	258,62	18,55	68,40	0,01	40,43	0,96	14,51	7,58
S4-MB-40-122020	86,33	7,64	19,21	0,01	13,14	0,89	5,63	6,15
N1-10-122020	24,41	0,04	4,93	0,00	6,69	1,75	2,00	7,8
N1-40-122020	72,48	0,01	17,20	0,00	9,75	55,96	1,77	7,27
N1-MB-10-122020	259,97	27,20	61,76	0,01	36,73	1,23	13,76	7,8
N1-MB-40-122020	368,18	37,86	82,44	0,02	40,42	3,31	17,54	6,83
N2-10-122020	17,13	0,21	4,57	0,01	16,86	4,03	5,05	7,82
N2-40-122020	162,48	0,10	39,22	0,00	15,37	113,74	1,86	7,24
N2-MB-10-122020	264,42	17,61	72,30	0,01	38,61	0,89	13,93	6,68
N2-MB-40-122020	332,88	34,63	90,32	0,03	46,78	3,66	21,95	7,05
N3-10-122020	nd	nd	nd	nd	nd	nd	nd	8,07
N3-40-122020	139,99	0,02	26,72	0,01	11,32	87,71	1,19	7,93
N3-MB-10-122020	275,86	22,65	73,70	0,02	38,89	2,35	16,16	7,7
N3-MB-40-122020	31,02	3,22	6,65	0,00	4,09	0,68	2,17	6,98
N4-10-122020	445,79	1,73	54,31	0,00	15,11		1,22	8,07
N4-40-122020	368,71	4,79	57,81	0,01	18,45	127,06	3,75	7,48
N4-MB-10-122020	105,81	5,68	26,27	0,01	17,92	0,88	6,17	6,93
N4-MB-40-122020	135,76	9,34	36,33	0,01	22,65	1,34	7,15	6,23
W2-10-122020	24,57	0,03	4,52	0,00	19,43	3,28	2,66	8,05
W2-40-122020	68,39	0,03	11,82	0,00	16,10	4,12	1,71	7,35
W2-MB-10-122020	270,00	8,56	49,99	0,01	49,34	1,25	11,38	7,11
W2-MB-40-122020	366,07	29,76	76,15	0,02	47,75	3,00	17,85	nd
W4-10-122020	458,07	0,54	50,98	0,00	18,32	201,06	1,24	7,82
W4-40-122020	582,95	6,06	69,09	0,01	22,17	225,37	1,65	7,49
W4-MB-10-122020	346,76	13,39	63,47	0,01	48,80	1,34	13,00	7,45
W4-MB-40-122020	478,71	28,29	83,13	0,02	51,56	3,19	14,30	7,81
Surface water	nd	nd	nd	nd	nd	nd	nd	7,4

Deltares

FEB 2021	Ca	Fe	Mg	Ni	Si	P	S	pH	AlK	DOC
210	mg/l	mg/l	mg/l	mg/l	mg/l	mg/l	mg/l	On-site	mg/l	mg/l
R-10-221	nd	nd	nd	nd	nd	nd	nd	nd	nd	nd
R-40-221	52,26	0,02	10,02	0,0026	8,78	1,14	1,47	6,6	211	nd
R-MB10-221	240,74	19,52	62,91	0,0066	35,28	14,27	1,57	6,6	1131,4	110,4
R-MB40-221	305,94	38,06	87,09	0,0123	36,41	15,72	2,18	6,8	1585,9	nd
S1-10-221	26,23	0,01	5,82	0,0028	3,97	0,30	2,22	6,9	115,2	nd
S1-40-221	101,35	0,03	11,14	0,0004	9,75	0,58	9,60	6,9	380,5	9,0
S1-MB10-221	289,53	24,77	71,22	0,0048	31,64	11,49	0,97	6,7	1342,8	70,9
S1-MB40-221	347,50	32,23	89,44	0,0186	33,36	10,55	2,64	6,7	1531,4	nd
S2-10-221	12,35	0,07	3,15	0,0044	4,35	1,13	1,01	nd	nd	nd
S2-40-221	86,08	2,43	25,56	0,0049	11,51	2,32	1,51	6,7	415,1	13,9
S2-MB10-221	233,54	22,55	71,34	0,0129	38,54	16,73	1,41	6,7	1298,1	nd
S2-MB40-221	175,25	14,34	52,72	0,0191	22,08	7,96	1,72	6,7	833,7	88,9
S3-10-221	11,49	0,05	3,37	0,0050	2,79	0,86	0,31	7,1	65,6	nd
S3-40-221	61,32	0,00	6,62	0,0005	7,01	0,37	2,93	6,8	208,1	6,1
S3-MB10-221	260,78	21,75	73,62	0,0139	35,21	16,18	1,24	6,6	1384,6	73,4
S3-MB40-221	212,25	18,30	58,83	0,0160	26,56	9,83	1,93	6,7	1033,6	103,6
S4-10-221	153,98	0,01	18,46	0,0041	10,72	0,77	19,47	7,1	523,0	nd
S4-40-221	270,97	6,87	57,42	0,0015	24,46	7,11	10,23	6,9	1035,4	25,4
S4-MB10-221	258,90	18,49	74,73	0,0077	34,37	14,18	1,00	6,7	1247,2	70,0
S4-MB40-221	124,55	12,30	30,97	0,0050	13,39	5,14	0,91	6,5	560,5	46,8
N1-10-221	21,06	0,06	4,42	0,0052	8,28	1,34	0,75	nd	nd	nd
N1-40-221	66,49	0,01	14,76	0,0001	8,48	0,93	16,34	7,2	235,2	15,3
N1-MB10-221	262,59	21,04	66,95	0,0083	28,16	10,61	0,96	nd	1250,3	nd
N1-MB40-221	401,28	47,28	98,21	0,0162	34,15	11,80	2,81	6,7	1685,8	nd
N2-10-221	nd	nd	nd	nd	nd	nd	nd	nd	nd	nd
N2-40-221	57,94	0,01	12,61	0,0021	10,52	0,98	5,57	6,9	259,8	nd
N2-MB10-221	284,71	24,41	84,96	0,0079	35,69	15,25	0,97	6,7	1393,1	69,5
N2-MB40-221	356,31	34,42	109,08	0,0250	38,76	13,91	3,09	6,8	1592,6	157,4
N3-10-221	nd	nd	nd	nd	nd	nd	nd	nd	nd	nd
N3-40-221	77,77	0,01	12,12	0,0026	10,01	0,89	6,80	7,1	290,6	17,2
N3-MB10-221	291,85	21,42	83,49	0,0061	32,94	10,83	1,54	6,8	1399,0	136,2
N3-MB40-221	162,65	15,93	48,90	0,0087	18,94	7,23	1,46	6,6	723,2	73,5
N4-10-221	302,03	0,02	37,95	0,0006	13,34	0,30	40,54	7	1049,6	24,6
N4-40-221	323,60	7,10	44,44	0,0026	16,75	2,94	47,30	6,9	1136,0	29,5
N4-MB10-221	286,38	21,03	97,92	0,0180	40,67	13,07	2,71	7	1584,3	nd
N4-MB40-221	212,94	16,80	65,52	0,0119	24,41	7,19	1,53	6,7	1001,2	84,8
W2-10-221	26,14	0,07	4,42	0,0143	24,70	1,68	1,20	nd	nd	nd
W2-40-221	59,64	0,01	6,76	0,0017	10,01	0,39	3,71	7,2	211,8	nd
W2-MB10-221	308,57	10,07	61,59	0,0034	42,35	12,12	0,88	6,8	1313,5	82,7
W2-MB40-221	411,79	31,51	93,96	0,0084	40,88	13,32	2,75	6,8	1744,1	nd
W4-10-221	245,07	0,29	29,52	0,0014	16,83	0,84	14,13	7,1	941,0	24,9
W4-40-221	430,28	12,75	52,89	0,0033	23,89	3,38	3,07	6,9	1676,1	56,0
W4-MB10-221	349,45	16,72	68,58	0,0064	41,57	13,87	1,22	6,8	1637,1	93,1
W4-MB40-221	521,47	31,83	100,90	0,0071	43,32	11,69	2,48	6,9	2130,9	nd
Surface water	124,35	0,37	15,13	0,0010	3,87	0,05	41,22	7,7	337,9	11,3

MAY 2021	Ca	Fe	Mg	Ni	Si	P	S	pH	TC	TIC	DOC
300	mg/l	mg/l	mg/l	mg/l	mg/l	mg/l	mg/l	On-site	mg/l	mg/l	mg/l
R-10-621								nd			
R-40-621	22,65	0,16	4,95	0,0013	8,70	1,70	0,80	6,6	77,11	50,69	26,4
R-MB10-621	260,09	23,63	61,19	0,0095	38,63	16,55	2,04	6,6	329,90	228,05	101,8
R-MB40-621	338,82	32,51	80,24	0,0087	38,70	12,05	2,38	6,7	398,16	290,23	107,9
S1-10-621	23,36	0,03	4,93	0,0001	5,46	0,59	2,36	nd			
S1-40-621	90,23	0,01	9,36	0,0023	10,59	0,43	9,05	6,9	74,19	55,21	19,0
S1-MB10-621	295,72	24,32	65,50	0,0049	33,21	11,25	1,08	6,8	346,23	286,01	60,2
S1-MB40-621	369,24	30,52	86,49	0,0186	35,72	8,07	3,05	6,9	485,21	338,80	146,4
S2-10-621	8,65	0,07	1,89	0,0036	3,85	0,50	0,11	nd			
S2-40-621	61,70	0,02	16,37	0,0045	12,54	0,40	3,64	6,6	76,63	49,44	27,2
S2-MB10-621	242,53	12,78	67,08	0,0148	40,34	10,92	1,62	6,6			
S2-MB40-621	201,26	22,64	53,98	0,0179	23,36	8,43	1,56	6,6	308,21	232,71	75,5
S3-10-621	16,13	0,13	3,98	0,0057	6,11	0,93	2,56	nd			
S3-40-621	91,62	0,01	9,01	0,0040	10,73	0,40	3,71	6,6	74,10	57,07	17,0
S3-MB10-621	234,18	20,76	60,48	0,0115	34,39	13,06	1,17	6,8	332,42	253,95	78,5
S3-MB40-621	108,26	11,29	26,46	0,0065	13,39	4,68	1,10	6,8	178,44	131,04	47,4
S4-10-621	110,92	0,03	12,27	0,0023	12,06	0,71	21,33	7,3	93,50	59,98	33,5
S4-40-621	259,57	8,15	49,77	0,0013	23,89	5,76	2,28	7	197,16	177,04	20,1
S4-MB10-621	230,62	17,31	60,08	0,0083	32,79	13,27	0,94	6,8	308,01	242,63	65,4
S4-MB40-621	218,62	23,35	52,46	0,0067	22,12	7,84	1,42	6,9	329,22	246,04	83,2
N1-10-621	14,82	0,04	2,71	0,0040	4,60	0,63	0,23	nd			
N1-40-621	108,93	0,02	17,78	0,0024	12,02	1,23	31,66	7,2	93,78	59,61	34,2
N1-MB10-621	305,26	23,32	69,53	0,0066	33,17	10,97	1,25	6,9	337,93	266,17	71,8
N1-MB40-621	384,19	31,39	85,32	0,0129	32,79	6,33	2,66	6,7	505,31	375,16	130,1
N2-10-621								nd			
N2-40-621	72,64	0,03	13,59	0,0009	16,45	1,44	3,44	7			
N2-MB10-621	281,44	22,05	75,68	0,0090	37,92	13,45	1,07	6,8	335,13	290,01	45,1
N2-MB40-621	357,81	29,43	97,88	0,0240	38,03	9,72	2,91	6,8	514,77	353,03	161,7
N3-10-621								nd			
N3-40-621	112,82	0,02	15,90	0,0011	12,32	0,91	29,84	7,2			
N3-MB10-621								6,9	234,17	165,70	68,5
N3-MB40-621	165,58	16,51	45,60	0,0097	17,59	5,71	1,61	6,6	232,05	164,22	67,8
N4-10-621	181,19	0,03	20,97	0,0010	12,02	0,30	32,20	7	138,90	100,15	38,8
N4-40-621	178,65	0,57	32,02	0,0019	17,04	0,18	9,48	nd	146,17	137,54	8,6
N4-MB10-621	294,48	19,86	86,84	0,0224	42,79	11,79	2,81	7,3			0,0
N4-MB40-621	237,73	23,60	63,26	0,0133	22,69	8,10	1,64	6,7	320,31	240,79	79,5
W2-10-621								nd			
W2-40-621	75,96	0,02	7,69	0,0021	16,73	0,55	3,01	7,1			
W2-MB10-621	294,52	12,03	50,44	0,0015	43,58	11,56	0,81	7	313,54	253,93	59,6
W2-MB40-621	445,64	27,62	88,52	0,0113	43,60	9,84	2,60	7	458,47	347,68	110,8
W4-10-621	177,72	0,02	19,10	0,0035	18,11	0,38	25,95	7,2	129,57	114,97	14,6
W4-40-621	385,09	8,29	42,22	0,0012	32,86	3,57	2,16	6,9	300,03	280,79	19,2
W4-MB10-621	347,27	16,01	60,46	0,0025	45,04	11,32	1,13	7	371,02	291,28	79,7
W4-MB40-621	490,29	21,79	92,68	0,0081	45,26	6,34	2,43	7,3	51,86	37,77	14,1
Surface water	118,20	0,15	16,16	0,0003	4,54	0,06	30,19	7,6	65,96	57,93	8,0

Deltares

OCT 2021	Ca	Fe	Mg	Ni	Si	P	S	pH	TC	TIC	DOC	APR 2022	Ca	Fe	Mg	Ni	Si	P	S	pH
460	mg/l	mg/l	mg/l	mg/l	mg/l	mg/l	mg/l	On-site	mg/l	mg/l	mg/l	680	mg/l	mg/l	mg/l	mg/l	mg/l	mg/l	mg/l	
R-10-1021	54,46	0,15	10,12	0,12	8,51	1,63	10,33	nd	133,7	23,4	110,4	R-10-								
R-40-1021												R-40-	42,54		8,32	1,1564	8,14			6,6
R-MB10-1021	264,95	30,40	63,11	5,83	34,51	16,50	3,56	6,40	397,3	317,7	79,6	R-MB-10-								
R-MB40-1021	339,82	24,21	82,07	8,60	36,46	8,21	4,42	6,50	473,2	403,3	69,9	R-MB-40-	304,76		90,80	6,48	35,95			6,5
S1-10-1021												S1-10-	22,22		6,04	1,12	6,83			7,1
S1-40-1021	115,96	0,03	12,77	0,35	9,35	0,20	58,92	6,90	61,0	54,7	6,3	S1-40-	98,34		10,63	0,35	12,74			6,9
S1-MB10-1021	279,92	8,24	65,16	0,47	31,05	3,54	2,81	6,90	355,2	339,7	15,5	S1-MB-10-								
S1-MB40-1021	373,15	20,67	87,95	14,06	33,60	5,39	5,12	6,90	522,8	427,5	95,3	S1-MB-40-	341,80		79,56	6,76	32,12			6,9
S2-10-1021												S2-10-	14,64		7,26	2,39	7,84			7
S2-40-1021	83,43	0,09	22,52	3,57	12,85	0,61	53,29	7,00	60,0	46,4	13,6	S2-40-	72,11		18,30	1,85	9,65			6,8
S2-MB10-1021	176,69	8,63	50,31	9,27	29,19	4,46	2,21	6,90	268,7	232,5	36,2	S2-MB-10-								
S2-MB40-1021	157,58	7,65	41,52	8,36	18,44	2,67	2,27	6,80	224,0	187,8	36,2	S2-MB-40-	168,99		45,10	9,87	20,40			6,8
S3-10-1021	26,13	0,18	6,80	5,16	11,76	0,58	4,70	6,90				S3-10-								
S3-40-1021	76,17	0,03	11,59	2,70	15,29	1,29	14,37	7,00	54,6	45,2	9,4	S3-40-	61,19		9,03	3,34	11,19			6,8
S3-MB10-1021												S3-MB-10-								
S3-MB40-1021	190,13	10,57	48,76	5,56	23,58	4,35	3,33	6,80	251,1	220,3	30,8	S3-MB-40-	111,87		37,71	5,86	18,75			6,9
S4-10-1021	734,43	0,16	89,22	3,66	11,03	0,15	546,11	7,00				S4-10-								
S4-40-1021	502,44	0,10	69,39	0,63	14,67	0,15	221,19	6,90	184,8	169,1	15,7	S4-40-	312,80		43,45	0,000	18,23			7,1
S4-MB10-1021									187,7	185,2	2,5	S4-MB-10-								
S4-MB40-1021	143,03	6,55	33,90	0,64	14,16	2,42	1,90	6,90				S4-MB-40-	160,01		24,31	0,83	17,21			6,9
N1-10-1021				0,00								N1-10-								
N1-40-1021	37,99	0,12	7,33	2,18	14,26	1,44	3,90	nd				N1-40-	47,44		11,28	2,00	13,32			7,2
N1-MB10-1021	303,53	7,76	73,71	1,02	31,21	3,39	3,28	nd	411,8	376,5	35,3	N1-MB-10-	299,10		59,40	0,56	28,76			6,9
N1-MB40-1021	404,89	36,47	90,40	7,51	32,54	8,02	5,33	nd	534,9	454,8	80,1	N1-MB-40-								
N2-10-1021												N2-10-								
N2-40-1021	66,67	0,05	12,97	2,92	12,88	1,87	9,61	nd				N2-40-	50,50		11,62	0,88	13,46			7,0
N2-MB10-1021	267,43	8,40	75,86	7,94	34,31	5,10	2,95	nd	381,2	348,1	33,1	N2-MB-10-								
N2-MB40-1021	350,51	17,22	98,26	18,77	37,12	5,57	5,13	nd	560,8	449,5	111,3	N2-MB-40-	360,44		72,14	12,65	31,12			6,8
N3-10-1021												N3-10-								
N3-40-1021	40,35	0,08	10,38	4,58	10,32	0,27	2,61	6,90				N3-40-	110,26		13,73	0,001	13,84			6,9
N3-MB10-1021				0,00								N3-MB-10-								
N3-MB40-1021									88,4	42,5	45,9	N3-MB-40-								
N4-10-1021												N4-10-								
N4-40-1021	469,38	0,23	65,61	0,44	16,96	0,13	244,42	7,00	159,5	149,9	9,6	N4-40-	330,78		42,12	1,00	16,39			7,1
N4-MB10-1021												N4-MB-								
N4-MB40-1021												N4-MB-40-								
W2-10-1021												W2-10-								
W2-40-1021	48,71	0,03	7,86	0,35	21,46	1,17	6,15	6,80	154,1	36,2	117,9	W2-40-	83,11		8,17	0,02	12,67			7,1
W2-MB10-1021									547,3	467,3	80,0	W2-MB-10-								
W2-MB40-1021	451,86	23,69	90,83	1,73	43,73	8,59	5,31	6,90				W2-MB-40-	423,78		81,86	2,23	44,72			7,0
W4-10-1021	100,21	0,03	10,99	0,32	15,26	0,24	39,07	7,20	90,1	45,1	44,9	W4-10-	112,90		11,05	1,00	13,71			7,2
W4-40-1021												W4-40-	223,21		44,32	0,10	25,25			7,3
W4-MB10-1021									598,5	577,7	20,8	W4-MB-10-								
W4-MB40-1021	552,62	12,67	94,66	0,19	48,40	3,97	5,87	7,10				W4-MB-40-	560,74		73,26	1,10	42,66			7,1
Surface water	62,19	0,26	9,85	0,12	6,33	0,25	10,49	7,50	52,6	44,1	8,6	Surface water	80,02		12,60	0,23	8,45			7,6

Deltares

E Chemical soil extractions

Aqua regia destruction and 0.43M HNO_3 extraction of soils in field plots and mesocosms.

Aqua Regia	mg/kg																										
	Al	As	Ba	Be	Ca	Cd	Ce	Co	Cr	Fe	K	Li	Mg	Mn	Na	Ni	P	Pb	Sc	Sr	Ti	V	Zn
blanc 1	0,00	5,84	<	<	2,88	2,94	<	<	0,32	268,22	45,39	7,11	2,30	<	859,8	1,71	0,59	4,08	0,42	<	0,15	<	7,28
N1-10	4880	12,25	33,01	0,33	5795	0,50	10,26	6,50	15,85	8568	1095	14,90	12014	246,2	863,7	117,19	340,2	10,25	1,54	20,60	105,1	10,36	55,00
N1-40	7319	12,47	36,74	0,35	3091	0,26	12,81	2,94	16,58	10182	1443	18,99	3867	271,9	741,7	37,51	379,3	8,14	1,91	13,41	155,6	13,81	50,21
S1-MB-10	7353	13,41	38,31	0,38	4559	0,37	11,48	5,69	39,00	9485	1678	17,05	10136	185,6	535,7	94,36	379,8	10,41	2,07	16,38	153,4	14,09	46,79
S1-MB-40	5109	12,82	31,49	0,28	3412	0,75	7,23	1,42	10,32	6864	1297	14,01	1272	209,2	477,2	11,42	422,2	10,87	1,44	13,20	137,1	10,50	38,11
N2	5868	15,64	32,07	0,30	3194	0,13	12,99	2,39	12,84	8166	1267	14,46	3366	184,3	343,5	32,12	324,8	9,62	1,58	13,05	140,3	11,22	41,02
N2-MB	4813	6,33	27,12	0,24	2657	0,38	10,87	3,66	9,99	6235	1151	12,25	4614	165,0	232,6	39,10	257,0	6,03	1,41	11,73	130,3	9,33	34,47
S2	3919	17,56	24,23	0,98	2988	1,01	12,08	1,80	11,48	5224	801	11,91	1600	116,5	170,8	17,18	243,9	4,86	2,08	11,18	79,3	7,91	31,72
S2-MB	4020	17,66	25,22	1,00	3102	1,02	12,00	1,70	11,78	5431	821	11,12	1650	120,3	170,1	17,23	262,0	4,95	2,10	12,00	81,7	8,00	32,91
N3	5964	12,09	34,61	0,31	3689	0,38	11,41	2,61	12,98	7499	1362	14,92	2984	219,9	214,5	26,67	358,6	11,34	1,65	14,59	133,6	11,88	41,50
N3-MB	5453	10,03	32,43	0,30	3403	0,12	12,58	2,61	11,66	7100	1395	14,47	2386	182,3	236,6	20,54	326,6	7,55	1,48	15,36	131,5	11,00	37,60
S3	6542	12,43	36,66	0,35	4539	0,38	11,50	2,44	15,10	7895	1436	16,25	2614	237,4	208,5	24,53	348,0	9,59	1,76	17,69	145,0	12,91	43,45
S3-MB	4638	10,98	26,85	0,26	2700	0,32	10,36	1,14	11,44	5630	1223	13,40	1760	151,0	162,1	12,50	271,9	10,28	1,39	10,65	126,8	9,50	31,18
R	4709	11,67	28,55	0,24	2942	<	9,87	0,24	9,72	5938	1067	13,62	1018	188,7	64,0	9,09	262,8	8,09	1,39	11,48	131,7	9,16	31,08
R-MB	5779	11,95	33,17	0,32	3420	0,24	15,32	1,70	11,20	7524	1373	14,14	1320	198,7	125,0	10,24	398,2	12,42	1,49	15,86	123,9	12,73	48,69
W2	5569	12,47	31,25	0,27	3890	0,23	10,09	0,68	10,69	6518	1139	14,27	1285	148,6	46,7	9,50	280,5	6,89	1,40	17,07	127,7	9,75	34,40
W2-MB	4132	10,13	26,17	0,23	3207	0,10	7,00	0,37	8,66	5142	1068	11,82	880	134,4	34,7	9,25	231,8	4,85	1,22	13,56	119,8	7,94	28,66
N4	5942	10,42	33,74	0,31	5520	0,70	9,61	1,97	12,77	7248	1214	14,96	3513	235,6	123,8	32,68	299,1	12,21	1,65	21,56	140,9	12,73	42,05
N4-MB	5601	10,24	31,89	0,31	5551	0,70	9,56	1,78	12,97	7331	1321	14,00	3535	246,8	122,2	33,02	304,6	12,00	1,70	19,93	139,9	13,90	44,20
S4	5209	18,68	31,79	0,31	3741	1,10	12,47	1,01	11,19	6176	1052	16,48	1383	185,6	427,2	13,10	264,8	9,62	1,53	15,77	137,4	10,29	39,30
S4-MB	5256	18,90	32,00	0,31	3799	1,20	12,78	1,00	11,76	6230	1200	16,30	1401	210,0	439,0	13,20	270,0	10,01	1,43	15,88	134,1	9,97	41,27
W2	4125	9,12	24,72	0,23	5161	0,55	9,77	0,54	8,78	5524	1048	12,82	900	145,8	90,9	7,90	342,7	5,56	1,27	14,00	139,9	8,68	26,27
W4	4127	10,23	25,72	0,23	5244	0,55	10,16	0,54	10,90	5433	1057	12,82	917	160,4	90,4	8,11	324,9	5,54	1,27	14,31	141,0	8,77	28,44
W4-MB	7973	17,23	42,31	0,42	6750	0,33	26,59	2,49	15,74	11195	1485	19,76	1286	236,3	271,9	14,99	394,3	12,78	2,10	26,61	159,5	16,35	55,78
blanc 2	1,29	14,78	<	0,01	2,37	0,36	<	<	0,70	267,82	>	5,91	1,94	<	<	1,85	<	<	0,46	<	0,13	<	<
Recovery%	45	135	68	65	94	105	65	76	80	86	50	92	83	102	53	93	110	103	48	72	14	79	100

Aqua Nitrosa	mg/kg																						
	Al	As	Ba	Be	Ca	Cd	Ce	Co	Cr	Fe	K	Li	Mg	Mn	Na	Ni	P	Pb	Sc	Sr	Ti	V	Zn
blanc 1	0,05	0,48	0,00	0,00	0,21	0,01	<	<	0,00	13,17	-0,39	<	0,05	<	<	0,02	<	<	0,02	<	0,01	<	<
N1-10	384	1,35	16,60	0,09	3118	0,08	3,19	1,27	0,56	1025	141,9	0,19	553,3	140,1	<	4,85	138,7	7,21	0,04	10,23	4,10	2,20	16,64
N1-40	434	1,37	17,08	0,11	3412	0,11	3,58	1,20	0,61	1200	119,7	0,23	404,5	142,2	<	2,29	166,8	8,61	0,05	10,28	3,28	2,54	18,83
S1-MB-10	360	1,38	14,98	0,11	3140	0,10	3,21	2,16	2,41	1534	223,0	0,16	928,3	127,5	<	20,09	192,0	7,43	0,07	9,11	4,04	2,73	17,32
S1-MB-40	471	1,87	17,29	0,12	3025	0,08	4,35	1,39	0,76	1701	289,3	0,24	343,2	152,7	5,19	2,52	247,6	9,67	0,08	9,19	5,70	3,46	18,75
N2	399	1,25	17,18	0,10	3482	0,13	3,79	1,21	0,59	1282	135,3	0,19	396,4	153,4	<	2,59	168,6	8,99	0,05	10,01	3,78	2,51	19,81
N2-MB	390	1,24	16,17	0,11	2961	0,08	3,78	1,32	0,64	1566	280,0	0,19	394,6	148,3	<	2,78	212,5	8,99	0,06	9,14	3,94	3,20	19,69
S2	390	1,09	15,56	0,09	3201	0,09	3,06	1,26	0,61	969	83,2	0,23	379,2	126,0	<	3,59	131,7	7,22	0,03	10,01	3,05	2,18	17,70
S2-MB	389	1,03	15,00	0,09	3176	0,09	3,06	1,26	0,68	1012	81,1	0,22	362,4	142,0	<	3,71	130,2	7,00	0,03	10,00	3,00	2,12	17,98
N3	420	1,31	16,68	0,10	3648	0,11	3,28	1,10	0,55	1008	178,5	0,26	430,2	139,3	<	2,81	165,6	8,11	0,03	11,18	3,72	2,36	18,14
N3-MB	420	1,37	18,12	0,12	3161	0,11	3,87	1,36	0,50	1456	323,4	0,18	360,2	154,2	1,01	2,31	205,3	9,04	0,05	12,93	3,58	3,10	19,01
S3	460	1,15	17,63	0,11	3487	0,10	3,47	1,13	0,76	997	136,3	0,27	359,4	149,5	<	2,51	136,9	8,17	0,04	13,99	3,85	2,61	18,12
S3-MB	330	1,90	13,50	0,09	2630	0,07	3,04	1,07	0,47	1276	287,1	0,13	316,1	121,4	0,43	2,38	177,4	7,74	0,05	8,36	4,12	2,54	16,58
R	352	1,41	13,48	0,08	2370	0,06	2,82	1,02	0,46	1181	251,5	0,17	246,9	106,7	8,01	1,39	146,2	6,36	0,05	8,01	4,09	2,37	15,36
R-MB	419	1,01	17,09	0,10	3664	0,12	3,63	1,18	0,53	1049	136,7	0,21	342,5	155,3	<	1,61	163,1	8,32	0,04	10,69	3,61	2,41	18,76
W2	391	1,07	16,63	0,09	4165	0,10	3,16	1,11	0,52	1052	88,1	0,22	280,5	143,6	<	1,43	165,1	8,03	0,03	14,17	3,23	2,42	18,53
W2-MB	360	0,86	15,45	0,10	3502	0,08	3,49	1,13	0,56	1298	241,1	0,19	276,9	119,0	<	1,61	188,7	8,59	0,05	11,61	4,07	2,74	18,56
N4	554	1,40	18,77	0,14	5145	0,10	4,10	1,11	0,63	1271	82,6	0,41	405,2	211,0	24,48	2,93	143,2	10,27	0,05	17,67	5,15	3,92	19,47
N4-MB	555	1,27	19,00	0,14	5170	0,10	4,10	1,12	0,65	1311	83,8	0,39	412,4	221,5	24,61	2,99	156,7	8,12	0,04	16,90	6,91	4,22	21,37
S4	481	1,27	19,09	0,12	4416	0,10	3,74	1,27	0,72	1191	87,9	0,31	399,5	174,2	25,29	3,70	149,2	8,26	0,04	15,05	4,18	3,17	18,43
S4-MB	483	1,54	19,76	0,12	4441	0,10	3,73	1,19	0,75	1211	88,0	0,30	412,9	197,4	22,20	3,82	165,0	8,11	0,03	12,79	3,98	3,33	19,25
W2	412	1,60	15,65	0,10	3594	0,08	3,51	1,04	0,54	1317	256,3	0,18	269,3	131,3	3,91	1,44	210,9	8,09	0,05	12,55	4,51	2,73	16,87
W4	411	1,75	17,11	0,11	3928	0,08	3,83	1,14	0,59	1439	280,1	0,20	294,4	143,5	4,28	1,57	230,5	8,84	0,05	13,72	4,93	2,98	18,44
W4-MB	438	1,14	16,93	0,11	4727	0,10	3,72	1,21	0,54	1118	69,3	0,31	314,5	149,0	50,55	1,84	131,1	8,95	0,03	16,42	3,35	2,70	17,84
blanc 2	0,05	0,89	0,00	0,00	0,78	0,01	<	-0,09	0,03	13,34	<	0,01	0,08	<	<	0,04	<	<	0,02	<	0,01	<	0,05

F PNEC calculations nickel toxicity

Input parameters, calculated PNEC, probability of exceedance (p), and RCR calculated with PNEC-pro V6 based on Biotic Ligand Models for nickel.

Calculations all data pore water CO-Action okt 2022								
ID	DOC	pH	Ca	Mg	Ni	PNEC	Probability	RCR
	mg/L		mg/L	mg/L	ug/L	ug/L	p	
S1-10	9	6,7	46,74	10,18	3,65	30,06	0,00	0,12
S1-10	9	6,7	119,84	26,38	10,56	31,52	0,00	0,33
S1-10	9	6,7	29,76	5,59	2,80	29,64	0,00	0,09
S1-10	9	6,7	30,23	5,97	0,73	29,68	0,00	0,02
S1-10	9	6,7	26,23	5,82	2,80	29,66	0,00	0,09
S1-10	9	6,7	23,36	4,93	0,06	29,58	0,00	0,00
S1-10	9	6,7	22,22	6,04	1,12	29,68	0,00	0,04
S1-40	9	6,7	28,25	5,49	4,42	29,64	0,00	0,15
S1-40	9	6,7	72,08	12,80	7,32	30,29	0,00	0,24
S1-40	9	6,7	120,11	23,75	0,39	31,28	0,00	0,01
S1-40	9	6,7	142,60	31,27	3,13	31,96	0,00	0,10
S1-40	9	6,7	101,35	11,14	0,39	30,14	0,00	0,01
S1-40	9	6,7	90,23	9,36	0,00	29,98	0,00	0,00
S1-40	9	6,7	115,96	12,77	0,35	30,29	0,00	0,01
S1-40	9	6,7	98,34	10,63	0,35	30,10	0,00	0,01
S2-10	13,9	6,7	70,01	18,15	10,53	37,63	0,00	0,28
S2-10	13,9	6,7	109,64	28,39	11,67	38,56	0,00	0,30
S2-10	13,9	6,7	17,23	4,26	4,43	36,38	0,00	0,12
S2-10	13,9	6,7	26,41	6,33	5,88	36,57	0,00	0,16
S2-10	13,9	6,7	12,35	3,15	4,43	36,28	0,00	0,12
S2-10	13,9	6,7	8,65	1,89	3,56	36,17	0,00	0,10
S2-10	13,9	6,7	14,64	7,26	2,39	36,65	0,00	0,07
S2-40	13,9	6,7	17,55	4,54	2,42	36,41	0,00	0,07
S2-40	13,9	6,7	16,85	3,82	8,02	36,34	0,00	0,22
S2-40	13,9	6,7	98,70	28,07	4,89	38,53	0,00	0,13
S2-40	13,9	6,7	110,74	29,32	5,39	38,64	0,00	0,14
S2-40	13,9	6,7	86,08	25,56	4,89	38,30	0,00	0,13
S2-40	13,9	6,7	61,70	16,37	4,51	37,47	0,00	0,12
S2-40	13,9	6,7	83,43	22,52	3,57	38,03	0,00	0,09
S2-40	13,9	6,7	72,11	18,30	1,85	37,65	0,00	0,05
S3-10	6,1	6,7	33,68	9,40	7,56	25,93	0,00	0,29
S3-10	6,1	6,7	54,31	16,13	9,05	26,53	0,00	0,34
S3-10	6,1	6,7	18,50	5,23	4,96	25,55	0,00	0,19
S3-10	6,1	6,7	13,16	3,74	0,86	25,42	0,00	0,03
S3-10	6,1	6,7	11,49	3,37	4,96	25,38	0,00	0,20
S3-10	6,1	6,7	16,13	3,98	5,66	25,44	0,00	0,22
S3-10	6,1	6,7	26,13	6,80	5,16	25,69	0,00	0,20
S3-40	17	6,7	1,98	0,47	5,21	40,38	0,00	0,13
S3-40	17	6,7	1,44	0,02	1,10	40,34	0,00	0,03
S3-40	17	6,7	78,46	12,49	0,51	41,47	0,00	0,01
S3-40	17	6,7	85,86	24,92	2,57	42,58	0,00	0,06
S3-40	17	6,7	61,32	6,62	0,51	40,94	0,00	0,01
S3-40	17	6,7	91,62	9,01	4,00	41,15	0,00	0,10
S3-40	17	6,7	76,17	11,59	2,70	41,38	0,00	0,07
S3-40	17	6,7	61,19	9,03	3,34	41,15	0,00	0,08
S4-10	33,5	6,7	149,26	17,49	4,07	65,02	0,00	0,06
S4-10	33,5	6,7	322,18	36,84	3,49	66,76	0,00	0,05
S4-10	33,5	6,7	153,98	18,46	4,07	65,10	0,00	0,06
S4-10	33,5	6,7	110,92	12,27	0,00	64,55	0,00	0,00
S4-10	33,5	6,7	734,43	89,22	3,66	71,47	0,00	0,05
S4-40	15,7	6,7	98,71	27,82	8,38	41,02	0,00	0,20
S4-40	15,7	6,7	193,00	55,18	15,90	43,49	0,00	0,37
S4-40	15,7	6,7	327,09	46,73	8,50	42,73	0,00	0,20
S4-40	15,7	6,7	326,44	79,28	10,26	45,66	0,00	0,22
S4-40	15,7	6,7	270,97	57,42	8,50	43,69	0,00	0,19
S4-40	15,7	6,7	259,57	49,77	1,31	43,00	0,00	0,03
S4-40	15,7	6,7	502,44	69,39	0,63	44,77	0,00	0,01
S4-40	15,7	6,7	312,80	43,45	0,00	42,43	0,00	0,00
N1-10	34,2	6,7	50,11	0,08	64,81	64,43	0,54	1,01
N1-10	34,2	6,7			8,50	64,78	0,00	0,13
N1-10	34,2	6,7	27,69	10,14	5,18	65,33	0,00	0,08
N1-10	34,2	6,7	24,41	6,69	3,80	65,02	0,00	0,06
N1-10	34,2	6,7	21,06	8,28	5,18	65,17	0,00	0,08
N1-10	34,2	6,7	14,82	4,60	3,95	64,84	0,00	0,06
N1-40	34,2	6,7			8,50	64,78	0,00	0,13
N1-40	34,2	6,7			8,50	64,78	0,00	0,13
N1-40	34,2	6,7	59,96	13,81	0,13	65,66	0,00	0,00
N1-40	34,2	6,7	72,48	17,20	1,35	65,97	0,00	0,02
N1-40	34,2	6,7	66,49	14,76	0,13	65,75	0,00	0,00
N1-40	34,2	6,7	108,93	17,78	2,44	66,02	0,00	0,04
N1-40	34,2	6,7	37,99	7,33	2,18	65,08	0,00	0,03
N1-40	34,2	6,7	47,44	11,28	2,00	65,44	0,00	0,03
N2-10	45,1	6,7			8,50	80,15	0,00	0,11
N2-10	45,1	6,7	92,35	44,60	6,35	83,69	0,00	0,08
N2-10	45,1	6,7	20,63	6,04	8,50	80,22	0,00	0,11

Continued								
ID	DOC	pH	Ca	Mg	Ni	PNEC	Probability	RCR
	mg/L		mg/L	mg/L	ug/L	ug/L	p	
N2-10	45,1	6,7	17,13	4,57	10,22	80,09	0,00	0,13
N2-10	45,1	6,7		3,07	8,50	79,96	0,00	0,11
N2-10	45,1	6,7			0,00	80,15	0,00	0,00
N2-10	45,1	6,7			0,00	80,15	0,00	0,00
N2-40	33,1	6,7	18,22	0,04	39,01	62,88	0,00	0,62
N2-40	33,1	6,7			8,50	63,23	0,00	0,13
N2-40	33,1	6,7	72,12	14,80	2,11	64,21	0,00	0,03
N2-40	33,1	6,7	162,48	39,22	2,14	66,41	0,00	0,03
N2-40	33,1	6,7	57,94	12,61	2,11	64,02	0,00	0,03
N2-40	33,1	6,7	72,64	13,59	0,89	64,10	0,00	0,01
N2-40	33,1	6,7	66,67	12,97	2,92	64,05	0,00	0,05
N2-40	33,1	6,7	50,50	11,62	0,88	63,93	0,00	0,01
N3-10	17,2	6,7			8,50	40,81	0,00	0,21
N3-10	17,2	6,7			8,50	40,81	0,00	0,21
N3-10	17,2	6,7	302,68	84,38	8,50	48,22	0,00	0,18
N3-10	17,2	6,7			8,50	40,81	0,00	0,21
N3-10	17,2	6,7			8,50	40,81	0,00	0,21
N3-10	17,2	6,7			0,00	40,81	0,00	0,00
N3-10	17,2	6,7			0,00	40,81	0,00	0,00
N3-40	17,2	6,7	10,65	0,04	19,89	40,62	0,00	0,49
N3-40	17,2	6,7	160,91	37,19	24,90	43,97	0,00	0,57
N3-40	17,2	6,7	113,64	23,59	2,65	42,74	0,00	0,06
N3-40	17,2	6,7	139,99	26,72	6,51	43,03	0,00	0,15
N3-40	17,2	6,7	77,77	12,12	2,65	41,71	0,00	0,06
N3-40	17,2	6,7	112,82	15,90	0,00	42,05	0,00	0,00
N3-40	17,2	6,7			0,00	40,81	0,00	0,00
N3-40	17,2	6,7		13,73	0,00	41,86	0,00	0,00
N4-10	24,6	6,7			19,25	51,24	0,00	0,38
N4-10	24,6	6,7			9,45	51,24	0,00	0,18
N4-10	24,6	6,7	276,88	33,49	10,20	54,00	0,00	0,19
N4-10	24,6	6,7	445,79	54,31	12,55	55,87	0,00	0,22
N4-10	24,6	6,7	302,03	37,95	8,50	54,40	0,00	0,16
N4-10	24,6	6,7	181,19	20,97	1,91	52,87	0,00	0,04
N4-10	24,6	6,7			0,44	51,24	0,00	0,01
N4-10	24,6	6,7			1,00	51,24	0,00	0,02
N4-40	29,5	6,7	85,63	23,19	19,25	59,93	0,00	0,32
N4-40	29,5	6,7	106,46	30,27	9,45	60,57	0,00	0,16
N4-40	29,5	6,7	376,91	58,69	10,20	63,12	0,00	0,16
N4-40	29,5	6,7	368,71	57,81	12,55	63,04	0,00	0,20
N4-40	29,5	6,7	323,60	44,44	8,50	61,84	0,00	0,14
N4-40	29,5	6,7	178,65	32,02	1,91	60,72	0,00	0,03
N4-40	29,5	6,7	469,38	65,61	0,44	63,75	0,00	0,01
N4-40	29,5	6,7	330,78	42,12	1,00	61,63	0,00	0,02
W2-10	59,6	6,7	132,15	24,71	23,08	102,21	0,00	0,23
W2-10	59,6	6,7	30,64	67,61	10,66	106,07	0,00	0,10
W2-10	59,6	6,7	31,24	5,76	14,33	100,50	0,00	0,14
W2-10	59,6	6,7	24,57	4,52	4,49	100,39	0,00	0,04
W2-10	59,6	6,7	26,14	4,42	14,33	100,38	0,00	0,14
W2-10	59,6	6,7			0,00	100,59	0,00	0,00
W2-10	59,6	6,7	48,71	7,86	0,35	100,69	0,00	0,00
W2-40	59,6	6,7	11,94	0,02	9,97	99,98	0,00	0,10
W2-40	59,6	6,7	10,13	0,09	6,47	99,99	0,00	0,06
W2-40	59,6	6,7	62,29	8,61	1,69	100,76	0,00	0,02
W2-40	59,6	6,7	68,39	11,82	2,35	101,04	0,00	0,02
W2-40	59,6	6,7	59,64	6,76	1,69	100,59	0,00	0,02
W2-40	59,6	6,7	75,96	7,69	2,12	100,67	0,00	0,02
W2-40	59,6	6,7	87,68		0,00	104,70	0,00	0,00
W2-40	59,6	6,7	83,11	8,17	0,02	100,72	0,00	0,00
W4-10	24,9	6,7			8,50	51,67	0,00	0,16
W4-10	24,9	6,7			8,50	51,67	0,00	0,16
W4-10	24,9	6,7	597,34	72,90	1,38	57,96	0,00	0,02
W4-10	24,9	6,7	458,07	50,98	2,06	55,99	0,00	0,04
W4-10	24,9	6,7	245,07	29,52	1,38	54,06	0,00	0,03
W4-10	24,9	6,7	177,72	19,10	3,55	53,12	0,00	0,07
W4-10	24,9	6,7	100,21	10,99	0,32	52,39	0,00	0,01
W4-10	24,9	6,7	112,90	11,05	1,00	52,40	0,00	0,02
W4-40	56	6,7	159,19	24,60	3,80	97,15	0,00	0,04
W4-40	56	6,7	425,64	90,53	15,80	103,09	0,00	0,15
W4-40	56	6,7	327,61	33,01	8,50	97,91	0,00	0,09
W4-40	56	6,7	582,95	69,09	7,82	101,16	0,00	0,08
W4-40	56	6,7	430,28	52,89	8,50	99,70	0,00	0,09
W4-40	56	6,7	385,09	42,22	1,22	98,74	0,00	0,01
W4-40	56	6,7	180,39		0,00	110,86	0,00	0,00
W4-40	56	6,7	223,21	44,32	0,10	98,93	0,00	0,00
SW	8,6	7,4	76,19	11,91	0,01	19,94	0,00	0,00

Deltares is an independent institute for applied research in the field of water and subsurface. Throughout the world, we work on smart solutions for people, environment and society.

Deltares

www.deltares.nl